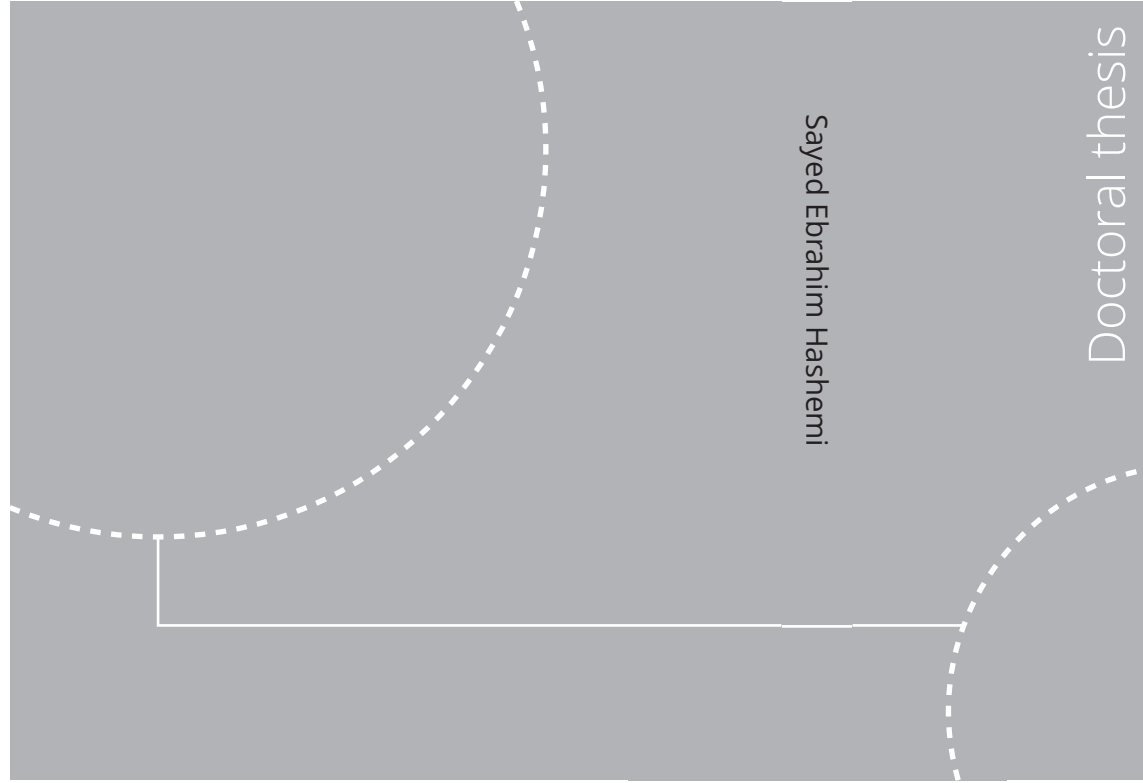


ISBN 978-82-326-5651-6 (printed ver.)
ISBN 978-82-326-5713-1 (electronic ver.)
ISSN 1503-8181 (printed ver.)
ISSN 2703-8084 (electronic ver.)



Doctoral theses at NTNU, 2022:107

Sayed Ebrahim Hashemi

Development and Optimization of Processes for Liquefied Biomethane Production

Doctoral theses at NTNU, 2022:107

NTNU
Norwegian University of
Science and Technology
Thesis for the degree of
Philosophiae Doctor
Faculty of Engineering
Department of Energy and Process Engineering

Sayed Ebrahim Hashemi

Development and Optimization of Processes for Liquefied Biomethane Production

Thesis for the degree of Philosophiae Doctor

Trondheim, March 2022

Norwegian University of Science and Technology
Faculty of Engineering
Department of Energy and Process Engineering



Norwegian University of
Science and Technology

NTNU

Norwegian University of Science and Technology

Thesis for the degree of Philosophiae Doctor

Faculty of Engineering

Department of Energy and Process Engineering

© Sayed Ebrahim Hashemi

ISBN 978-82-326-5651-6 (printed ver.)

ISBN 978-82-326-5713-1 (electronic ver.)

ISSN 1503-8181 (printed ver.)

ISSN 2703-8084 (electronic ver.)

Doctoral theses at NTNU, 2022:107



Printed by Skipnes Kommunikasjon AS

Abstract

The contribution of renewable energies to the globally fast-expanding transport sector is the lowest among the other sectors like power generation. Many alternative fuels have been suggested to boost the green transition towards sustainable transportation. Liquefied biomethane (LBM) has recently gained much attention within this context. LBM has similar characteristics as liquefied natural gas. Moreover, the abundance and origin of LBM from biogas make it an exciting energy source in the transport sector.

LBM production involves multiple energy-intensive processes. Biogas upgrading to remove CO_2 and low-temperature refrigeration to liquefy the final product are the most critical parts of an LBM production plant. For a long time, the development of processes regarding biogas upgrading focused on applications such as compressed gaseous fuel and gas grid injection, where a purity of 90-97 mol% of CH_4 is required. Hence, the design of the biogas upgrading process complied with such purity requirements.

The emergence of LBM as an alternative transportation fuel has imposed an even more restrictive purity requirement (i.e., CO_2 content below 50 ppm in upgraded biogas known as biomethane). The liquefaction process after the biogas upgrading process is the main reason for considering such stringent CO_2 requirements; exceeding the CO_2 concentration limit in the biomethane can damage low-temperature heat exchangers due to CO_2 ice-formation.

Developing processes for LBM production that are energy-efficient and cost-efficient requires further considerations for the highly restrictive CO_2 content in biomethane. Hence, the focus of this thesis has been to develop and optimize the design of LBM production plants through thermodynamic and cost analyses. Further, a novel process concept has been developed to convert CO_2 available in the biogas mixture to additional LBM using the CO_2 methanation process fed by renewable hydrogen.

In this thesis, detailed process models of state-of-the-art technologies for biogas upgrading, CO_2 methanation, and biomethane liquefaction have been simulated with a commercial process simulation tool. Amine-based absorption and cryogenic gas separation have been considered for the upgrading process. Different refrigeration cycles, including N_2 expander cycles and single mixed refrigerant cycles, have been

used for liquefaction. The CO₂ methanation process model has been developed so that it can be integrated in the LBM production plant. The processes have been optimized using a sequential quadratic programming (SQP) algorithm.

Determination of potential synergies and overall energy efficiency improvements of LBM production plants due to integration of the upgrading and liquefaction processes has been performed by comparing LBM production using amine-based biogas upgrading and cryogenic biogas upgrading. The results indicated that integrating biogas upgrading with the liquefaction process using the cryogenic gas separation would reduce the specific energy requirement of the LBM production plant. However, cryogenic gas separation for biogas upgrading was associated with challenges regarding CO₂ ice-formation that limit its application in practice, even with a better thermodynamic performance.

Optimization studies have aimed to propose alternative approaches to improve the performance of the conventional LBM production plant using amine-based biogas upgrading. The results illustrated that the interaction between the upgrading and liquefaction processes within the conventional LBM production plant was limited to only the pressure level of the biomethane produced from the upgrading process. Hence, a sequential optimization approach was adequate to determine the optimal operating conditions for minimum exergy demand within the plant. Further, the results revealed that the thermodynamic optima obtained from minimizing the exergy supply and the total annualized cost for the upgrading process would be similar since operating at high pressure was required to satisfy the restrictive CO₂ content specification. Concerning the total exergy demand within the overall plant, the difference between solutions obtained from different objective function formulations for the upgrading process would be insignificant.

In this thesis, a comprehensive investigation has been carried out to design a CO₂ methanation reactor considering the improvement of CO₂ conversion and irreversibility rate within the reactor. It was observed that a series of methanation reactors with intermediate water removal operating under non-isothermal conditions could provide maximum CO₂ conversion with an improved irreversibility rate within the reactor. Further, the required reactor length to perform CO₂ methanation was determined. The results indicated that the CO₂ methanation reaction could be run in a shorter reactor when the intermediate water removal was considered as the gaining for additional CO₂ conversion due to extra length was not significant.

Finally, a conceptual process design has been proposed to combine the conventional LBM production plant with the methanation process. Here, the feasibility of such a process concept has been thoroughly studied. The results illustrated that the methanation process could be partly responsible for upgrading; however, an additional polishing step was required to meet the CO₂ content specification. The feasibility study concluded that the applicability of the proposed process design was highly dependant on the price of H₂. Further, the overall exergy efficiency of the proposed concept could outweigh the exergy efficiency of the conventional LBM production plant if the available exergy of heat was utilized.

Preface

This thesis was submitted to the Department of Energy and Process Engineering at the Norwegian University of Science and Technology (NTNU) in partial fulfilment of the requirements for the degree of philosophiae doctor (Ph.D.). The thesis represents four years of work, of which 25 % is allocated for teaching duties.

The work was financially supported by Norwegian University of Science and Technology (NTNU) through the Strategic Research Program ENERSENSE. Associate Professor Bjørn Austbø served as main supervisor of the work together with Associate Professor Sondre K. Schnell and Professor Kristian M. Lien as co-supervisors.

Sayed Ebrahim Hashemi
December 2021
Trondheim

Acknowledgements

During my journey in PhD project since September 2017, many people have helped me reach this point. All of them deserve my gratitude. First of all, I wish to express my sincere appreciation to my main supervisor, associate professor Bjørn Austbø for his patience, guidance, trust, and motivation. He was always available for discussions and help. After our meetings, I had plenty of ideas to progress further. I thank him for his thorough feedback regarding my research work. I truly enjoyed working with him.

I want to thank my co-supervisors, professor Kristian M. Lien and associate professor Sondre K. Schell for their supports, fruitful discussions during our meetings. I especially thank professor Lien for his help to initiate the direction of PhD project with his insightful ideas. I learned a lot from his comprehensive understanding of every problem. I am also grateful to Dr. Schnell for considering my questions with understanding and motivating me during the PhD project. I would also like to thank professor Magne Hillestad for his active collaboration on my research work. He was always available for profound discussions and developing ideas. His comments on my research work improved their quality.

I am grateful to Shiplu Sarker and Donghoi Kim for their collaborations in my research articles. Their feedback and discussion helped me improve my research work quality. I also want to thank Sander Wijnsma for his MATLAB help and for sharing initial scripts for reactor models.

During my stay in Norway, I have been lucky to know a few people who became more than just a friend. They are now an essential part of my life. I am grateful to Lena and Bahar for the unlimited kindness and positive energy that they have given me. Thank you for finding a way to cheer me up when I felt down. I am grateful to Markus for letting me become a very important part of his life. His always inspiring and thoughtful encouragements made everything seem easy. I especially thank Michi for his presence whenever I needed to talk to someone. He is the one who helped me to go through all ups and downs during the PhD project. I am thankful to Benjamin for his valuable advice and the great time we spent together. He has been the one with who I never felt ignored.

I had the privilege of being part of ENERSENSE, where I met terrific people. I

thank the leader, Odne Burheim, and my colleagues in ENERSENSE, Pauline, Gaurav, Kjersti, Yash, Ian, Robert, Jake, Islam, Faranak, Silje, Simon, Zohreh, Laurina. I will never forget all our social activities and the wonderful time together. I also want to greatly appreciate my dear office mates Felix and Ailo, who tolerated escalating room temperature and fruitful discussions, both scientific and off topics. I want to thank Engin, Sam and Ahmad for their encouragement and trust in me.

Attending the lunch meeting in the Process Integration (PI) group was a great honor for me, where I had the chance to meet knowledgeable people with excellent insight into thermodynamics. I would like specifically to thank Prof. Truls Gundersen, the leader of the PI group. His presentations and welcoming attitudes, especially in our several hiking and cabin trips, were always good motives for going forward.

♥ Last but most of all, I express my deepest gratitude to my parents, Fakhri and Ghader, my brother, Behnam, and his wife, Sepideh, for their unlimited support and unconditional love. Where I stand now is because of them. Their inspiration made everything happen. You are the meaning of my life, and I am grateful to have you beside me. This thesis is dedicated to you. ♥

Contents

Abstract	i
Preface	iii
Acknowledgements	v
	Page
1 Introduction	1
1.1 Motivation	1
1.2 Objectives	2
1.3 Scope	4
1.4 Contributions	4
1.5 Structure and outline of the thesis	5
1.6 List of publications	5
2 Background	7
2.1 Situation of energy use in transportation	7
2.2 Alternative fuels in transport sector	8
2.3 Biogas production and its composition	11
2.4 Biogas utilization	12
2.5 Biogas to liquefied biomethane	13
2.5.1 Biogas cleaning	14
2.5.2 State-of-the-art biogas upgrading	14
2.5.3 State-of-the-art liquefaction of biomethane	16
2.5.4 Potentials and barriers	17
2.6 Power-to-gas for liquefied biomethane production	19
2.6.1 State-of-the-art water electrolysis	19
2.6.2 State-of-the-art methanation	21
3 Methods	25
3.1 Process description and modeling	25
3.1.1 Simulation tools	28
3.1.2 Feed and product	28
3.1.3 Assumptions	28
3.2 Process evaluation	29
3.3 Process optimization	29

4	Summary of articles	31
4.1	Article I	31
4.2	Article II	32
4.3	Article III	33
4.4	Article IV	34
4.5	Article V	35
4.6	Article VI	36
5	Conclusions and future work	39
	Bibliography	43
	Collection of papers	49
	Article I	51
	Article II	65
	Article III	73
	Article IV	107
	Article V	115
	Article VI	139

1.1 Motivation

Fossil fuels mainly dominate the energy use in the transport sector, and the penetration of renewable energy sources in this sector is remarkably limited. Concerns regarding energy density and readiness of infrastructures for alternative fuels originated from renewable sources are recognized as major barriers to further increasing renewable energy share in transportation, particularly for long distances.

Purified biogas, often known as biomethane, is considered an appropriate fuel for transportation due to its abundance and similar features to conventional natural gas (NG). In order to utilize biomethane in transport, it is often stored in liquid form or compressed gaseous form. Further, liquefied biomethane (LBM) is considered more economically feasible for long-range transportation.

Nonetheless, LBM production requires satisfying very restricted CO_2 content since the presence of CO_2 in liquefaction processes causes severe issues like CO_2 ice formation in heat exchangers. This strict CO_2 content limit imposes additional care to the design of the LBM production plant. Therefore, common technologies for removing CO_2 from biogas, known as biogas upgrading technologies, should be adjusted accordingly.

Within this context, it is essential to understand the effect of such specifications on the design of the LBM production plant. Moreover, since the LBM production plant consists of multiple processes, integration of these processes and optimizing them are crucial when developing an energy-efficient and economically feasible process design.

Another aspect regarding the conventional LBM production plant is that the captured CO_2 from biogas is usually emitted into the atmosphere without further

utilization or is stored underground in liquid form. Recently, the production of synthetic methane through the Power-to-Gas (PtG) concept using green H_2 has been considered an alternative approach to utilize the CO_2 from biogas.

The PtG concept using CO_2 methanation can be part of the biogas upgrading process to boost the LBM production. However, the feasibility of employing CO_2 methanation jointly with the upgrading and liquefaction process has not been evaluated. This motivates to examine the practicality of integrating the PtG concept with conventional LBM production plants.

1.2 Objectives

The primary objective of the PhD project is to enable potential improvements in energy efficiency and economy of LBM production plants. In order to achieve the main objective, three sub-objectives are defined as follows:

Objective I: Determining potential synergies between biogas upgrading and liquefaction

Objective II: Determining thermodynamic and economic optima of operating conditions for LBM production plants

Objective III: Developing a concept to integrate the PtG concept with conventional LBM production plants

This article-based thesis contains six research articles dedicated to responding to the mentioned objectives and filling the research gap in developing and optimizing process models for liquefied biomethane production as an alternative transportation fuel. Fig. 1.1 illustrates the objectives and the corresponding articles in response to the objectives.

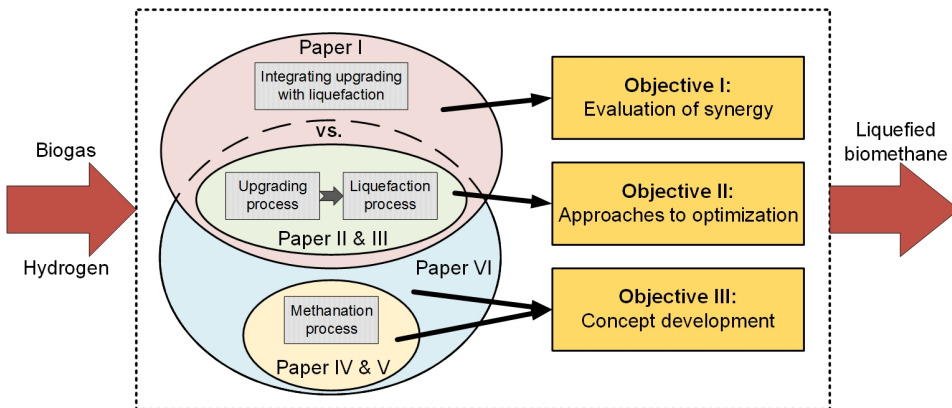


Figure 1.1: An outline regarding the objectives and dedicated articles

With respect to *Objective I*, potential synergy is assessed by comparing the energy efficiency of conventional and integrated LBM production schemes where upgrading and liquefaction process are combined. Here, the hypothesis is that biogas upgrading through cryogenic separation (within the integrated LBM scheme) would reduce the required cooling duty in liquefaction. Unlike the integrated scheme, within the conventional LBM production scheme considering amine-based biogas upgrading, unavoidable temperature increase due to amine regeneration conflicts with the cooling required for the subsequent liquefaction. The results examining this hypothesis is presented in **Article I**.

Potential performance improvement of the conventional LBM production scheme is considered for examination of *Objective II*. The reason for selecting this scheme rather than the integrated scheme is mainly because of crucial practical concerns regarding the cryogenic separation for biogas upgrading in large-scale applications. Further, optimization of the biogas upgrading using amine-based absorption has not been fully realized for LBM production.

This thesis examines optimization approaches for the conventional LBM production plant. First, the hypothesis is that any changes in the operating conditions of the upgrading process affect the cooling demand in the subsequent liquefaction process, while the opposite is not true. Therefore, several objective function formulations for sequential and simultaneous optimization of the conventional LBM production scheme are examined in order to address the dependency between the two processes. The results from the first approach are presented in **Article II**.

With knowledge gained from the first optimization approach, **Article III** focuses on optimization of the upgrading process, examining several objective function formulations to improve both thermodynamic and economic performance of the upgrading process. Further, their impact on the upgrading process is also investigated.

For *Objective III*, the design of a suitable methanation reactor for biogas upgrading is proposed and the feasibility of an integrated scheme consisting of methanation and conventional LBM production is evaluated. First, **Article IV** presents fundamental insight into the thermodynamic performance of a methanation reactor using pure CO₂ or a biogas mixture as the feed gas. Here, improvements in the design and operating conditions of the energy-efficient methanation reactor are highlighted in terms of improved heat integration potential and reduced irreversibilities within the methanation reactor. **Article V** investigates further CO₂ conversion improvement and irreversibility rate reduction within the methanation reactor, considering staging of reactors and water removal.

Finally, the insight gained from modeling the methanation reactor is used in **Article VI** to develop a conceptual process model for the combination of PtG and conventional LBM production plants. The proposed concept utilizes the CO₂ from the biogas mixture to produce additional LBM.

1.3 Scope

First, the thesis is a simulation-based study that follows the downstream operation of a biogas production plant. The development of the process models is performed using process simulation software (Aspen HYSYS[®]) and MATLAB.

Second, only biogas upgrading and utilization are considered in the final process design and proposed optimization approaches. LBM is regarded as the desired final product used for biogas utilization.

Third, only amine-based absorption and cryogenic gas separation are considered among possible technologies for biogas upgrading. The choice of these two technologies is mainly due to their capability to satisfy biomethane purity specifications without further polishing steps before the liquefaction.

Moreover, some topics are beyond the scope of this thesis. For instance, biogas production methods and pre-treatment of biogas are not included in this project. However, the inlet biogas composition is hypothesized based on the literature when modeling the processes. For PtG application, the production of green H₂ through water electrolysis is not considered in the models; instead, the necessary information is taken from relevant literature.

1.4 Contributions

The main contributions of this thesis can be listed as:

- Developed detailed process models for amine-based biogas upgrading, cryogenic biogas upgrading and multiple refrigeration cycles. Investigated extensively the performance of LBM production plants in terms of energy and exergy efficiency. Developed detailed cost estimation model for LBM production plant.
- Proposed optimization approaches for LBM production plants. Considered the dependency between biogas upgrading and liquefaction process in objective function formulations. Performed sensitivity analysis to determine the influence of design variables on the performance of the LBM production plant. Determined optimal operating conditions for LBM production plants in terms of thermodynamic and economic performance with respect to highly restrictive constraints.
- Developed rigorous models for a methanation reactor. Considered the kinetics of methanation, and mass and heat transport limitations to design a series of reactors with intermediate water removal. Proposed a novel process concept combining methanation and conventional LBM production. Determined the feasibility of the proposed concept. Specified the price of produced LBM under different scenarios.

1.5 Structure and outline of the thesis

This thesis is structured by five chapters representing an overview and summary of the research given in the six articles. A collection of articles is also provided as an annex.

Chapter 1 provides an overview of the PhD thesis, including motivation, objectives and contributions, and highlights the thesis structure.

Chapter 2 presents background regarding the energy situation in the transportation sector and alternative fuels. Further, this chapter reviews the state-of-the-art biogas upgrading technologies and LBM production. The principle of PtG and recent advances regarding methanation reactor design are also presented.

Chapter 3 describes the process models developed in this thesis. Primary assumptions for process models and setup of the optimization problems are highlighted. Moreover, elaborate descriptions of the methods employed to evaluate and optimize the processes are presented.

Chapter 4 provides a summary of the appended articles. The summaries elaborate on the main contributions of each article. Further, the leading findings are highlighted and discussed briefly.

Chapter 5 draws the main conclusions of the thesis and provides some suggestions for future work.

1.6 List of publications

The research articles that have been published or submitted to international peer-reviewed journals and peer-reviewed conference publications are listed below according to the sequence presented in this thesis. Regarding authorship in all articles, the PhD candidate was responsible for conceptualization, methodology, software, validation, formal analysis. The PhD candidate also wrote the original draft of all articles and participated in the theoretical discussions.

Article I. S. E. Hashemi, S. Sarker, K. M. Lien, S. K. Schnell and B. Austbø “*Cryogenic vs. absorption-based biogas upgrading in liquefied biomethane production – An energy efficiency analysis*” *Fuel*, (2019) 245: 294–304.

Article II. S. E. Hashemi, K. M. Lien, S. K. Schnell and B. Austbø “*Optimization of an absorption-based biogas upgrading and liquefaction process*” *Chem. Eng. Trans.*, (2019) 72: 697–702.

Article III. S. E. Hashemi, D. Kim and B. Austbø “*Objective function evaluation for optimization of an amine-based biogas upgrading and liquefaction process*” Submitted to *Ind. Eng. Chem. Res.*

Article IV. S. E. Hashemi, K. M. Lien, S. K. Schnell and B. Austbø “*Thermodynamic analysis of different methanation reactors for biogas upgrading*” *Comput. Aided Chem. Eng.*, (2020) 48: 367–372.

Article V. S. E. Hashemi, K. M. Lien, M. Hillestad, S. K. Schnell and B. Austbø “*Thermodynamic insight in design of methanation reactor with water removal considering nexus between CO₂ conversion and irreversibilities*” *Energies*, (2021) 14(23): 7861–7881.

Article VI. S. E. Hashemi, M. Hillestad and B. Austbø “*Direct vs. indirect biogas methanation for LBM production: A concept evaluation*” to be submitted to *Chem. Eng. Res. Des.*

The following conference presentations have been given during the PhD work:

S. E. Hashemi, S. Sarker, K. M. Lien, S. K. Schnell and B. Austbø “*Liquefied biomethane as an alternative transportation fuel*”, The European Conference on Fuel and Energy Research and its Applications (12th ECCRIA); September 2018, Cardiff, UK.

S. E. Hashemi, K. M. Lien, S. K. Schnell and B. Austbø “*Optimization of a chemical absorption biogas upgrading and liquefaction process*”, 22nd Conference Process Integration, Modelling and Optimisation for Energy Saving and Pollution Reduction (PRES’19); October 2019, Crete, Greece.

S. E. Hashemi, K. M. Lien, S. K. Schnell and B. Austbø “*Design of methanation reactor operating under different conditions*”, The 30th European Symposium on Computer Aided Process Engineering (ESCAPE 30); September 2020 (moved online), Milan, Italy.

In addition, the author has also contributed to the following article published in international peer-reviewed journal during his PhD work. This article is not included in the thesis.

Article VII. S. Hashemi, S. E. Hashemi, K. M. Lien and J. J. Lamb “*Molecular microbial community analysis as an analysis tool for optimal biogas production*” *Microorganisms*, (2021) 9(6): 1162–1186.

This chapter provides a brief description of liquefied biomethane production and relevant topics. Firstly, the global energy situation in the transport sector is provided, addressing alternative fuels. Secondly, a general recap of the process chain of production and the use of biogas is outlined, centered around the state-of-the-art LBM production. Finally, a brief background regarding the Power-to-Gas concept focusing on its application for methane production from CO₂ and green H₂ is given.

2.1 Situation of energy use in transportation

The energy demand in transportation section grows rapidly driven by fast growth of population, urbanization, and global mobility. In 2018, near a third of the total global energy demand was used in transport, but renewable sources provided only 3.7 % of this demand (see Fig. 2.1) [1]. Moreover, approximately one-quarter of global greenhouse gas emissions comes from the transportation due to high dependence on fossil fuels [2]. Fig. 2.2 illustrates contribution of different forms of transportation in the CO₂ emission in 2020. 77 % of global CO₂ emission from the transport is originated from on-road transportation (i.e., light-duty vehicles (LDV), heavy-duty vehicles (HDV), 2 and 3 wheelers, and buses), followed by CO₂ emissions from marine and aviation. It is worth mentioning that the HDVs and marines are crucial as their contribution to the emission of CO₂ and particulate matters is disproportionate for their numbers in the global vehicle fleet.

Unfortunately, with current upward trend of emissions from the transport and all announced policy measures in transportation sector, the CO₂ emission is expected to increase up to 60 % by 2050 [1]. Therefore, a rapid shift towards decarbonization of the transport sector is required to meet the objectives of the Paris Climate Agreement [3]. In order to boost the decarbonization of the transport sector, implementation of existing and developing low-carbon and zero-emissions technologies

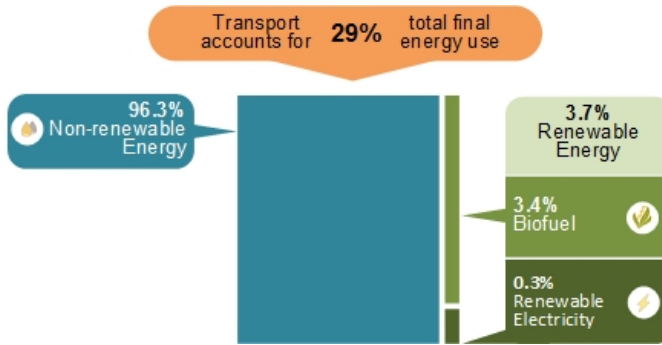


Figure 2.1: Energy use and renewable energy share in the transport sector in 2018 (The figure is reproduced with granted permission from [1])

among all forms of transportation is necessary [1,2]. This thesis focuses on technology options and alternative fuels that can be employed in the road transportation particularly for the heavy-duty vehicles.

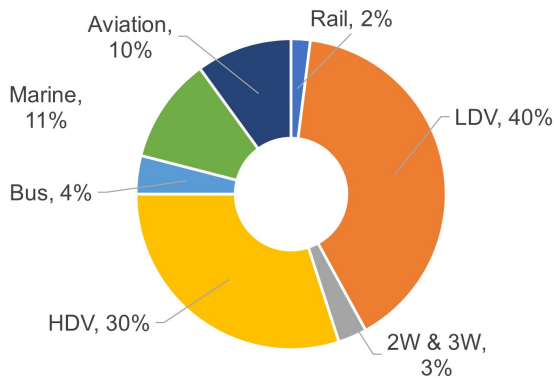


Figure 2.2: CO₂ emission from different forms of transportation in 2020 (The figure is reproduced with granted permission from [2])

2.2 Alternative fuels in transport sector

As illustrated in Fig. 2.3, the main alternative energy use for the road transport can be categorized in four groups: 1) direct use of renewable electricity 2) gaseous or liquid biofuels 3) renewable electricity-based H₂ 4) renewable electricity-based synthetic fuels.

The direct use of electricity refers to the use of renewable electricity produced from intermittent energy sources like solar photovoltaic (PV), wind power, geothermal

power, hydropower and etc. to run vehicles using batteries. Electrification of passenger cars, urban buses, 2 and 3 wheelers has been increased considerably in the past decade, thanks to high efficiency of batteries, and supports from policy makers to push the car industries towards selling electric and hybrid cars [1]. Nonetheless, the use of batteries faces several barriers such as lack of charging stations, long charging time, shortage in noble metals for battery fabrications and most importantly short distance range [4].

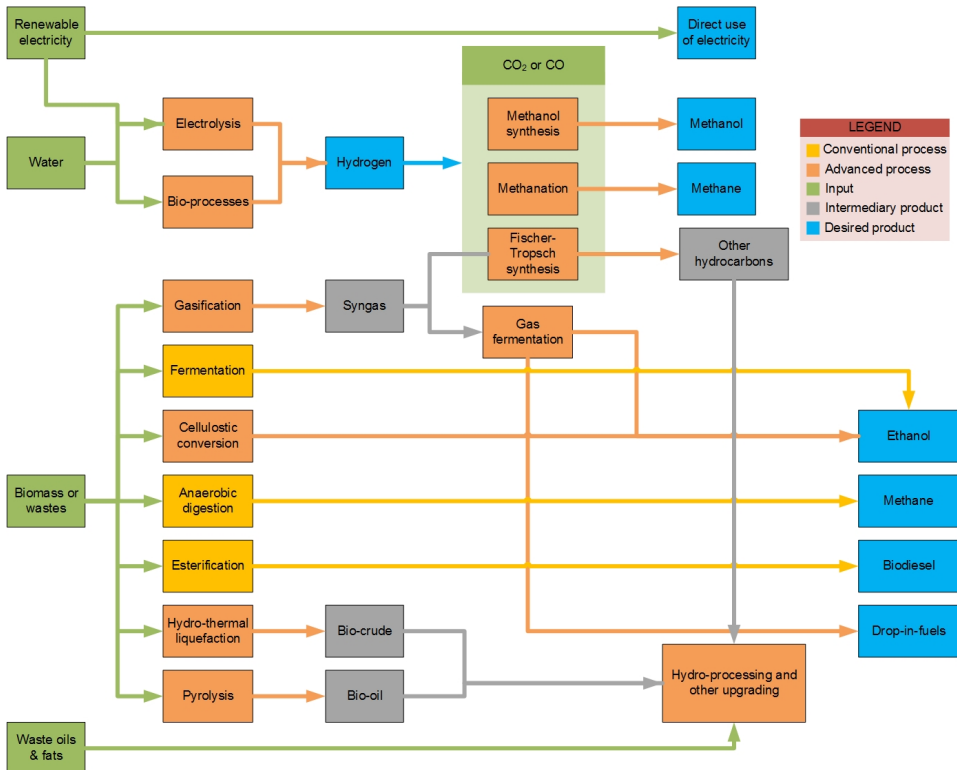


Figure 2.3: Alternative energy use for the road transport (The figure is reproduced with granted permission from [1])

Unlike the electrification of cars, available technologies to produce alternative fuels from renewable electricity are less established as most of them are still under development and in the demonstration stage. The gaseous and liquid biofuels are mainly originated from biomass and wastes from agriculture and domestic to produce biofuels such as biodiesel, bioethanol and methane. These biofuels are mostly blended with gasoline and diesel. Available technologies for biofuels have been in place for many years [5] and ongoing research are considering alternative raw materials and improving the efficiency of the technologies [6].

The demand for biofuels has been extensively increased due to energy pathway policies for transportation by increasing the share of biofuels in blends with fossil

fuels. Further, in comparison to fossil fuels, biofuels are more cost-competitive relative to other alternatives. However, biofuel production cannot fully meet the energy use in the transport section as the amount of space to produce biofuels is limited. Exclusively large land area, water, and fertilizer are expected for biomass crops, and when they have grown, a large amount of storage facilities is required before converting to energy.

The renewable electricity-based H_2 is often known as ‘green H_2 ’ which is generated through water electrolysis using the electricity from renewable sources. Further, bioprocesses such as fermentation-based systems, at which microorganisms like bacteria degrade organic matter, can be used to produce green H_2 [7]. However, the latter technology is limited by slow kinetics, thereby challenging for scale-up [7].

Currently, the majority of H_2 production is used in producing ammonia as fertilizer, in oil refineries, and in producing iron and aluminum [8]. In the past decade, there have been many research and interest to bring H_2 into play for transportation purposes in order to mitigate the CO_2 emission. H_2 in compressed form or in liquid form are main ways of utilizing H_2 in transport.

The main barrier with green H_2 compared to fossil-based H_2 from natural gas and coals, which accounts for about 99 % of current H_2 production globally, is the cost of green H_2 production [9]. Because the H_2 production from renewable electricity is directly related to the price of electricity. In order to fulfill the decarbonization of the economy and transport, the green H_2 should replace the current H_2 requirement and additional demand in the transport sector.

The renewable electricity-based synthetic fuels are often recognized as fuels produced through Power-to-Gas (PtG) as they involve multiple conversion steps from electricity to other forms of energy mainly chemical energy. This pathway can provide a solution to utilize CO_2 captured from other sources such as power plants or biogas upgrading plants and to turn them into fuels. The PtG will be discussed in detail later in this chapter.

Fig. 2.4 gives an overview on the energy density of different available fuels for transportation per unit of volume and mass. As mentioned earlier, having smallest energy density for batteries limits its applications for short range vehicles. H_2 in compressed or liquid form represents the highest energy density per unit of mass thanks to being the lightest element in nature (i.e., approximately 3 times higher than diesel) but the volumetric energy density of it requires large spaces. For synthetic fuels with similar characteristics as liquefied natural gas (LNG) or liquefied petroleum gas (LPG), the gravimetric energy density is better than diesel, but it requires approximately 1.5 times larger space to provide the same amount of energy as diesel.

Considering the impact of storage systems for alternative fuels would reduce the energy densities and it will be even worse for the compressed and liquid H_2 . Alternative fuels with similar characteristics as LNG or LPG would be beneficial for

long range transportation. One of the alternative synthetic fuels are compressed or liquefied biomethane from biogas upgrading, which is investigated in this thesis.

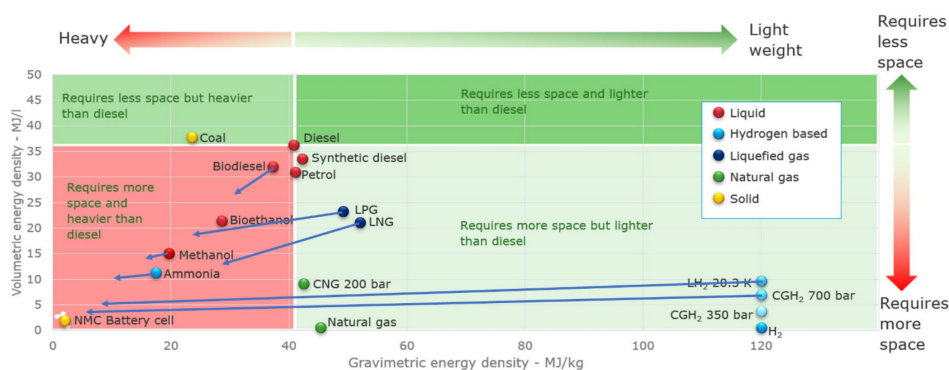


Figure 2.4: Volumetric/Gravimetric energy densities of different energy carriers. The arrows are indicative values representing the effect of storage systems on energy density (The figure is copied with granted permission from [10])

2.3 Biogas production and its composition

Thanks to the diversity and plentifulness of sources, biogas has been considered an important biofuel between energy policymakers and researchers due to its potential to reduce the dependency on fossil fuels [11]. Biogas can be produced from different feedstocks ranging from agricultural sources like farm animal waste and crops to municipal wastes and sewage treatment plants through biological degradation of carbohydrate-rich, protein-rich and fat-rich matters under anaerobic conditions, known as anaerobic digestion (AD) [12]. The biogas composition depends on the type of feedstock, operating parameters such as temperature and related technology for biogas production.

Essentially, biogas may be considered as natural gas (NG) with relatively high CO_2 content. There are several differences between biogas and conventional NG, for instance the size of treating plants for NG is generally much larger than that for biogas production plant and the concentration of components other than methane differs between two gases. Typically, NG contains higher hydrocarbons, while biogas instead includes more hydrogen sulfide (H_2S). A biogas mixture contains mainly CH_4 (50–70 %) and CO_2 (30–50 %) with minor amount of other components such as H_2O , N_2 , H_2S , H_2 and siloxanes [13]. Typical biogas composition for different feedstocks produced through different technologies is given in Table 2.1.

Table 2.1: Typical composition of biogas and NG [13]

Component	Unit	AD biogas	Landfill biogas	NG
CH ₄	vol%	53–70	30–65	81–89
CO ₂	vol%	30–50	25–47	0.67–1
N ₂	vol%	2–6	< 1–17	0.28–14
O ₂	vol%	0–5	< 1–3	0
H ₂	vol%	n.a.	0–3	n.a.
Higher hydrocarbon	vol%	n.a.	n.a.	3.5–9.4
H ₂ S	ppm	0–2000	30–5000	0–2.9
NH ₃	ppm	< 100	0–5	n.a.
Chlorines	mg/Nm ³	< 0.25	0.3–225	n.a.
Siloxanes	μg/g _{dry}	< 0.08–0.5	< 0.3–36	n.a.

2.4 Biogas utilization

Burning household biogas for heat generation without any processing or treatment has been in place for more than 100 years. Nowadays, biogas is utilized in many applications including burning biogas in combined heat and power plants (CHP) for heat and electricity generation, upgrading biogas for natural gas grid injection and various transportation fuels (see Fig. 2.5) [14].

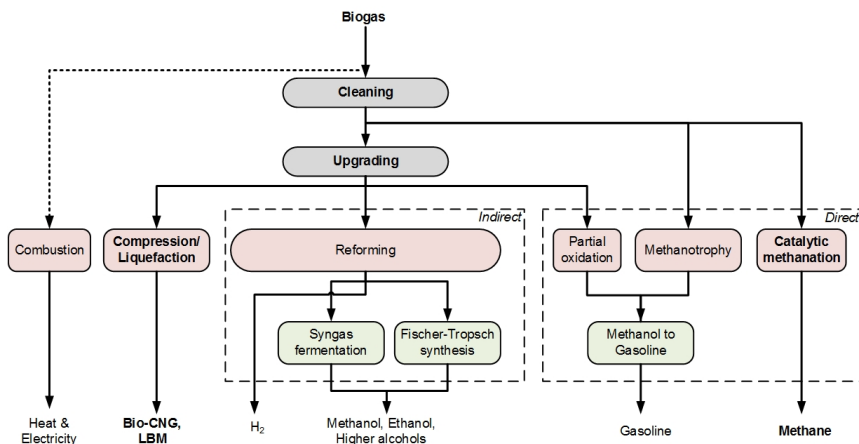


Figure 2.5: Different utilization of biogas (The figure is updated with granted permission from [14])

Unlike the use of biogas for heat and electricity generation, there are mandatory requirements in other applications to produce biogas with a methane content of more than 97 %, often known as biomethane. Clean biogas can be used in catalytic reforming processes to produce syngas and high purity H₂, from which further synthesis like syngas fermentation or Fischer-Tropsch process can lead to production

of other transportation fuels [15, 16].

The biomethane can reduce the dependency on fossil-fuels as it shares comparable properties as conventional natural gas (NG), which can be then transported in compressed form (bio-CNG) or in liquid form (LBM). Having similar characteristics as the NG makes injection of biogas into pipeline grids an option. Further, similar to NG, transportation of biomethane in liquid is considered as the most promising approach for long distance transportation (over 3500 km) in terms of economy and CO₂ emissions [11].

The biomethane in liquid form has approximately 600 times lower volume than that in gaseous form. The use of biogas in the transportation has advantages such as lower particulate matters (e.g., tar and soot) and approximately 80 % lower CO₂ emissions (i.e., 8–22 mg CO₂eq per MJ) compared to fossil fuels [11].

2.5 Biogas to liquefied biomethane

The production of LBM from the biogas involves multiple processes; biogas cleaning, upgrading and liquefaction. The biogas cleaning refers to remove the minor components like H₂S, O₂, N₂ and siloxanes. Upgrading biogas is a major step in LBM production. In upgrading, CO₂ is removed from the biogas in order to bring the concentration of biomethane close to quality standards for NG in terms of purity and heating value. Table 2.2 summarizes the impact of impurities in the biogas mixture and the permissible limit of impurities for LBM production. Finally, the upgraded biogas is liquefied through refrigeration cycles. For the sake of brevity, an overview regarding available technologies in market to clean, upgrade and liquefy the biogas is presented in this section.

Table 2.2: Undesired impact of impurities [17]

Component	Impacts
H ₂ O	Corrosion due to acid formation Concerns regarding damages due to condensation and freezing
H ₂ S	Corrosion due to acid formation (reacting with H ₂ O) SO _x formation and lethal Forming flammable mixtures (i.e., 4.5–45 % H ₂ S in air)
CO ₂	Lowering calorific value of biogas Corrosion due to acid formation (reacting with H ₂ O)
NH ₃	Corrosion due to acid formation (reacting with H ₂ O)
O ₂ & N ₂	Reduction in liquefaction rate of biomethane Reduction in calorific value of biogas
Siloxanes	SiO ₂ formation and microcrystalline quarts Abrasion
Dust	Clogging in equipment
Cl ⁻ and F ⁻	Corrosion concerns

2.5.1 Biogas cleaning

Performing biogas cleaning in advance to upgrading and liquefaction is beneficial to prevent corrosion and potential mechanical issues of the equipment. Further, the level of biogas cleaning is determined by the further processing and the use of biogas. Available biogas cleaning technologies are distinguished from each other with respect to the quality and conditions of inlet gas, the required purity of biogas and process efficiency. As the cleaning step is placed outside of the scope of this thesis, readers are encouraged to review the work by Sun et al. [18] for detailed overview regarding technologies employed for removing impurities.

2.5.2 State-of-the-art biogas upgrading

Multiple technologies have been employed for the biogas upgrading to biomethane. These technologies include a wide range of physical and chemical methods to purify the biogas such as physical/chemical absorption, pressure swing adsorption, cryogenic separation and membranes. Table 2.3 represents advantages and disadvantages of each technology used for the biogas upgrading. The state-of-the-art regarding biogas upgrading technologies is mostly related to exploration of new materials or solvents and modification of process configurations in order to handle challenges relevant to each technology [19].

Table 2.4 summarizes the characteristics of each technology used for biogas upgrading. Pellegrini et al. [20] illustrated that the type of feedstock influences the cost related to biogas production (i.e., associated cost to the digester) not the cost of upgrading as the concentration of CO_2 does not differ significantly from different feedstock.

In comparison with other upgrading technologies, cryogenic biogas upgrading not only is energy intensive but also demands high investment and operating cost. Nonetheless, the potential synergy between cryogenic and subsequent liquefaction process in LBM production provides some advantages compared to other technologies. This is investigated as part of the present thesis.

The majority of previous studies in the context of utilization of biogas have been focused on applications for gas grid injection or compressed synthetic gas production with concentration of methane in the range of 90-98 % depending on specified standards in different countries. However, the LBM production requires to meet extremely restricted CO_2 content up to 50 ppm in the biomethane. The present thesis determines the influence of the restricted specifications on optimal operating condition of the LBM production plant.

Among all biogas upgrading technologies, chemical absorption using amines and cryogenic separation are capable to produce biomethane with purity sufficient for LBM production without considering additional polishing steps. Therefore, these two technologies are chosen for advance investigation in terms of process development and optimization in this thesis.

Table 2.3: Advantages and disadvantages of different biogas upgrading technologies [17]

Technology	Principle mechanism	Advantages	Challenges	Integration with liquefaction
Water scrubbing (WS)	Solubility difference of components in water	-No need for precleaning	-Excess fresh water demand	Polishing requirement
Physical absorption (PA)	Solubility difference of components in organic solvents	-Simplicity	-Chemicals requirement	Polishing requirement
Chemical absorption (CA)	Chemical reactions between acid gases and amine solutions	-Cost effective	-Excess heat demand for regeneration	Compatible with liquefaction
Pressure swing adsorption (PSA)	Adsorbing acid gases at surface of adsorbent materials at elevated pressure	-High biomethane purity -Low methane loss -Dry process -Chemical-free	-Pre-treatment requirement -High investment -Complexity -High CH ₄ loss	Compatible with liquefaction
Membranes (M)	Selective permeation of components through permeable membranes induced by pressure differences on sides	-Dry process -Chemical-free -Compactness	-Pre-treatment requirement -High investment -High CH ₄ loss	Polishing requirement
Cryogenic separation (CS)	Low-temperature distillation or sublimation/desublimation of CO ₂ on surfaces	-Highest methane purity -Synergy between upgrading and liquefaction	-Energy intensive -Pre-treatment requirement -CO ₂ freezing	Compatible with liquefaction

Table 2.4: Characteristics of different biogas upgrading technologies [17]

Technology	CH ₄ purity (vol%)	CH ₄ loss (%)	Pres. (bar)	Temp. (°C)	Energy use (kWh/Nm ³)	Process efficiency (%)
WS	93–98	> 2	4–10	n.a.	0.2–0.45	92.7–96.0
PA	95–98	< 4	4–8	55–80	0.2–0.3	90.0–95.5
CA	97–99	< 0.5	10–80	70–110	0.05–0.18	88.5–97.7
PSA	95–99	< 3	3–10	n.a.	0.23–0.3	84.8–93.6
M	80–98	< 5	4–6	n.a.	0.18–0.35	82.4–98.0
CS	95–99	< 0.1	40–80	-90 – -100	0.45–0.76	84.9–96.7

2.5.3 State-of-the-art liquefaction of biomethane

Liquefaction of biomethane can be done either through conventional liquefied natural gas (LNG) processes or by combining small liquefaction plant with a cryogenic (or low-temperature) upgrading technologies. However, employing the combination of low-temperature biogas upgrading and small liquefaction for LBM production has not been realized in the practice. Further, the pressure letdown as one way for liquefaction is not a feasible option for biomethane liquefaction due to the low pressure of biomethane.

The conventional LNG processes are often considered in two groups: N₂ expanders and mixed refrigerant (MR)-based processes. In the N₂ expander refrigeration cycle, N₂ as refrigerant is maintained in the gaseous state throughout the liquefaction process. The N₂ expander refrigeration cycles are known for their simplicity and high energy use.

Different MR-based refrigeration cycles can be classified in accordance with the involved refrigerants and the number of refrigeration loops. In this context, single mixed refrigerant (SMR) refers to liquefaction process involving one refrigeration loop employing a mixture of nitrogen, methane, and other heavier hydrocarbons, whereas dual mixed refrigerant (DMR) involves two refrigeration loops with two different mixed refrigerants.

Propane-precooled mixed refrigerant (C3MR) combines the SMR with a separate precooling loop using pure propane as refrigerant. Cascade processes employ multiple refrigeration cycles for precooling, liquefaction and subcooling using different MRs. Table 2.5 provides an overview regarding available refrigeration cycles that can be applied for biomethane liquefaction.

The selection of refrigeration cycle depends on several factors such as capacity required for liquefaction, energy efficiency, environmental concerns and complexity. Further description and analysis for small- and large-scale liquefaction processes can be found in the literature [21, 22].

In comparison with N₂ expander refrigeration cycles, the MR-based refrigeration cycles give higher energy efficiency due to providing a better match to reduce the

Table 2.5: Available refrigeration cycles for biomethane liquefaction [17]

Biomethane liquefaction technology	Capacity (tonne _{LBM} /day)	Specific energy (kWh/kg _{LBM})
N ₂ single expander	25–60	0.78
N ₂ single expander with three intercooled compression stages	20–200	0.6–1.1
N ₂ dual expander	30–500	0.35
Single Mixed Refrigerant (SMR)	10–25	0.70
Pre-Cooled Mixed Refrigeration	40–6000	0.48
Combined process for biogas upgrading and liquefaction (cascade refrigeration)	0.6–18.5	1.4–1.77
Linde cycle with pre-cooling	12–16	0.75–0.84

gap between hot and cold composite curves in heat exchangers. However, there are several challenges with respect to MR-based refrigeration cycles including high capital investment cost, complexity, safety and environmental issues due to the use of flammable hydrocarbons.

In general, small-scale liquefaction processes and off-shore LNG processes can be considered for LBM production as the capacity of producing biomethane is much smaller than typical NG production. However, Concerns regarding small-scale liquefaction processes are related to energy efficiency and high operating cost. In applications such as LBM production, the N₂ expander refrigeration cycles are the most suitable and feasible options because of their small investment cost and easy implementation of the process. The SMR can also be a good candidate to be used for liquefying the biomethane owing to its compactness and simplicity.

Recently, Haider et al. [23] presented an integrated biogas upgrading and biomethane liquefaction process, where they employed nitrogen-methane (N₂-CH₂) expansion liquefaction process for LBM production. They indicated that the LBM production through conventional biogas upgrading technologies followed by liquefaction process could provide feasible solution for long-distance transportation. This indication is investigated in details considering alternative approaches to optimize the processes in this thesis.

2.5.4 Potentials and barriers

Currently, the share of biogas in the transport sector is very limited (< 1 %), but it is growing steadily [11]. Despite the significant potential of biogas production worldwide due to abundant biomass, the use of biogas for transport is mainly considered in Europe [1]. Fig. 2.6 illustrates the biomethane production and biomethane use in countries with most biomethane production worldwide.

In 2013, Germany produced the largest amount of biomethane, while only 1.4 % of produced biomethane was used in transport sector. Countries with lower biomethane

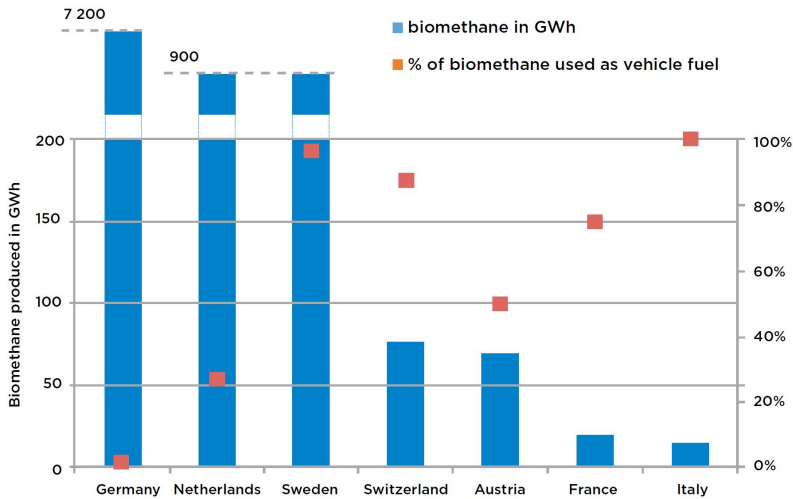


Figure 2.6: Biomethane production and the share of biomethane for transportation in countries with most biomethane production worldwide in 2013 (The figure is copied with granted permission from [11])

production such as Sweden, Switzerland and Italy have a greater focus on the use of biomethane as fuel. Estimation of actual accessible feedstock for production of biogas suited for transport is a challenging task due to lack of data and uncertainties. Nonetheless, there is a substantial potential for biogas production based on energy crops and animal by-products worldwide in the range of 1500-2000 PJ/year within each continent [11].

In addition to the potential capacity of biogas production, existing gas infrastructures and well-established knowledge regarding the transportation of biogas in the gaseous or liquid form provides a unique advantage for the biogas-as-fuel market in near future worldwide. However, the main obstacles for developing the use of biogas as a transportation fuel can be identified as lack of centralized biomass availability to increase the production capacity, relatively high price compared to fossil fuels, lack of highly efficient heavy-duty vehicles, lack of standards for biogas-based fuels, and short-lasting regulatory frameworks [11].

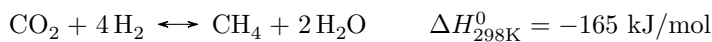
Specifically concerning LBM production, the supply chain of LBM is simpler than conventional NG. However, the availability of biogas at a lower pressure (i.e., near atmospheric pressure) compared to conventional NG (i.e., in the pressure range of 40-80 bar) makes the sustainable scale-up of LBM production a challenging issue. This is mainly due to additional energy requirements to produce feasible and economical transportation fuel out of biogas. Moreover, most technological advances concerning the design of energy- or cost-efficient LBM production plants are in the research or development stage, which will take time to be implemented in real-life applications. Within this context, this thesis evaluates different process

concepts for the LBM production.

2.6 Power-to-gas for liquefied biomethane production

The PtG process is proposed to connect surplus renewable electricity to the gas grid. The central technology used in PtG is H₂ production through electrolysis. The produced H₂ can either be used as a gaseous fuel or be further converted to methane by the methanation process when external CO/CO₂ sources are available [24]. The resulting methane from PtG, usually known as substitute or synthetic natural gas (SNG), can be used in the well-established natural gas infrastructures such as gas grid networks, storage tanks or fuelling stations [25]. It should be mentioned that often instead of PtG, the notion of Power-to-Methane (PtM) is used in the literature addressing methane as the final product.

Due to lack of infrastructure for H₂ storage and distribution and limited volumetric energy density of H₂, the conversion of H₂ to methane in PtG has gained much attention [26]. In the PtG applications, the conversion of CO₂ and H₂ into the CH₄, known as CO₂ methanation, takes place through a highly exothermic reaction, which was first proposed by Sabatier and Senderens in 1902 [27]:



One of advantages of PtG applications is the use of CO₂ as a raw material, which then the CO₂ captured from a power generation plant, a biomass plant (in the form of biogas) or other industrial plants is no longer a waste product. However, the main disadvantages with respect to PtG processes are the relatively low efficiency and high investment cost.

In principle, an increase in the chemical energy density from H₂ to CH₄ is possible through the CO₂ methanation. At the standard conditions, approximately 17 % of potential chemical energy is released as heat of reaction limiting the efficiency of the conversion [26]. Due to multiple conversion steps within PtG the overall efficiency drops to between 30-40 %, which is in the range of conventional power plant efficiencies [28]. A brief overview on the state-of-the-art of the PtM elements including electrolysis and methanation is provided in the following subsections.

2.6.1 State-of-the-art water electrolysis

In PtG applications, the presence and production of H₂ is essential. Currently, H₂ is produced from conversion of various feedstocks such as hydrocarbons, biomass and water (see Fig. 2.7). It should be noted that the H₂ production through electrolysis is environmentally friendly as long as the required electricity for the water electrolysis has originated from renewable energy. The produced H₂ from electrolysis is often known as “green H₂” [29].

Currently, the majority of H_2 production is based on fossil fuels employing steam reforming processes because of relatively high price of electricity used for the water electrolysis [30]. Recent advancements concerning the steady increase in electrical renewable energy production has made the water electrolysis process an interesting alternative for H_2 production in order to tackle challenges like production cost and air pollution reduction [29].

The electricity and water requirements for an ideal water electrolysis to produce 1 kilogram of H_2 at 25 °C and 1 atmospheric pressure are 39 kWh and 8.9 liters, respectively [31]. However, currently available water electrolyzers in the market have an efficiency between 62 and 90 %, which corresponds to 62.9 – 43.3 kWh/kg H_2 [8].

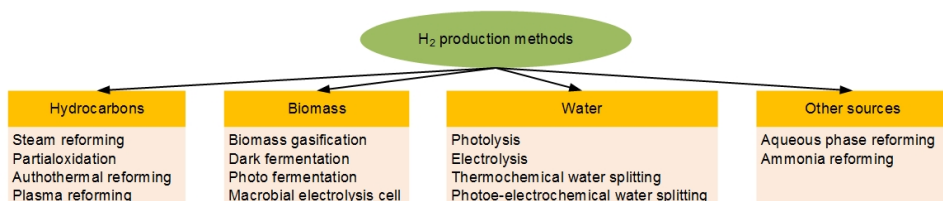
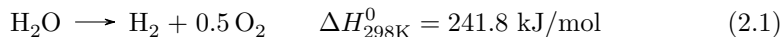


Figure 2.7: Possible hydrogen sources and production methods

H_2 is produced through electrolysis via an endothermic electrochemical reaction as follows:



As it can be seen from equation 2.1, according to Le Chatelier's principle, the conversion from the water molecules towards the products (i.e., H_2 molecules) improves at higher temperature and lower pressure [32].

Water electrolysis can be classified based on their operating temperature. The low temperature class (operational temperature lower than 100 °C) includes Alkaline Electrolyzer (AEL) and Proton Exchange Membrane Electrolyzer (PEMEL), whereas Solid Oxide Electrolyzer (SOEL) is classified as high temperature (operating at temperatures ranging 600-900 °C) [33].

Characteristics of different water electrolysis is summarized in Table 2.6. Nowadays, the core of research with respect to the water electrolysis is to improve the efficiency of electrolyses focusing on alternative electrodes/electrolytes, finding good metal supports for electrodes and solid electrolytes to boost the cell conductivity and stability, consideration of novel configurations [34–36]. As this thesis does not consider the production H_2 in the process development, readers are encouraged to consider exclusive overview by Stonic et al. [37] for further information regarding the fundamental of electrolysis.

Table 2.6: Summary of characteristics of different water electrolyzers [38]

	AEL	PEMEL	SOEL
Maturity	Mature	Commercial	Development
Electrolyte	25–30 wt% KOH	Polymer membrane	ZrO ₂ & Y ₂ O ₃
Charge carrier	OH ⁻	H ⁺	O ²⁻
Temperature (°C)	60–90	50–80	650–900
Pressure (bar)	30	100	1
Voltage (V)	1.8–2.4	1.6–2.1	0.95–1.3
Efficiency (%)	62–82	67–82	80
Specific energy kWh/Nm ³ H ₂	3.8–4.8	4.4–5	2.5–3.5
Current density A · cm ⁻²	0.4	1–2.5	0.3–1.3
System lifetime (year)	20–30	10–20	n.a.
Advantages	-High reliability -Low cost -Long lifetime	-Dynamic operation -High current density -Short start-up	-High efficiency -Co-electrolysis possibility -Possibility of heat integration
Disadvantages	-Low current density -High maintenance cost -Large cell area	-Expensive materials -Short lifetime	-Heat management -High investment cost

2.6.2 State-of-the-art methanation

There are two major pathways to carry out the CO₂ methanation process; biological methanation (biomethanation) and chemical methanation (catalytic methanation) [39–41]. In biomethanation, the CO₂ and H₂ are anaerobically metabolised via methanogenic archaea microorganisms to produce CH₄ and excess energy for other microorganisms' survival. Although the biological metabolism brings positive features such as operation at moderate temperature (30–60 °C) and atmospheric pressure, the biomethanation process has been challenged for its slow kinetics and poor mass transfer. This limits its application for large-scale CO₂ methanation [42].

Catalytic methanation has been in use for many years [43]. The conversion of CO₂ and H₂ is facilitated in the presence of a metal catalyst. Practically, the catalytic methanation process takes place at elevated temperatures (200–550 °C) and in pressure range between 1–40 bar [39]. Thanks to the operational conditions, the

catalytic methanation has faster kinetics and provides a higher conversion efficiency. Besides, the produced heat at elevated temperature is considered a valuable co-product that can be utilized in other processes [44].

Thermodynamics of the CO₂ methanation

Since the Sabatier reaction is exothermic and the number of moles (volume size) in the product reduces, operating at lower temperature and higher pressure is thermodynamically favourable according to Le Chatelier's principles [45]. In practice, the H₂/CO₂ ratio would increase/decrease depending on the selection of the limiting component. By manipulation of the H₂/CO₂ ratio, the concentration of the limiting component is controlled in the product side [45]. If the H₂/CO₂ ratio at the inlet is lower than 4, H₂ is the limiting component and excess CO₂ is expected to leave the reactor in product gas. Although a greater ratio than stoichiometry would increase the CO₂ conversion (since CO₂ is the limiting component), the additional valuable H₂ leaves the reactor without participating in the reaction in the product gas mixture.

Catalysts

CO₂ methanation is an eight-electron exchange reaction from fully oxidized carbon (-4) to methane (+4) [26]. Even though the reaction is thermodynamically favourable because of it being exothermic, the reduction of carbon has very slow kinetics. Therefore, the presence of an efficient and effective catalyst is essential to improve the reaction rate. Substantial research has been conducted to explore new materials for catalytic methanation [46]. Furthermore, the catalyst must have good thermal consistency for a wide range of temperatures, and good resistance to the coke formation [47].

Many parameters are involved to select an appropriate catalyst for CO₂ methanation such as activity, selectivity towards the CH₄ and the price for the catalyst. However, Mills and Steffgen [48], suggested the following orders for the available metal catalysts for the methanation in terms of activity and selectivity:

Activity: Ru > Fe > Ni > Co > Mo

Selectivity: Ni > Co > Fe > Ru

The most commonly used catalyst in industrial applications for catalytic methanation is Nickel (Ni) because of its highest selectivity towards CH₄ and being relatively cheap. Operating methanation at elevated temperatures exceeding 550 °C results in a runaway situation causing the deactivation of the catalyst and reactor damage [49].

Reactors

Knowing the fact that the methanation process has been used in industries like ammonia production processes for many years has not stopped many researchers to explore novel reactor designs with respect to improvement in CO₂ conversion, cost efficiency and dynamic behaviour of methanation reactor in response to the load fluctuations from renewable energy sources.

Depending on the catalyst material and operating conditions of the methanation reactor, consideration of heat management to remove the heat of reaction from the reactor is essential. Exceeding the temperature in thermal runaway (i.e., existence of the hotspots within the reactor length) reduces the functionality of catalyst, thereby limits the lifetime of the reactor.

The most developed type of methanation reactors are two-phase reactor concepts, where the metal catalysts form the solid bed interacting with the reacting gases. In this group, fixed-bed reactors have been on the market for many years, while the other types of reactors in this group, known as structured reactors (e.g., two-phase fluidized bed, microchannel, membrane and sorption-enhanced reactors) are mostly at the demonstration or research level [26]. Providing uniform and long contact time between the gas phase and the catalyst particles has made the fixed-bed reactors very popular in industrial applications [50].

In general, the fixed-bed reactor can operate under adiabatic or polytropic conditions. The main difference between different operation modes is the temperature profile within the reactors. In the adiabatic version, a series of fixed-bed reactors are linked to each other, where intermediate intercooling is placed between the reactors in order to cool down the inlet stream into the next reactor to the temperature that is desired for high CO₂ conversion. Therefore, the heat of reaction from the reactor is removed externally through intercoolers. In contrary, the heat of reaction from the polytropic reactor (known also as cooled fixed-bed reactors) is removed internally by a cooling medium [27]. In this system, the reacting gas goes through tube-bundles with relatively small diameter, which is mounted within large shells filled by coolant such as thermal oil, molten salt or water [26].

In comparison to adiabatic reactors, the heat management and temperature control in the cooled fixed-bed reactors are more efficient, thereby the number of required reactors to obtain a certain amount of CO₂ conversion reduces. However, the design of such systems is more complex and relatively expensive [43].

Besides the development of the reactor type itself, there are other approaches for methanation process design in order to optimize the number of required reactors or the heat management. For instance, partial feeding of reacting gases to the reactor, recycling a portion of products, diluting the reacting gas with inert gases or addition of inert particles to the catalyst bed are possibilities to improve the performance of the methanation reactor. Some of these approaches are investigated in this thesis to provide an insight for methanation reactor design suitable for integrating with LBM production plants.

The large-scale of PtG projects (i.e., capacity greater than 1 MW) focusing on the CH₄ production through the catalytic methanation are summarized in Table 2.7. As can be observed in Table 2.7, the integration of methanation process with LBM production plant has not been fully realized, therefore this thesis aims to develop conceptual process for a comprehensive analysis of integrated scheme of methanation and LBM production.

Table 2.7: Large-scale PtG projects focusing on the catalytic methanation [38, 51]

Project name	Country	Year of commission	Capacity (MW)	Electrolysis	CO ₂ source	Methanation reactor	Final application
STOREGO	DE	2013	1	AEL	Bioethanol plant	Fixed-bed reactor	NG grid injection
STOREGO	CH	2016	0.7	PEMEL	Wastewater treatment plant	Biological treatment	NG grid injection
STOREGO	IT	2016	0.2	AEL	Captured from atmosphere	Modular structured reactor	Liquefied NG
Audi e-gas	DE	2013	6	AEL	Biogas plant	Fixed-bed reactor	NG grid injection & pressurized CH ₄
Jupiter 1000 hybrid	FR	2018	1	AEL & PEMEL	Captured from industries	Structured micro-channels	NG grid injection
	DE	2023	100	AEL & PEMEL	Captured from industries	n.a.	NG grid injection
PEGASUS	IT	projected	n.a.	n.a.	Biogas plant	n.a.	NG grid injection
MethFuel	DE	2020	1	PEMEL & SOMEL	Captured from industries	Three-phases reactor	NG grid injection
MeGa-stoRE	DK	projected	10	AEL	Captured from industries	Fixed-bed reactor	NG grid injection

This chapter provides an outline regarding methods used in Articles I–VI. The general description of the studied processes and the process flow diagrams are given here. Further, different approaches to simulate and evaluate the processes are presented briefly. More specific descriptions can be found in appended articles.

3.1 Process description and modeling

In this thesis, three main processes (i.e., biogas upgrading, methanation, and liquefaction processes) are studied using process simulation software. For the biogas upgrading, the models include chemical absorption and cryogenic gas separation technologies. The reason to consider these two technologies is their ability to meet the desired level of CO₂ removal for LBM production without additional polishing steps. A series of fixed-bed reactors with intermediate water removal is considered for the methanation process. The liquefaction process is modeled using different refrigeration cycles. Here, brief descriptions of the employed processes are given.

Chemical absorption biogas upgrading

Fig. 3.1 illustrates a schematic of a chemical absorption biogas upgrading process. This process model is used in Articles I–VI. The process employs MDEA as an amine solution. In addition to compression units and distillation columns for CO₂ capture and amine regeneration, the process considers auxiliary dehydration units to remove water from the gas streams. The compression units consist of multiple stages with intermediate cooling water heat exchangers. The dehydration units are considered using black-box modeling for tri-ethylene-glycol (TEG) absorber/regeneration columns to calculate the energy requirement in the dehydration units.

Cryogenic gas separation

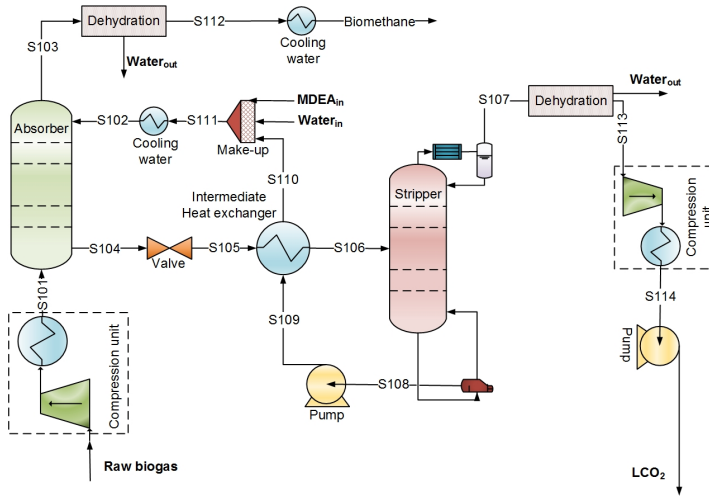


Figure 3.1: Schematic of a chemical absorption biogas upgrading process

The process model for cryogenic gas separation employs an integrated scheme that combines the upgrading and liquefaction processes. Fig. 3.2 illustrates a schematic of an integrated cryogenic biogas upgrading and liquefaction process. This process model is employed in Article I. The cryogenic upgrading consists of two distillation columns operating at different pressure levels. Cooling for condensers and the inlet stream to the first distillation column is provided by the liquefaction process. The heat duties are delivered to reboilers in the high- and low-pressure distillation columns through cooling-water heat exchangers.

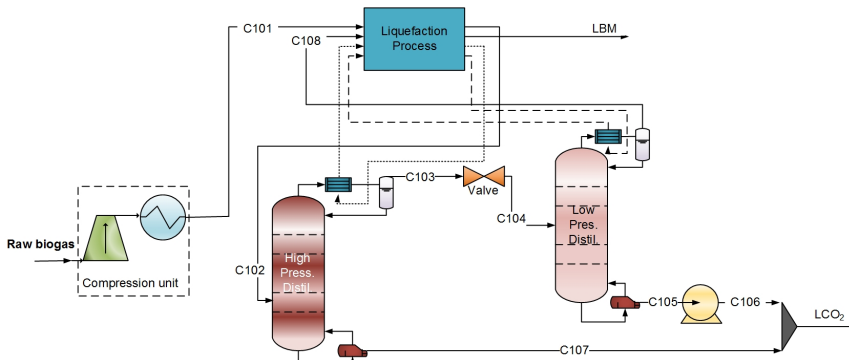


Figure 3.2: Schematic of a chemical absorption biogas upgrading process

Methanation

A step-wise approach is considered to develop the methanation process in this thesis. First, the Gibbs reactor available in the process simulation software (i.e., Aspen

HYSYS[®]) provides the principal understandings of the methanation process. This type of reactor considers equilibrium conditions, and it is employed in Article IV to investigate the effect of operating conditions on the overall performance of the methanation process. Later, a detailed model is developed in MATLAB for a fixed-bed reactor operating under isothermal conditions considering the kinetics of the methanation process. The developed model is used in Article V to study the effect of water removal on the CO₂ conversion improvement. Finally, an advanced and rigorous model is developed for the cooled-wall fixed-bed reactor in Article VI. The advanced model considers a series of multi-tubular methanation reactors where the water produced is removed between the reactors by condensation to ensure the maximum CO₂ conversion within the process.

A schematic of the final methanation process is given in Fig. 3.3. The reactor model accommodates the temperature profiles within the reactor using a pseudo-homogeneous plug flow model. In order to account for mass and heat transfer limitations between the gas streams and the solid phase (catalyst), a temperature-dependent effectiveness factor is considered in the model. In this thesis, the kinetics of the methanation process is based on only the Sabatier reaction. The assumption is because of not including CO in the feed gas. Further, the preliminary simulations regarding the CO₂ and biogas methanation illustrated that other side reactions such as CO methanation and carbon formation were negligible within the temperature and pressure ranges studied in this thesis.

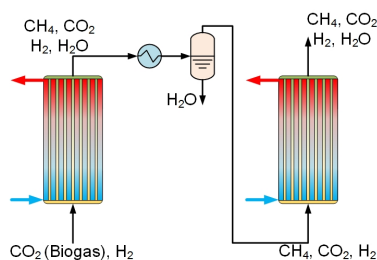


Figure 3.3: A schematic of methanation process

Liquefaction

Three refrigeration cycles are modeled for the liquefaction process; N₂ single expander cycle, N₂ dual expander cycle, and single mixed refrigerant cycle. The reasons to select these cycles are due to their relatively simple design and applicability for the liquefaction capacity required in typical biogas production plants. The N₂ single expander cycle is employed in Articles I, II, III and VI, while the other refrigeration cycles are only considered in Article III.

In principle, the cooling duty required in each refrigeration cycle is provided through changes in the pressure level of the refrigerant using compressors and expanders. As part of the liquefaction cycle, an additional expander is employed to bring the

pressure of the liquefied biomethane to atmospheric pressure. The working fluid within the single and the dual expander refrigeration cycles is N_2 , while a mixture of hydrocarbons (i.e., CH_4 , C_2H_6 , C_3H_8 , and C_4H_{10}) and N_2 is used as working fluid in the mixed refrigerant cycles.

3.1.1 Simulation tools

All above-mentioned biogas upgrading and liquefaction processes are simulated using Aspen HYSYS[®] V9.0 (Aspen Technology Inc.). Different thermodynamic models are used to calculate the properties of the different mixtures. For amine-based CO_2 capture, the "Acid gas – chemical solvent" package recommended by Aspen HYSYS[®] is considered. The Soave-Redlich-Kwong (SRK) equation of state is employed for other operating units within the processes (such as compressors, expanders, heat exchangers and mixers) and the refrigeration cycles. The exception is for Article VI, where the "Refprop" package from the Aspen properties is considered for the compression units, the refrigeration cycle and the methanation reactors. The selection is based on the presence of H_2 in the mixture within the liquefaction process, which requires an accurate thermodynamic model for flash calculations. The methanation reactor is modelled in MATLAB and imported to the Aspen HYSYS[®] model using MATLAB CAPE-OPEN unit operation [52].

3.1.2 Feed and product

A biogas mixture of 60 mol% CH_4 , 39.9 mol% CO_2 , and 0.1 mol% H_2S , representing a typical biogas composition, with a molar flow rate of 1000 kmol/h at 35 °C and 1 atm is considered as feed to the LBM production plant in Articles I–III. In Articles IV–VI, the inlet biogas condition is adapted to a large biogas plant located at Skogn in Norway with a capacity of around 25 million Nm^3 /year biogas production, which is equivalent to approximately 200 kmol/h of raw biogas, with a composition of 60 mol% CH_4 and 40 mol% CO_2 at 35 °C and 1 atm. In articles containing the methanation process, it is assumed that H_2 is fed to the process from an alkaline-type electrolyzer, with similar temperature and pressure as the raw biogas.

The desired product from the LBM production plant is liquefied biomethane with a CO_2 content below 50 ppm at atmospheric pressure. Further, in Articles I–III, liquefied CO_2 at 35 °C and 110 bar is considered a by-product of the LBM production plant for CO_2 pipeline transportation.

3.1.3 Assumptions

With respect to development of process flowsheets within Aspen HYSYS[®], several assumptions are made. First, isentropic efficiency of compressors and expanders is assumed to be 80 %, while an isentropic efficiency of 85 % is assumed for the pumps. Second, the inlet and outlet temperature of cooling water used in the condensers and intermediate heat exchangers are 20 and 25 °C, respectively. Third, saturated steam at 5 bar is assumed as a heat source for the reboiler of the stripper column

and the heater, and saturated steam at 40 bar is considered as a heat sink for the methanation reactors. Finally, pressure drops in heat exchangers and columns are not considered.

With respect to the methanation reactor, it is assumed that the reactor is multi-tubular. Further, the velocity field within the methanation reactor is modeled through the plug flow model. Pressure drop along the reactor length is neglected as primary simulation tests showed that the pressure drop (calculated from the Ergun equation) was on a scale of 0.1 kPa for the studied dimensions and flow rates in this thesis.

3.2 Process evaluation

The assessment of the studied processes is based on thermodynamic and economic performance. The thermodynamic performance of the processes is evaluated with respect to energy efficiency and exergy efficiency. For the economic assessment, total annualized cost associated with each process is considered.

In Article I, the studied configurations are compared for overall energy efficiency and methane utilization. The overall energy efficiency is defined as the ratio of all useful energy to all required energy to produce the LBM. Further, methane utilization is defined as the amount of methane in the raw biogas that converts to LBM. In order to calculate the methane utilization, the work and the heat requirements are converted into corresponding amounts of methane needed to provide such energy demands through conventional engineering processes.

Due to limitations of energy analysis, such as considering heat and work with the same quality, exergy analysis is used to assess and optimize the thermodynamic performance of the proposed processes in Articles II–VI. Further, the exergy analysis highlights exergy loss (irreversibility) locations. For the exergy analysis, the methodology described by Kotas [53] is employed.

Cost analysis is considered in Articles III and VI, where the feasibility of proposed configurations are of interests. In order to perform the cost analysis, a detailed model considering both investment and operating costs is developed for all operation units within the process flowsheet. The cost estimation model is based on the module costing technique described by Turton et al. [54].

3.3 Process optimization

The optimization in Article I is performed through a primary search method. For the sake of providing better solutions for optimization, the Hyprotech SQP optimizer in Aspen HYSYS® V9.0 is used in other articles. The optimization objective in Article I is to maximize the energy efficiency, while minimizing the exergy supply into the processes is considered as optimization objective in Articles II and III. In Article III, minimizing the total annualized cost of the LBM production plant

is also considered. Several objective function formulations are examined in order to determine alternative approaches to optimize the conventional LBM production plant using amine-based biogas upgrading in Articles II and III. In Article VI, the optimization objective is to maximize the LBM production.

The design variables for the upgrading process include pressure levels of absorber and stripper columns, the amine flow rate and concentration, and rich- and lean-amine temperatures. In the methanation process, the design variables are inlet temperatures, coolant temperatures, and number of tubes of the reactors. With respect to the liquefaction process, low- and high-pressure levels, refrigerant flow rates, and intermediate temperatures are considered in the optimization.

In addition to sets of equality constraints (mass and energy balances, and correlations to compute physicochemical properties), which Aspen HYSYS[®] model handles, there are inequality constraints to satisfy practical limits in the process design. The most important specification is for the CO₂ content in the produced biomethane from the upgrading process (i.e., below 50 ppm) in order to prevent CO₂ freezing in the liquefaction process. Further, a minimum temperature approach of 10 and 2 °C is assumed for cooling water and low-temperature heat exchangers, respectively, to account for the capital cost of the heat exchangers.

For the amine-based biogas upgrading, a maximum temperature of 126.7 °C is considered for the reboiler temperature of the stripper column to avoid degradation of the amine. Regarding the methanation reactors, a maximum temperature of 550 °C and a maximum velocity within the reactors 1 m/s were considered in order to avoid deactivation of the catalyst and significant pressure drops within the reactor.

Table 3.1 gives an overview of the methods that are used in articles.

Table 3.1: Overview on the employed methods in each article

Articles		I	II	III	IV	V	VI
Involved processes	Absorption upgrading	*	*	*			*
	Cryogenic upgrading	*					
	Methanation				*	*	*
	Liquefaction	*	*	*			*
Simulation tool	HYSYS	*	*	*	*		*
	MATLAB					*	*
Process evaluation	Energy analysis	*		*			
	Exergy analysis		*	*	*	*	*
	Cost analysis			*			*
Optimization		*	*	*			*

Summary of articles

The present chapter provides a summary of each article given in this thesis. As each article's detailed results and discussion are presented in the appended articles, the summaries here aim to highlight the main contribution of the articles and grant a short outline of the major findings and discussion from each article.

4.1 Article I

This article aimed to determine the effect of integrating upgrading and liquefaction processes on the overall energy efficiency of the LBM production plant. In order to evaluate the synergy between the processes, two different configurations were considered. The first configuration represented a conventional LBM production plant with amine-based biogas upgrading followed by a nitrogen single expander refrigeration cycle. In the second configuration, a cryogenic gas separation system using two distillation columns was integrated with a nitrogen single expander refrigeration cycle.

In this article, rigorous process models including all unit operations were developed for both configurations in order to provide a fair comparison for the overall performance of the LBM production plant. Further, the first part of this article was dedicated to a comprehensive overview of available technologies that could be employed for biogas upgrading.

The results illustrated that the specific energy (i.e., a combination of work and heat) required for the LBM production plant decreased by increasing the CH_4 content in the biogas mixture, while it was independent of the H_2S concentration. It was observed that the influence of the CH_4 content was larger in the conventional LBM production plant.

For the conventional and integrated configurations, energy analysis for a biogas mixture with 60 mol% CH₄ showed an overall energy efficiency of 80.1 % and 87.2 %, respectively. Here, the overall energy efficiency was defined as the ratio of all useful energy (i.e., lower heating value (LHV) of LBM and produced work and heat) to all required energy (i.e., LHV of raw biogas and supplied work and heat). Regarding specific energy requirements, the conventional configuration needed 1.54 kWh/kg LBM of work and 1.81 kWh/kg LBM of heat, while the integrated configuration just required 2.07 kWh/kg LBM of work.

The results demonstrated that 62.8 % and 72.7 % of the available methane in the raw biogas could be converted to LBM in conventional and integrated configurations, respectively, when considering a self-sustained process design (i.e., converting the available methane in biogas mixture through conventional engineering processes to provide energy requirements within the process).

Although preliminary optimization was applied before providing the energy analysis in this article, a robust optimization approach should be employed to optimize the configurations due to the number of involved design variables, particularly for the upgrading process. Further, as cryogenic gas separation for biogas upgrading is associated with challenges regarding CO₂ ice-formation, limiting its application in practice even with better thermodynamic performance. Hence, the rest of this research study focused on optimizing the performance of the conventional LBM production plants using amine-based biogas upgrading.

4.2 Article II

This article focused on minimizing the exergy supply to the conventional LBM production plant. A detailed model was provided for the conventional LBM production plant consisting of an amine-based biogas upgrading and a liquefaction process. The approach investigated in this article evaluated the effect of dependency between the upgrading process and the liquefaction process on the optimization by comparing sequential and simultaneous optimization. In the simultaneous optimization approach, all the variables of the overall LBM production plant were considered at the same time, while in the sequential optimization approach, first the upgrading process was optimized and then the liquefaction process.

Different objective functions were tested for the sequential optimization approach to accommodate the link between the two processes. Here, objective functions considered the exergy supply in the upgrading process combined with either heat removal in the liquefaction process or the exergy of the heat removed in the liquefaction process.

It was indicated that the interaction between the upgrading and the liquefaction process was limited to only the pressure level of produced biomethane from the upgrading process. The results illustrated that similar solutions would be obtained from optimizing the LBM production plant through sequential and simultaneous

optimization. The results showed that the best solution obtained from different objective function formulations used in the sequential optimization were close to each other. Nonetheless, the best solution obtained from the sequential optimization was when the exergy demand in the upgrading and the liquefaction was considered in the objective function formulation.

In addition to proposing the optimization approach for the conventional LBM production plant, challenges regarding simulation convergence, particularly for the upgrading process, were highlighted.

4.3 Article III

This article was a continuation and further development of the optimization approach presented in Article II. Here, a sequential optimization approach was employed to optimize the conventional LBM production plant in terms of both thermodynamic and economic performance. This article focused on optimizing the upgrading process since this process was found more complex than the liquefaction, while also facing challenges regarding simulation convergence and accounting for the majority of the exergy demand in the plant.

The major aim of this article was to provide a comparison between thermodynamic optima and economic optima obtained from optimizing the upgrading process and suggestions for alternative objective function formulation for optimization of the upgrading process. Because providing a detailed economic evaluation, particularly for the upgrading process usually involves many uncertainties. The alternative objective functions for the upgrading process were formulated in accordance with energy use, energy quality, energy cost and total annualized cost. For the liquefaction process, the optimization objective was to minimize the net work required.

With respect to the convergence issues for the upgrading process simulation addressed in Article II, it was found that determining appropriate specifications for the stripper column model and allocating convergence error tolerance in the range between 10^{-6} and 10^{-8} for all unit operations, particularly for columns and recycle units, were essential. Preliminary simulation tests showed that one variable from the top and one variable from the bottom of the stripper should be considered for stripper column specifications. In this work, condenser temperature and lean CO_2 loading were found suitable for the amine-based biogas upgrading process since their values were known by the process specifications.

The mentioned modifications allowed to perform the optimization with an increased number of design variables and wider variable bounds without experiencing convergence errors. Further, it was observed that a smooth transition at each iteration during the optimization assisted in avoiding the convergence issues. Therefore, adjusting the optimizer setup with smaller step size and error tolerance appeared to be necessary to achieve smooth transitions.

From a thermodynamic point of view, the results illustrated that optimizing the

upgrading process considering the energy quality (i.e., exergy-based formulation) would shift the solution towards more heat and less work in comparison with the solution obtained from considering energy use within the upgrading process (i.e., energy-based formulation). This was because the energy quality of the work is higher than that of the heat. Further, it was shown that the objective function formulation based on energy use or energy cost would lead to similar solutions.

From an economic point of view, the results illustrated that the total annualized cost for the upgrading process could be reduced by decreasing the investment cost. This was mainly due to the fact that the investment cost for the units operating at high pressures was dominant (i.e., the investment cost of these units were sensitive to the pressure level). Therefore, solutions with a lower operating pressure resulted in a reduction in the total annualized cost. A similar solution was obtained from the exergy-based formulation. It was indicated that using the exergy-based formulation for optimizing the upgrading process could be a good alternative to obtain both the highest thermodynamic and economic performance as this process was forced to operate at high pressures to meet the stringent requirements regarding CO₂ content in the biomethane. The exergy-based formulation could find the solution that considers requirements concerning pressure level by adapting work and heat supplied to the process.

When considering the overall LBM production plant (i.e., upgrading and liquefaction), the results indicated that the total exergy demand would be approximately equal for all of the employed objective function formulations for the upgrading process. This is because the higher exergy demand within the upgrading process obtained from some of the formulations would be compensated by savings in the required exergy for the liquefaction process. Further, the results illustrated that the total exergy supply to the overall LBM production plant could reduce significantly by choosing an appropriate refrigeration cycle. Regarding the selection of refrigeration cycle for LBM production, it was shown that a single mixed refrigerant cycle required the lowest net work due to providing smaller temperature differences within heat exchangers compared to single and dual nitrogen cycles.

In addition to optimization, a comprehensive sensitivity analysis was performed to investigate the influence of each design variable associated with the upgrading process on the final optimal solution. The results from the sensitivity analysis revealed that reducing the absorber pressure was followed by a reduction in the amine concentration and an increase in the amine flow rate. Nonetheless, at optimal solutions, the stripper pressure was found to be independent of changes in the amine concentration and the amine flow rate.

4.4 Article IV

In addition to investigation regarding conventional LBM production plants, potential improvement for LBM production has been considered in this thesis through

converting CO_2 in the biogas mixture to CH_4 , often referred to as CO_2 methanation.

This article aimed to provide thermodynamic insight into designing an energy-efficient methanation reactor. Developing the methanation reactor model was essential as the methanation reactor was intended to be integrated within the overall process model for the LBM production in the subsequent articles. This article examined potential heat integration and irreversibilities within a methanation reactor that operated under adiabatic or isothermal conditions.

Here, biogas was used as the feed gas to the reactor, and the methanation process was modeled through the Gibbs reactor model (i.e., operating under equilibrium conditions). In order to have the same CO_2 conversion as in the isothermal reactor, a series of adiabatic reactors with intermediate cooling was considered.

The results indicated that the heat integration potential due to the exergy of heat removed from the process increased when the methanation process operated under adiabatic conditions. The higher heat integration potential under adiabatic conditions was accompanied by a lower irreversibility rate within the process than for the isothermal conditions. It was also illustrated that the necessary number of adiabatic reactors reduced with increasing pressure and decreasing temperature.

It was highlighted in this article that a complete analysis regarding irreversibilities within the reactors and the heat available for integration required considering kinetic models rather than equilibrium models since the reactor performance was highly dependent upon the operating temperature.

4.5 Article V

This article focused on the effect of water removal on CO_2 conversion and irreversibilities within a methanation reactor. Similar to Article IV, this article aimed to provide thermodynamic insight into designing the methanation reactor. In this article, a fixed-bed reactor operating under isothermal condition was modeled in detail, considering kinetic models and an effectiveness factor for intra-particle mass and heat transport limitations.

Here, water was removed at one point along the reactor, meaning that the original reactor was divided into two reactors in series. With this assumption, the design of the methanation reactor considering moving the water removal point along the length of the reactor was investigated for different reactor lengths (i.e., representing reactor volume). The investigation considered pure CO_2 or a biogas mixture as feed for different operating temperatures and pressures. The required length to obtain equilibrium condition within the reactor was determined.

The results illustrated that for short reactors (i.e., the reactor length was shorter than the required length to reach equilibrium), the optimal water removal point

was located at the middle of the reactor in order to obtain maximum CO_2 conversion. Increasing the reactor length towards the equilibrium length would move the optimal water removal point closer to the end. Moreover, the optimal water removal point was independent of the operating temperature, but the presence of CH_4 in the feed gas (i.e., in biogas mixture) caused moving the optimal water removal point towards the end of the reactor.

For the irreversibilities within the reactor, it was illustrated that the optimal water removal point for CO_2 conversion in a short reactor would provide the largest irreversibility rate. Further, for reactor lengths close to the equilibrium length, it was observed that the improvement in the CO_2 conversion due to the water removal would accompany a minor irreversibility penalty.

Overall, it was indicated that the reactor length was an essential parameter to determine the optimal water removal point. Further, the results demonstrated that additional gains for the CO_2 conversion and the irreversibilities were insignificant when the equilibrium length was used. This suggested that when water removal is considered for a methanation reactor, the reactor length could be shorter than the equilibrium length.

This article also discussed different conceptual ideas for designing the methanation reactor, such as partial water removal and partial reactant feeding. It was highlighted that obtaining isothermal conditions is a challenging task in practice due to the highly exothermic nature of the methanation process. Therefore, extending the reactor model to non-isothermal operating modes was suggested. By employing this suggestion, more degrees of freedom to manipulate the driving forces within the reactor were expected to obtain an energy-efficient reactor design.

4.6 Article VI

This article merged the findings from Articles II–V in order to develop a conceptual process design for conventional LBM production with integrated methanation, attempting to produce a higher amount of LBM. The main aim of this article was to evaluate the feasibility of the proposed concept using exergy and cost analysis. For the methanation process, direct and indirect biogas methanation were considered. The main difference between the two methanation approaches was the feed gas composition; captured pure CO_2 and a biogas mixture was used in the indirect and direct methanation scheme, respectively.

The results confirmed that the methanation process could replace most of the biogas upgrading. Compared to the indirect methanation configuration, the direct methanation configuration provided several advantages; higher CO_2 conversion because of lower temperature in the catalytic bed, lower H_2 loss, less boil-off gas, smaller reactor volume and higher exergy efficiency.

The exergy analysis demonstrated that the production of highly purified biomethane constituted a major part of the total irreversibilities. Further, the available exergy

of heat within the indirect and direct methanation configurations provided great potential for additional energy integration to improve overall exergy efficiency.

The results indicated that the direct and indirect methanation configurations produced 52.2 and 47.1 % additional LBM, respectively, compared to the conventional LBM production configuration. Nonetheless, the overall exergy efficiency of the integrated configurations was lower than that of the conventional configuration. It was illustrated that considering the available exergy of heat and the exergy of the boil-off stream could significantly enhance the overall exergy efficiency of the integrated configurations, obtaining even better exergy efficiency than the conventional configuration.

From an economic point of view, the investment cost for biomethane production was similar for the conventional and the direct methanation configurations. However, the investment cost associated with liquefaction was slightly higher for the direct methanation configuration than the conventional LBM production (i.e., because of higher LBM flow rate). Further, the cost analysis revealed that the main cost-driving factor for the integrated configurations was the H_2 price, resulting in significantly higher operating costs for the integrated configurations than for conventional LBM production.

The results indicated that the feasibility of integrating the conventional LBM production with the methanation process was highly dependent on the H_2 price. It was demonstrated that the H_2 price should be approximately 0.5 USD/kg H_2 to produce LBM with compatible price by the conventional LBM production. However, a H_2 price close to 1 USD/kg H_2 could also be reasonable if the possibility of selling high-pressure steam is considered.

Conclusions and future work

The present thesis targeted to propose methods to produce liquefied biomethane. In order to achieve the goals of the thesis, several detailed process models for LBM production were developed and optimized. This chapter recapitulates the overall conclusions of the appended articles, and strives to provide some directions for future work.

From the results in Article I, it was concluded that integrating upgrading and liquefaction processes improved the overall energy efficiency of the LBM production plant. As the temperature of the final product was extremely low, employing cryogenic gas separation for biogas upgrading could provide a good synergy between the two processes. However, the main challenge is risk of CO₂ ice-formation in the cryogenic upgrading process.

With respect to the optimization method presented in Articles II and III for a conventional LBM production plant that uses amine-based biogas upgrading, it was concluded that optimizing the overall LBM production with regards to thermodynamic efficiency could be done through a sequential approach; the pressure level of the biomethane produced from the upgrading process was found to be the only variables influencing both the upgrading process and the liquefaction process.

In a sequential optimization approach, it was concluded that optimizing the biogas upgrading process for total exergy demand for the studied process that requires a high level of biomethane purity would be similar to optimizing for the total annualized cost. This finding was essential as it helped optimize the upgrading process with less effort since providing cost estimates for the plant was cumbersome. Further, it was shown that the objective function formulations for the upgrading process would have a limited influence on the overall thermodynamic efficiency of the plant. However, different objective function formulations for the upgrading

process might affect the total annualized cost of the overall plant (considering both upgrading and liquefaction processes).

Overall, for objectives I and II presented in Chapter 1, this thesis provided an energy-efficient design approach for LBM production and showed that the performance of conventional LBM production plants can be optimized by minimizing the exergy supply.

Regarding reactor design for the methanation process presented in Articles IV and V, the results outlined that staged reactors operating under non-isothermal conditions would better utilize the exergy of heat with lower irreversibility rate within the reactors. Further, it was illustrated that intermediate water removal between reactor stages increased the CO₂ conversion, obtaining equilibrium conditions in a shorter reactor. This indicated that it was unnecessary to run the reaction within long reactors as the additional improvement in CO₂ conversion and reduction in the irreversibility due to extra length would not be significant.

From Article VI, it was concluded that integrating the methanation process with the conventional LBM production plant, aiming for complete CO₂ conversion, was not feasible in terms of the LBM production cost. Nonetheless, the proposed concept's efficiency could be higher than the conventional LBM production plant. The current price for green H₂ production was the primary reason for the high LBM price through the proposed concept. This finding responds to the objective III of the thesis that aimed to provide an alternative approach to utilize the CO₂ in the biogas mixture.

Limitations and recommendations for future work

The following recommendations for future work are based on the limitations and findings of this thesis.

It would be interesting to consider the sequential optimization approach with respect the total annualized cost for the entire plant. Here, optimization of the upgrading process considering exergy efficiency resulted in similar solutions as when minimizing the total annualized cost of the upgrading process, but the influence of selecting different objective functions on the total cost for the plant was not fully covered.

The limitation corresponding to the optimization in this thesis was related to selecting design variables. Here, the operating variables were intentionally chosen for optimization by fixing some parameters, particularly equipment size, such as distillation columns. The main reason for this decision was due to convergence concerns. Therefore, the feasible region for optimizing the process was restricted to a particular process description. Performing a sensitivity analysis regarding the impact of these parameters and examining alternative design parameters are essential and worth conducting in future work.

The possibility of manipulating the reaction rate within the reactor to change driving forces along the reactor was illustrated in this thesis. This possibility provides opportunities for the design of the methanation reactor, considering partial feeding or partial removal of products, obtaining an energy-efficient reactor design. An efficient heat management strategy within the reactor can be expected while assuring high CO_2 conversion and low irreversibility rate. Nonetheless, the proposed reactor design in this thesis only comprised two reactors considering the complete water removal (as a product) between reactors. Therefore, a combination of water removal and partial feeding of the reactants is worth examining in future work.

Even though the concept of integrating the methanation process with a conventional LBM production plant did not lead to a feasible solution, the possibility of using methanation as part of the biogas upgrading process suggests finding a good compromise between methanation and final polishing steps in future work. In this way, instead of obtaining complete CO_2 conversion within the methanation reactor (as considered in this thesis), the methanation process can be run with a smaller amount of H_2 , aiming for converting all H_2 . The unreacted CO_2 from the methanation can then be removed in the subsequent polishing process. Here, the determination of the optimal operating conditions and H_2/CO_2 ratio, leading to a promising solution, should be considered.

Bibliography

- [1] REN21 & FIA Foundation. Renewable energy pathways in road transport. Report, REN21 & FIA Foundation, 2020.
- [2] INTERNATIONAL COUNCIL ON CLEAN TRANSPORTATION (ICCT). Vision 2050: A strategy to decarbonize the global transport sector by mid-century. Report, ICCT, 2020.
- [3] UNFCCC. Adoption of the paris agreement. report no. fccc/cp/2015/1.9/rev.1. <https://unfccc.int/resource/docs/2015/cop21/eng/109r01.pdf>. Accessed: 2021-12-16.
- [4] Pradeep Kumar Tarei, Pushpendu Chand, and Himanshu Gupta. Barriers to the adoption of electric vehicles: Evidence from india. *Journal of Cleaner Production*, 291:125847, 2021.
- [5] Richard Cabrera-Jiménez, Josep M. Mateo-Sanz, Jordi Gavaldà, Laureano Jiménez, and Carlos Pozo. Comparing biofuels through the lens of sustainability: A data envelopment analysis approach. *Applied Energy*, In Press, Corrected Proof:118201, 2021.
- [6] Zaira Navas-Anguita, Diego García-Gusano, and Diego Iribarren. A review of techno-economic data for road transportation fuels. *Renewable and Sustainable Energy Reviews*, 112:11–26, 2019.
- [7] Anish Ghimire, Luigi Frunzo, Francesco Pirozzi, Eric Trably, Renaud Escudie, Piet N. L. Lens, and Giovanni Esposito. A review on dark fermentative biohydrogen production from organic biomass: Process parameters and use of by-products. *Applied Energy*, 144:73–95, 2015.

- [8] Furat Dawood, Martin Anda, and G. M. Shafiullah. Hydrogen production for energy: An overview. *International Journal of Hydrogen Energy*, 45(7):3847–3869, 2020.
- [9] Tom DiChristopher. Experts explain why green hydrogen costs have fallen and will keep falling. <https://www.spglobal.com/marketintelligence/en/news-insights/latest-news-headlines/experts-explain-why-green-hydrogen-costs-have-fallen-and-will-keep-falling-63037203>. Accessed: 2021-11-25.
- [10] Jon Anders Ryste, Martin Wold, Joakim Frimann-Dahl, Christos Chryssakis, Magnus S. Eide, and Håkon Endresen, Øyvind Hustad. Comparison of alternative marine fuels. https://safety4sea.com/wp-content/uploads/2019/09/SEA-LNG-DNV-GL-Comparison-of-Alternative-Marine-Fuels-2019_09.pdf. Accessed: 2021-12-12.
- [11] International Renewable Energy Agency (IRENA). Biogas for road vehicles: Technology brief. Report, IRENA, 2018.
- [12] Behnam Hashemi, Shiplu Sarker, Jacob J. Lamb, and Kristian M. Lien. Yield improvements in anaerobic digestion of lignocellulosic feedstocks. *Journal of Cleaner Production*, 288:125447, 2021.
- [13] Irimi Angelidaki, Laura Treu, Panagiotis Tsapekos, Gang Luo, Stefano Campanaro, Henrik Wenzel, and Panagiotis G. Kougias. Biogas upgrading and utilization: Current status and perspectives. *Biotechnology Advances*, 36(2):452–466, 2018.
- [14] Liangcheng Yang, Xumeng Ge, Caixia Wan, Fei Yu, and Yebo Li. Progress and perspectives in converting biogas to transportation fuels. *Renewable and Sustainable Energy Reviews*, 40(Supplement C):1133–1152, 2014.
- [15] Qinghong Zhang, Weiping Deng, and Ye Wang. Recent advances in understanding the key catalyst factors for fischer-tropsch synthesis. *Journal of Energy Chemistry*, 22(1):27–38, 2013.
- [16] Sunggyu Lee, Makarand Gogate, and Conrad J. Kulik. Methanol-to-gasoline vs. dme-to-gasoline ii. process comparison and analysis. *Fuel Science and Technology International*, 13(8):1039–1057, 1995.
- [17] Muhammad Abdul Qyyum, Junaid Haider, Kinza Qadeer, Valentina Valentina, Amin Khan, Muhammad Yasin, Muhammad Aslam, Giorgia De Guido, Laura A. Pellegrini, and Moonyong Lee. Biogas to liquefied biomethane: Assessment of 3p’s–production, processing, and prospects. *Renewable and Sustainable Energy Reviews*, 119:109561, 2020.
- [18] Qie Sun, Hailong Li, Jinying Yan, Longcheng Liu, Zhixin Yu, and Xinhai Yu. Selection of appropriate biogas upgrading technology-a review of biogas clean-

-
- ing, upgrading and utilisation. *Renewable and Sustainable Energy Reviews*, 51:521–532, 2015.
- [19] Imran Ullah Khan, Mohd Hafiz Dzarfan Othman, Haslenda Hashim, Takeshi Matsuura, M. Ismail, A.F. and Rezaei-DashtArzhandi, and Wan I. Azelee. Biogas as a renewable energy fuel – a review of biogas upgrading, utilisation and storage. *Energy Conversion and Management*, 150:277–294, 2017.
- [20] Laura Annamaria Pellegrini, Giorgia De Guido, Stefano Consonni, Giulio Bortoluzzib, and Manuele Gatti. From biogas to biomethane: how the biogas source influences the purification costs. In *ICheaP12 International Conference on Chemical & Process Engineering*, volume 43, pages 409–414. Italian Association of Chemical Engineering-AIDIC, 2015.
- [21] Mohd Shariq Khan, Iftekhar. A. Karimi, and David A. Wood. Retrospective and future perspective of natural gas liquefaction and optimization technologies contributing to efficient lng supply: A review. *Journal of Natural Gas Science and Engineering*, 45:165–188, 2017.
- [22] Tianbiao He, Iftekhar A. Karimi, and Yonglin Ju. Review on the design and optimization of natural gas liquefaction processes for onshore and offshore applications. *Chemical Engineering Research and Design*, 132:89–114, 2018.
- [23] Junaid Haider, Muhammad Abdul Qyyum, Bilal Kazmi, Muhammad Zahoor, and Moonyong Lee. Simulation study of biomethane liquefaction followed by biogas upgrading using an imidazolium-based cationic ionic liquid. *Journal of Cleaner Production*, 231:953–962, 2019.
- [24] Andrea Mazza, Ettore Bompard, and Gianfranco Chicco. Applications of power to gas technologies in emerging electrical systems. *Renewable and Sustainable Energy Reviews*, 92:794–806, 2018.
- [25] Manuel Götz, Jonathan Lefebvre, Friedemann Mörs, Amy McDaniel Koch, Frank Graf, Siegfried Bajohr, Rainer Reimert, and Thomas Kolb. Renewable power-to-gas: A technological and economic review. *Renewable Energy*, 85:1371–1390, 2016.
- [26] Karim Ghaib and Fatima-Zahrae Ben-Fares. Power-to-methane: A state-of-the-art review. *Renewable and Sustainable Energy Reviews*, 81:433–446, 2018.
- [27] Stefan Rönsch, Jens Schneider, Steffi Matthischke, Michael Schlüter, Manuel Götz, Jonathan Lefebvre, Praseeth Prabhakaran, and Siegfried Bajohr. Review on methanation – from fundamentals to current projects. *Fuel*, 166:276–296, 2016.
- [28] Jianli Ma, Qi Li, Michael Kühn, and Natalie Nakaten. Power-to-gas based subsurface energy storage: A review. *Renewable and Sustainable Energy Reviews*, 97:478–496, 2018.

- [29] Bruna Rego de Vasconcelos and Jean-Michel Lavoie. Recent advances in power-to-x technology for the production of fuels and chemicals. *Frontiers in Chemistry*, 7(392), 2019.
- [30] Martín David, Carlos Ocampo-Martínez, and Ricardo Sánchez-Peña. Advances in alkaline water electrolyzers: A review. *Journal of Energy Storage*, 23:392–403, 2019.
- [31] John Turner, George Sverdrup, Margaret K. Mann, Pin-Ching Maness, Ben Kroposki, Maria Ghirardi, Robert J. Evans, and Dan Blake. Renewable hydrogen production. *International Journal of Energy Research*, 32(5):379–407, 2008.
- [32] Pierre Millet. *Hydrogen Production*, chapter Fundamentals of Water Electrolysis, pages 33–62. Wiley Online Library, 2015.
- [33] S. Shiva Kumar and V. Himabindu. Hydrogen production by pem water electrolysis – a review. *Materials Science for Energy Technologies*, 2(3):442–454, 2019.
- [34] Lubomír Staňo, Michal Stano, and Pavol Ďurina. Separators for alkaline water electrolysis prepared by plasma-initiated grafting of acrylic acid on microporous polypropylene membranes. *International Journal of Hydrogen Energy*, 45(1):80–93, 2020.
- [35] K. C. Sandeep, Sachin Kamath, Krunal Mistry, Ashok Kumar M, S. K. Bhattacharya, Kalyan Bhanja, and Sadhana Mohan. Experimental studies and modeling of advanced alkaline water electrolyser with porous nickel electrodes for hydrogen production. *International Journal of Hydrogen Energy*, 42(17):12094–12103, 2017.
- [36] Ting Chen, Yucun Zhou, Minquan Liu, Chun Yuan, Xiaofeng Ye, Zhongliang Zhan, and Shaorong Wang. High performance solid oxide electrolysis cell with impregnated electrodes. *Electrochemistry Communications*, 54:23–27, 2015.
- [37] Dragica Lj Stojić, Milica P. Marčeta, Sofija P. Sovilj, and Šćepan S. Miljanić. Hydrogen generation from water electrolysis—possibilities of energy saving. *Journal of Power Sources*, 118(1):315–319, 2003.
- [38] Alexander Buttler and Hartmut Spliethoff. Current status of water electrolysis for energy storage, grid balancing and sector coupling via power-to-gas and power-to-liquids: A review. *Renewable and Sustainable Energy Reviews*, 82:2440–2454, 2018.
- [39] Luís Alves, Vítor Pereira, Tiago Lagarteira, and Adélio Mendes. Catalytic methane decomposition to boost the energy transition: Scientific and technological advancements. *Renewable and Sustainable Energy Reviews*, page 110465, 2020.

-
- [40] Irimi Angelidaki, Dimitar Karakashev, Damien J. Batstone, Caroline M. Plugge, and Alfons J. Stams. Biomethanation and its potential. *Methods Enzymol*, 494:327–351, 2011.
- [41] Kyle A. Stone, Matthew V. Hilliard, Q. Peter He, and Jin Wang. A mini review on bioreactor configurations and gas transfer enhancements for biochemical methane conversion. *Biochemical Engineering Journal*, 128:83–92, 2017.
- [42] Shiplu Sarker, Anna S. R. Nordgård, Jacob J. Lamb, and Kristian M. Lien. *Hydrogen, Biomass and Bioenergy*, book section five - Biogas and Hydrogen, pages 73–87. Academic Press, 2020.
- [43] Woo Jin Lee, Chaoen Li, Hermawan Prajitno, Jiho Yoo, Jim Patel, Yunxia Yang, and Seng Lim. Recent trend in thermal catalytic low temperature co₂ methanation: A critical review. *Catalysis Today*, 2020.
- [44] Duo Sun and David S. A. Simakov. Thermal management of a sabatier reactor for co₂ conversion into ch₄: Simulation-based analysis. *Journal of CO₂ Utilization*, 21:368–382, 2017.
- [45] Lars Jürgensen, Ehiازه Augustine Ehimen, Jens Born, and Jens Bo Holm-Nielsen. Dynamic biogas upgrading based on the sabatier process: Thermodynamic and dynamic process simulation. *Bioresource Technology*, 178:323–329, 2015.
- [46] Ziwei Li, Qian Lin, Min Li, Jianxin Cao, Fei Liu, Hongyan Pan, Zhigang Wang, and Sibudjing Kawi. Recent advances in process and catalyst for co₂ reforming of methane. *Renewable and Sustainable Energy Reviews*, 134:110312, 2020.
- [47] Ye Wang, Lu Yao, Shenghong Wang, Dehua Mao, and Changwei Hu. Low-temperature catalytic co₂ dry reforming of methane on ni-based catalysts: A review. *Fuel Processing Technology*, 169:199–206, 2018.
- [48] G. Alex Mills and Fred W. Steffgen. Catalytic methanation. *Catalysis Reviews*, 8(1):159–210, 1974.
- [49] Chalachew Mebrahtu, Florian Krebs, Salvatore Abate, Siglinda Perathoner, Gabriele Centi, and Regina Palkovits. *Chapter 5 - CO₂ Methanation: Principles and Challenges*, volume 178, pages 85–103. Elsevier, 2019.
- [50] Ronny Tobias Zimmermann, Jens Bremer, and Kai Sundmacher. Optimal catalyst particle design for flexible fixed-bed co₂ methanation reactors. *Chemical Engineering Journal*, 387:123704, 2020.
- [51] Manuel Bailera, Pilar Lisbona, Luis M. Romeo, and Sergio Espotolero. Power to gas projects review: Lab, pilot and demo plants for storing renewable energy and co₂. *Renewable and Sustainable Energy Reviews*, 69:292–312, 2017.

- [52] Mohammad Ostadi. *New and Innovative Conceptual Designs of Gas-to-Liquid Processes*. Thesis for the degree of philosophiae doctor, Norwegian University of Science and Technology, 2017.
- [53] T.J. Kotas. *The Exergy Method of Thermal Plant Analysis*. Exergon Publishing Company, London, UK., 2012.
- [54] Richard Turton, Richard C. Bailie, Wallace B. Whiting, Joseph A. Shaeiwitz, and Debangsu Bhattacharyya. *Analysis, synthesis, and design of chemical processes*. Upper Saddle River, N.J.: Prentice Hall, 2012.

Collection of articles

Cryogenic vs. absorption-based biogas upgrading in liquefied biomethane production – An energy efficiency analysis

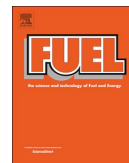
SAYED EBRAHIM HASHEMI¹, SHIPLU SARKER¹, KRISTIAN M. LIEN¹, SONDRÉ K. SCHNELL² AND BJØRN AUSTBØ^{1,*}

1. DEPARTMENT OF ENERGY AND PROCESS ENGINEERING,
NORWEGIAN UNIVERSITY OF SCIENCE AND TECHNOLOGY,
NO-7491 TRONDHEIM, NORWAY

2. DEPARTMENT OF MATERIAL SCIENCE AND ENGINEERING,
NORWEGIAN UNIVERSITY OF SCIENCE AND TECHNOLOGY,
NO-7491 TRONDHEIM, NORWAY

* CORRESPONDING AUTHOR

THIS ARTICLE WAS PUBLISHED IN *FUEL* (2019) 245: 294.



Full Length Article

Cryogenic vs. absorption biogas upgrading in liquefied biomethane production – An energy efficiency analysis



Sayed Ebrahim Hashemi^a, Shiplu Sarker^a, Kristian M. Lien^a, Sondre K. Schnell^b, Bjørn Austbø^{a,*}

^a Department of Energy and Process Engineering, Norwegian University of Science and Technology (NTNU), NO-7491 Trondheim, Norway

^b Department of Materials Science and Engineering, Norwegian University of Science and Technology (NTNU), NO-7491 Trondheim, Norway

ARTICLE INFO

Keywords:

Liquefied biomethane
Cryogenic upgrading
Chemical absorption upgrading
Methane utilization

ABSTRACT

Production of liquefied biomethane (LBM) from biogas comprises two major energy intensive processes; upgrading to increase the methane concentration and refrigeration to liquefy the upgraded biogas. Amine-based absorption has been considered an attractive option for biogas upgrading in industrial applications. The temperature increase associated with amine regeneration is, however, in conflict with the cooling requirement of the subsequent liquefaction process. Hence, cryogenic biogas upgrading, integrated with liquefaction, has emerged as an interesting alternative.

In this paper, a rigorous energy analysis was performed for comprehensive models of the two aforementioned LBM production alternatives. Both processes were modeled using Aspen HYSYS[®] and optimized to minimize the energy use. The results indicate that the integrated cryogenic upgrading process is favorable in terms of both overall energy efficiency and methane utilization. Moreover, the energy analysis implies that the liquefaction process accounts for the major part of the energy input to an LBM plant, demonstrating the significance of improving the energy efficiency of the liquefaction process in order to improve the overall performance of the LBM process.

1. Introduction

The use of fossil fuels in the transportation sector has remained dominant although renewable energy sources being introduced in the energy market. According to a recent report from the *Renewable Energy Policy Network for the 21st century* [1], the global renewable share of total energy use was 20.5% in 2016. However, the permeation of renewable energy in different sectors is not identical; for instance: energy use in the transportation sector comprises 32% of the total energy use in the world, out of which renewable energies like biofuels and renewable electricity account for only 3.1% [1].

Lately, *liquefied biomethane* (LBM) from biogas has attracted much interest as an alternative fuel [2]. Similar to liquefied natural gas (LNG), the energy density of LBM is about 21 MJ/L, which is approximately 2.4 times higher than that of compressed biomethane (Bio-CNG) [3]. The higher energy density of LBM makes it feasible as long distance transportation fuel. Currently, the global LBM production is limited to only 43,100 tonnes per annum, which is considerably lower than global trade of liquefied natural gas (LNG) with 293.1 million tonnes in 2017 [4]. However, it is estimated that demands for LBM will increase not only for the vehicle transportation sector, but also in maritime transport

over the next decades [4].

As a downstream product of biogas production plants, LBM production requires two energy intensive processes: upgrading and liquefaction. Biogas produced through either an anaerobic digester or landfill must be upgraded in order to increase the methane (CH₄) concentration (i.e. increase the heating value of the biogas) and remove harmful impurities in the final product. The upgraded biogas is known as biomethane, which contains mainly CH₄. Typical biogas compositions and LBM purity requirements are presented in Table 1. Based on the purpose of biogas utilization, one or a combination of conventional upgrading technologies such as water scrubbing, chemical absorption, pressure swing adsorption, or membrane separation can be applied [5].

In order to produce applicable biomethane in liquid form, the obtained biomethane from the upgrading processes must be liquefied in an external refrigeration cycle. Knowledge regarding refrigeration cycles is mature in terms of process design and energy optimization since it has been implemented in LNG plants for the past 100 years [6–8]. Cascade liquefaction processes, mixed refrigerant processes, and expander liquefaction processes (i.e. reverse Bryton cycles) are commercialized for liquefaction purposes [9].

In advance of performing a comprehensive energy assessment of

* Corresponding author.

E-mail address: bjorn.austbo@ntnu.no (B. Austbø).

<https://doi.org/10.1016/j.fuel.2019.01.172>

Received 29 September 2018; Received in revised form 13 January 2019; Accepted 30 January 2019

Available online 21 February 2019

0016-2361/ © 2019 The Authors. Published by Elsevier Ltd. This is an open access article under the CC BY-NC-ND license (<http://creativecommons.org/licenses/by-nc-nd/4.0/>).

Table 1
Typical biogas composition and LBM specification [10,11].

Compound	Unit	Anaerobic Digestion	Landfills	LBM purity requirement
CH ₄	mol%	50–70	45–62	> 99.99
CO ₂	mol%	19–38	24–40	< 10 ⁻³
H ₂ S	ppm	72–700	15–427	< 3.5
H ₂ O	mol%	< 0.6	NA	< 5·10 ⁻⁵
N ₂	mol%	0–5	1–17	
H ₂	mol%	NA	NA	
O ₂	mol%	0–1	1–2.6	
Siloxane	ppm	trace	NA	
Total chlorines	mg/Nm ³	100–800	NA	

different LBM production plants in this paper, an overview regarding energy use of different biogas upgrading methods and liquefaction processes is provided in order to highlight advances and with respect to energy use.

1.1. Biogas upgrading

To date, a number of studies have focused on the energy aspects of different biogas upgrading methods. Rotunno et al. [12] simulated a pressurized water scrubbing process considering a biogas mixture of 60 mol% CH₄ and 40 mol% CO₂. They reported that a purity of 98.1 mol % CH₄ was obtained at 10 bar and 25 °C, which is suitable for gas grid injection and bio-CNG production. They stated that the energy efficiency of the upgrading plant producing biomethane with quality of gas grid injection was 89.8%. Budzianowski et al. [13] considered various configurations of water scrubbing and water regeneration for a biogas mixture of 65 mol% CH₄ and 35 mol% CO₂. Their results indicated that a specific energy use of 0.32 kWh/Nm³ of raw biogas was required to produce biomethane with a purity of 98 mol% CH₄, which was equivalent to 15.2% of the energy content of the raw biogas.

Haider et al. [14] simulated different types of membrane operating at different pressure for a mixture of CH₄ and CO₂ containing 50–70 mol% CH₄. They stated that polyimide membranes in three stages upgraded the biogas up to 97 mol% CH₄ with specific energy of 0.22 kWh/Nm³ of raw biogas. Iovane et al. [15] conducted experimental studies considering a biogas composition including H₂S and other trace elements with polymeric membranes. They reported that the purity of biomethane reached 99 mol% CH₄ when the feed gas pressure was increased to 25 bar. Valenti et al. [16] investigated various designs for cellulose acetate membranes at 26 bar in order to upgrade a mixture of 55 mol% CH₄ and 45 mol% CO₂. They reported that a specific energy use from 0.33 to 0.47 kWh/Sm³, depending on the design, was required to achieve purity of 97 mol% CH₄.

An overview of literature indicates that upgrading biogas to high quality biomethane, satisfying the purity requirements for LBM production, hardly can be achieved only through water scrubbing or membrane separation [17]. Thereby, a polishing step should also be considered. Although the polishing step is costly and essential for achieving high quality biomethane, the specific energy requirement of the polishing step has not been fully considered in literature.

Pressure swing adsorption (PSA) is a technology that can be used for both upgrading and polishing [4]. Ferella et al. [18] performed experiments for low pressure PSA with different sorbents such as zeolite and activated carbon. They reported that biomethane with a purity of above 98 mol% CH₄ and a methane loss of 5% obtained using synthesized zeolite from fly ash. Augelletti et al. [19] simulated a novel two-stage PSA configuration that upgraded a biogas mixture of 60 mol% CH₄ and 40 mol% CO₂. They demonstrated that a biomethane stream with a purity of above 97 mol% CH₄, and CO₂ with a purity of up to 99.4% were obtained from the novel configuration, while the required specific energy and methane loss were 0.35 kWh/kg of biomethane and

about 3%, respectively. Recently, Liu et al. [20] simulated a vacuum swing adsorption process for three-step adsorption beds and obtained CH₄ purity of 99.4 mol% from a feed gas of 50 mol% CH₄ and 50 mol% CO₂. Their simulation showed a specific energy requirement of 0.22 kWh/kg of biomethane and biomethane recovery of 96.9%. Although the LBM requirements can be satisfied, high methane loss remains a challenge with PSA.

Amine-based absorption is suitable not only for large industrial scale applications, but also for obtaining the targeted LBM specifications without requiring additional polishing steps [4]. The energy requirement for chemical absorption consists of work for biogas compression and heat at high temperature in range of 100–130 °C for amine regeneration in a stripper column [21]. It is worth mentioning that the type of amine has great impact on the energy use in chemical absorption. For instance, biogas upgrading using monoethanolamine (MEA) requires more heat to regenerate the amine in stripper column than Methyl diethanolamine (MDEA) [22]. However, while the operating pressure is in the range 3–8 bar when using MEA, a pressure range of 45–70 bar is required for MDEA, depending on the purification requirements [22,23]. This means that a smaller amount of work is required for biogas compression prior to the absorber column with MEA than with MDEA.

Vo et al. [24] evaluated chemical absorption with MEA for biogas upgrading. They demonstrated that approximately 2.5 kWh/m³ of biomethane was required in the form of electricity and steam in order to obtain biomethane with 96 mol% CH₄. Most of the research concerning chemical absorption was focused on how to reduce the heating duties in the reboiler. For instance, Nejat et al. [23] showed that the reboiler heat duty reduced by approximately 47% once MDEA was substituted with a mixture of MDEA and Sulfolane.

In another study, Pellegrini et al. [25] investigated the energy requirement for LBM production from a biogas mixture of 60 mol% CH₄ and 40 mol% CO₂. They evaluated MEA absorption as upgrading method in order to reach the LBM purity requirements, considering an external refrigeration duty for liquefaction. They found that about 29% of the methane available in the raw biogas stream would be consumed if the process was to be self-supplied with work and heat, considering conventional engineering processes. The results indicated that biogas upgrading accounted for 57.4% of the total energy requirement.

CO₂ removal through chemical absorption is an exothermic reaction, which leads to an increase of biomethane temperature leaving the column. This is in conflict with the cooling duty for subsequent liquefaction process. Therefore, a comprehensive simulation model including both absorption-based upgrading and liquefaction assists in determining the actual energy use and potential improvements.

In addition to the aforementioned upgrading methods, cryogenic separation in distillation columns has attracted much attention [5,26]. In cryogenic separation, the difference in boiling point for the various gas components is exploited to separate the components [27]. Obtaining high CH₄ content and CO₂ recovery account as advantages of this technology. Moreover, cryogenic separation reduces the cooling requirement in LBM production since biogas upgrading takes place at lower temperature.

Yousef et al. [28] proposed a one-stage distillation column for a biogas mixture of 60 mol% CH₄ and 40 mol% CO₂ that purified biomethane up to 94.5 mol% CH₄ and obtained a CO₂ stream with a purity of 99.7 mol% as by-product. In a successive study [29], they employed two distillation columns operating above and below the critical pressure of pure CH₄, respectively, in order to upgrade biogas up to 97 mol % of CH₄. When considering heat recovery in the process design, the specific energy requirement was reduced to 0.25 kWh/Nm³ of raw biogas for producing liquefied CO₂ with purity of 99.7 mol% at 110 bar and biomethane with purity of 97.1 mol% CH₄ at 5 bar [29].

Lange et al. [22] proposed dual-pressure distillation columns, with one column operating at high pressure as a stripper section without condenser and one column operating at lower pressure as an

enrichment section without reboiler. They concluded that the use of low temperature separation technologies was advantageous, compared to a conventional MDEA absorption, when the CO₂ concentration in the feed gas was high. In successive studies [25,30], they simulated various types of cryogenic separation concepts including the Ryan-Holmes process [31,32], an anti-sublimation process [33,34] and dual-pressure distillation columns. Refrigeration cycles were not included in their simulation. The results indicated that approximately 14% of the methane in the raw biogas would be consumed if the process with dual-pressure distillation columns was supposed to be self-supplied with work and heat, which was half of the methane consumption for chemical absorption upgrading. Furthermore, their simulations showed that nearly 22% of the methane in the raw biogas was consumed for a synergetic process including anti-sublimation separation and liquefaction. Baccioli et al. [35] simulated a small-scale LBM production plant applying the anti-sublimation process for upgrading and a dual-expander refrigeration cycle for liquefaction. For a biogas mixture with 40 mol% CH₄, 59 mol% CO₂ and 0.5 mol% of H₂S and 0.5 mol% H₂O, the specific energy requirement was 1.45 kWh/kg of LBM in order to produce LBM with a purity of 97 mol% CH₄.

1.2. Biogas liquefaction

In conventional approaches, the high quality biomethane obtained from the upgrading is cooled down through a separate liquefaction unit in order to produce LBM. Birgen and Jarque [36] performed simulation using Aspen PLUS[®] for liquefying biomethane generated from an upgrading process with a production capacity of 100 MW_{LHV} of LBM. They showed that the total power requirement for a single expander liquefaction process was about 12.4 MW. Baccioli et al. [35] simulated a dual-expander liquefaction process for small-scale LBM production. Results from their simulation indicated that 0.75 kWh/kg LBM was required for liquefaction process.

In comparison with biogas upgrading, biomethane liquefaction has received limited attention in the literature.

1.3. Objective

Despite existing research regarding LBM production, few studies have focused on optimization of different design variables affecting the total energy use of the LBM production plants. This paper aims to develop comprehensive models of two different process configurations by simulating and optimizing the complete processes, including both upgrading and liquefaction. In the present paper, a cryogenic gas separation process integrated with liquefaction is compared with a conventional approach of LBM production through chemical absorption followed by liquefaction. Models have been developed in Aspen HYSYS[®] V9.0 considering a common raw biogas composition. Additionally, the design variables are optimized with respect to energy use. The performance of the two configurations is evaluated by means of energy analysis in order to identify potential improvement.

The layout of the paper is as follows: In Section 2, descriptions of the two process models are presented. The methodology of the optimization procedure and energy efficiency calculations are provided in Section 3. Results from the energy simulation and energy analysis are presented in Section 4. In Section 5, conclusions and suggestions for future work are presented.

2. Process descriptions

Two different approaches of producing LBM have been studied in this paper:

- Case 1: Cryogenic separation integrated with liquefaction in a synergetic approach
- Case 2: Amine-based absorption with subsequent liquefaction in a

conventional approach

In case 1, cryogenic separation is integrated with the liquefaction process. In case 2, an amine-based absorption upgrading followed by a liquefaction unit is considered. Identical feed and product conditions are applied for both processes. The raw biogas stream consists of 60 mol % CH₄, 39.9 mol% CO₂ and 0.1 mol% H₂S at 35 °C and 1 atm. Liquefied biomethane (LBM) and liquefied CO₂ (LCO₂) are considered as final product and byproduct of the LBM production plant, respectively. The CO₂ content should be below 50 ppm for the LBM stream and above 99.7 mol% for the LCO₂ stream. Moreover, all the H₂S from the raw biogas leaves the LBM production plant with the LCO₂ stream.

In general, raw biogas generated from a biogas production plant contains water (see Table 1). Depending on the type of biogas upgrading method, dehydration can be accomplished before or after the upgrading step. For instance, removal of water in a cryogenic gas separation is carried out before the upgrading step. For upgrading based on chemical absorption, the dehydration unit is placed after the upgrading step, as the amount of water removal depends on the water content at the outlet of the absorber. In this study, it is assumed that the raw biogas does not contain water, or alternatively is removed prior to upgrading. Therefore, no dehydration unit was considered for case 1, while a dehydration unit was considered for case 2 due to water being present during the chemical absorption upgrading.

It is assumed that the water from the biomethane stream and the high content CO₂ stream, respectively, from the outlet of the absorber and the outlet of the stripper in case 2 is removed using tri-ethylene-glycol (TEG) absorber/regeneration columns. The energy requirement of the dehydration process is mainly due to TEG regeneration, which involves heat at elevated temperature in the reboiler [37,38]. In the present study, the energy costs of the dehydration are estimated in accordance with the work by Kinigoma [39]. Furthermore, in accordance with recommendations from Aspelund et al. [40], the processes have been designed in such a way that cooling duties are delivered at high pressure. Therefore, an expander is placed at the end of LBM stream in order to adapt the pressure and temperature levels to the final LBM conditions.

2.1. Cryogenic upgrading scheme (case 1)

The flow sheet of an integrated cryogenic upgrading process for LBM production is given in Fig. 1. Biogas upgrading is accomplished at high pressure by means of two cascading distillation columns operating at different pressure level. Besides the columns, the model consists of a gas compression unit and one expander. Cooling is provided by a single expander refrigeration cycle with nitrogen, which is coupled to the upgrading process.

Initially, a high pressure raw biogas stream (S101) is produced by passing through the compression unit. After leaving the compression unit, the raw biogas (S102) is pre-cooled in a multi stream heat exchanger (HX1) before entering the high-pressure distillation column (D1). CO₂ exits from the bottom as a liquid with a small amount of CH₄ and H₂S (S104). The top product (S103) of D1 passes through a valve (V1) producing a low-pressure stream (S105) that goes into the low-pressure distillation column (D2). In D2, biomethane with a CO₂ content below 50 ppm and without H₂S leaves from the top (S106). The stream with high concentration CO₂ and H₂S (S107) departs bottom of D2 in liquid form towards pump (P1) in order to increase the stream pressure (S108) before mixing with S104 in liquid mixer (M1). Liquefied CO₂ leaves M1 as a byproduct of the LBM production plant. The biomethane (S106) from the top of D2 is further cooled in a multi stream heat exchanger (HX2) followed by an expander (E1) in order to produce the final liquefied biomethane (LBM).

Data for both distillation columns are presented in Table 2. A sensitivity analysis is performed to select the number of theoretical trays for the two columns, in order to minimize the cooling duties in the

Table 3
Optimization problems and design variables ranges for the cryogenic upgrading scheme (case 1).

Upgrading (step 1)			Liquefaction (step 2)		
Objective	min { $Q_{\text{precooling}} + Q_{\text{cond1}} + Q_{\text{cond2}} + Q_{\text{subcool}}$ }		Objective	min { $W_{\text{N}_2 \text{ compression}} - W_{\text{E}_2}$ }	
Constraints	<ul style="list-style-type: none"> - CO₂ content in LBM < 50 ppm - CH₄ loss < 1 mol% - No H₂S content in LBM 		Constraints	Minimum temperature approach in multi stream heat exchangers of 2 °C	
Optimization Variables	Range	Step size	Optimization Variables	Range	Step size
High pre. (P _{S101})	46–55 bar	0.5 bar	N ₂ flow rate (M _{S201})	3000–8000 kmol/h	100 kmol/h
Low pre. (P _{S105})	30–45 bar	0.5 bar	Low pre. (P _{S201})	1–5 bar	0.5 bar
1st column inlet temp. (T _{S102})	−60–−10 °C	2 °C	High pre. (P _{S202})	40–70 bar	1 bar
1st distillation column reflux ratio (RF ₁)	1.5–5	0.1	Stage temp. (T _{S203})	−50–−10 °C	2 °C
1st distillation column reboiler temp. (RT ₁)	10–15 °C	0.1 °C			
2nd distillation column reflux ratio (RF ₂)	1.5–5	0.1			
2nd distillation column reboiler temp. (RT ₂)	3–6 °C	0.1 °C			

net electrical work that is used in the refrigeration cycle. Initially, the absorber column is optimized in such a way that the standard LBM specifications are satisfied considering the minimum work for biogas compression. In the second step, the heating duty of the reboiler of the stripper column is minimized. Finally, the liquefaction process is optimized in order to achieve minimum electrical work. The optimization problem for case 2, corresponding to Fig. 2, is given in Table 4.

3.3. Energy analysis

Calculations regarding energy requirements for the dehydration units consider the heat duties in the reboiler for TEG regeneration. The energy demand for the dehydration step is estimated in accordance with the methodology proposed by Kinigoma and Ani [39]. It is assumed that the hydration unit is able to dewater the stream completely. Moreover, heat loss from the dehydration unit is considered negligible. The lean TEG flow rate ($\dot{m}_{\text{lean TEG}}$) in the dehydration unit is given as

$$\dot{m}_{\text{lean TEG}} = C_{\text{lean TEG}} \dot{V}_{\text{TEG}}, \quad (1)$$

where $C_{\text{lean TEG}}$ is the concentration of lean TEG and \dot{V}_{TEG} is volumetric TEG circulation rate. The volumetric TEG circulation rate is calculated considering a TEG circulation ratio (CR_{TEG}) of 0.035 m³ TEG/kgH₂O [38]:

$$\dot{V}_{\text{TEG}} = CR_{\text{TEG}} \dot{m}_w \quad (2)$$

Here, \dot{m}_w indicates the amount of water that is removed in the dehydration unit. The total heat rate requirement (\dot{Q}_{dh}) (kJ/h) for the dehydration unit consists of the sensible heat rate for TEG (\dot{Q}_s), the vaporization heat rate for water removal (\dot{Q}_v) and the heat rate for the reflux flow stream (\dot{Q}_r):

$$\dot{Q}_{\text{dh}} = \dot{Q}_s + \dot{Q}_v + \dot{Q}_r. \quad (3)$$

Considering a reflux ratio (R) of 0.25, a TEG regeneration temperature of 200 °C and constant heat capacity (c_p) of 3.014 kJ/kg °C, given by Kinigoma and Ani [39], the heat requirement in the dehydration unit can be calculated by the following equations:

$$\dot{Q}_s = \dot{m}_{\text{lean TEG}} \cdot c_p \cdot \Delta T \quad (4)$$

$$\dot{Q}_v = 2.023 \cdot (\dot{m}_w \cdot \dot{V}_{\text{gas flow}}) \quad (5)$$

$$\dot{Q}_r = R \cdot \dot{Q}_v \quad (6)$$

Here, $\dot{V}_{\text{gas flow}}$ (Nm³/h) is the volumetric gas flow rate entering the dehydration unit. The temperature differences (ΔT) for DH1 and DH2 corresponding to the model in Fig. 2 are defined as the difference between the TEG regeneration temperature and the temperature of the top

stream of the stripper and the absorber columns, respectively.

The thermodynamic performance of the proposed configurations in Section 2 are evaluated by means of energy. The overall energy efficiency is defined as the ratio of all useful energy to all required energy to produce the LBM [36]:

$$\eta = \frac{\dot{m}_{\text{LBM}} \cdot LHV_{\text{LBM}} + \sum \dot{W}_{\text{produced}} + \sum \dot{Q}_{\text{produced}}}{\dot{m}_{\text{raw biogas}} \cdot LHV_{\text{raw biogas}} + \sum \dot{W}_{\text{required}} + \sum \dot{Q}_{\text{required}}}. \quad (7)$$

Here, \dot{m}_{LBM} and $\dot{m}_{\text{raw biogas}}$ are the mass flow rates of LBM and raw biogas, respectively. \dot{W} and \dot{Q} represent the work and heat rate produced or consumed in the plant. In this study, LCO₂ is considered a valuable byproduct from the plant that can be used in other applications. The lower heating value (LHV) of the streams, work and heat rates are obtained from simulation in Aspen HYSYS[®].

Besides the overall energy efficiency, for the sake of enabling of comparison different energy forms, the amount of methane in the raw biogas that can be utilized as LBM is interpreted as an energy indicator in accordance with the net equivalent methane method proposed by Pellegrini et al. [25]. In this method, the work and the heat requirements are converted into corresponding amounts of methane required to provide such energy requirements through conventional engineering processes. Considering energy efficiencies of engineering processes given by Pellegrini et al. [25], it is assumed that the work is generated from a combined cycle power plant with energy efficiency of $\eta_{\text{cc}} = 0.55$ when the power plant is fueled by the methane with a lower heating value of 50 MJ/kg [25]. However, the assumed energy efficiency of the power plant would in reality be lower on a typical LBM scale in range of 10–15 MW. The equivalent methane requirement for work (\dot{m}_{work}) can be expressed as

$$\dot{m}_{\text{work}} = \frac{\dot{W}_{\text{net}}}{\eta_{\text{cc}} \cdot LHV_{\text{methane}}}, \quad (8)$$

where \dot{W}_{net} is the net work required for LBM production. In addition, it is assumed that the heat delivery at high temperature level in the reboiler of the stripper is supplied through a low-pressure steam generated by a methane-fired boiler with an energy efficiency of $\eta_b = 0.80$ [25]. Hence, the equivalent methane requirement of the methane-fired boiler (\dot{m}_{heat}) is given as

$$\dot{m}_{\text{heat}} = \frac{\dot{Q}_{\text{reb}}}{\eta_b \cdot LHV_{\text{methane}}}. \quad (9)$$

Here, \dot{Q}_{reb} is the amount of heat required in the reboilers at high temperatures. Calculation of the equivalent methane for the required work and heat provides a practical measure to compare the proposed

Table 4
Optimization problems and design variables ranges for the chemical absorption upgrading scheme (case 2).

Absorber (step 1)			Stripper (step 2)			Liquefaction (step 3)		
Objective	min { $W_{biogas\ compression}$ }		Objective	min {heating duty in reboiler}		Objective	min { $W_{N_2\ compression} - W_{Et} - W_{Et_2}$ }	
Constraints	- CO_2 content in LBM < 50 ppm - No H_2S content in LBM	Step size	Constraints	Minimum temperature approach in intermediate heat exchanger (HX1) of 2 °C	Step size	Constraints	Minimum temperature approach in multi stream heat exchangers of 2 °C	Step size
Optimization Variables	Range		Optimization Variables	Range		Optimization Variables	Range	
Feed gas pre. (P_{S101})	35–55 bar	1 bar	Stripper pre. (P_{S106})	1–5 bar	0.5 bar	N_2 flow rate (M_{S201})	2000–7000 kmol/h	100 kmol/h
lean amine flow rate (L_{S102})	4000–9000 kmol/h	500 kmol/h	Number of tray in stripper	15–25	1	Low pre. (P_{S201})	1–5 bar	0.5 bar
MDEA concentration	15–55 wt%	5 wt%	Feed tray	8–13	1	High pre. (P_{S202})	40–70 bar	2 bar
Number of tray in absorber column	15–30	1	Stripper reflux ratio (RR _f)	1.5–5	0.5	Stage temp. (T_{S203})	–60 to –20 °C	1 °C
			Stripper condenser temp. (CT_1)	30–50 °C	5 °C	Intermediate temp. (T_{S113})	–60 to –20 °C	5 °C

configurations. Methane utilization (MU) indicates the amount of methane in the raw biogas ($\dot{m}_{CH_4, raw\ biogas}$) that can be converted to LBM when all energy interactions involved in the process is treated as the equivalent methane:

$$MU = \left(1 - \frac{\dot{m}_{work} + \dot{m}_{heat} + \dot{m}_{loss}}{\dot{m}_{CH_4, raw\ biogas}} \right) \quad (10)$$

Here, $\dot{m}_{loss, loss}$ denotes the amount of methane lost with the other streams of the LBM production plant. Results from the energy analysis are presented in Section 4.

3.4. Sensitivity analysis

Once the processes were optimized for a biogas mixture of 60 mol% CH_4 , 39.9 mol% CO_2 and 0.1 mol% H_2S , the optimum processes were used to perform sensitivity studies. In this study, the influence of the composition of the raw biogas on the specific energy use is considered for different CH_4 contents ranging from 40 mol% to 70 mol% while the H_2S concentration varies between 0.01 mol% and 1.0 mol%.

4. Results and discussion

The pressure, temperature, molar flow rates, and gas composition of streams corresponding to the optimized configurations of case 1 and case 2 are presented in Tables 5 and 6, respectively. The strict specification of producing biomethane with CO_2 content below 50 ppm results in the optimum value of 47 bar for the operating pressure of the absorber column in case 2. However, the optimized pressure value of the high-pressure distillation column in the case 1 is lower (i.e. 50.5 bar). This means the required work for biogas compression is greater in case 1. Moreover, results from Tables 5 and 6 illustrate that the molar flow rate of nitrogen in the optimized liquefaction process of case 2 is half of case 1, while the high pressure of the liquefaction process in both configurations equals 70 bar.

Distribution of the energy use in different processes for the two optimized configurations is given in Table 7. The total energy demand for case 1 includes electrical work used in compressors and pumps, and the refrigeration cycle. For case 1, the refrigeration cycle consumes more than 80% of the total required work of the plant because cooling duties in the condensers of the distillation columns are provided at different temperature levels. In addition, due to a higher refrigerant flow rate, the work requirement of the nitrogen compression unit is higher in case 1 than in case 2. In case 1, CO_2 compression requires a minor amount of the total work (i.e. less than 0.1%) since the

Table 5
The optimized thermodynamic data of case 1 corresponding Fig. 1.

Stream	Molar flow (kmol/h)	Temp. (°C)	Pre. (bar)	Composition (mol%)			
				CH_4	CO_2	H_2S	N_2
Raw biogas	1000.0	35.0	1.0	60.00	59.90	0.10	–
S101	1000.0	35.0	50.5	60.00	59.90	0.10	–
S102	1000.0	–10.0	50.5	60.00	59.90	0.10	–
S103	659.5	–70.3	50.5	90.79	9.19	0.02	–
S104	340.5	13.8	50.5	0.36	99.37	0.27	–
S105	659.5	–78.5	39.5	90.79	9.19	0.02	–
S106	598.6	–87.7	39.5	99.99	43 ppm	–	–
S107	60.9	4.1	39.5	0.25	99.62	0.13	–
S108	60.9	5.6	50.5	0.25	99.62	0.13	–
S109	598.6	–160.9	39.5	99.99	43 ppm	–	–
S201	6400.0	32.7	2.5	–	–	–	100
S202	6400.0	35.0	70.0	–	–	–	100
S203	6400.0	–36.0	70.0	–	–	–	100
S204	6400.0	–162.9	2.5	–	–	–	100
S205	6400.0	–136.2	2.5	–	–	–	100
LBM	598.6	–161.4	1.0	99.99	43 ppm	–	–
LCO ₂	401.4	12.7	50.5	0.34	99.41	0.25	–

Table 6
The optimized thermodynamic data of case 2 corresponding Fig. 2.

Stream	Molar flow (kmol/h)	Temp. (°C)	Pre. (bar)	Composition (mol%)					
				CH ₄	CO ₂	H ₂ S	H ₂ O	MDEA	N ₂
Raw biogas	1000.0	35.0	1.0	60.00	59.90	0.10	–	–	–
S101	1000.0	35.0	47.0	60.00	59.90	0.10	–	–	–
S102	8000.0	45.0	47.0	–	0.03	47 ppm	88.96	11.01	–
S103	594.5	45.0	47.0	99.71	47 ppm	–	0.29	–	–
S104	8406.0	70.9	47.0	0.09	4.77	0.01	84.65	10.48	–
S105	8406.0	69.2	2.5	0.09	4.77	0.01	84.65	10.48	–
S106	8406.0	102.4	2.5	0.09	4.77	0.01	84.65	10.48	–
S107	416.6	35.0	2.5	1.74	95.71	0.24	2.31	–	–
S108	7989.0	130.0	2.5	–	0.03	4 ppm	88.94	11.03	–
S109	7989.0	130.8	47.0	–	0.03	4 ppm	88.94	11.03	–
S110	7989.0	71.2	47.0	–	0.03	4 ppm	88.94	11.03	–
S111	8000.0	71.2	47.0	–	0.03	4 ppm	88.96	11.01	–
S112	407.0	35.0	2.5	1.79	97.97	0.24	–	–	–
S113	407.0	35.0	47.0	1.79	97.97	0.24	–	–	–
S114	592.8	45.0	47.0	99.99	47 ppm	–	–	–	–
S115	592.8	–40.0	47.0	99.99	47 ppm	–	–	–	–
S116	592.8	–160.8	47.0	99.99	47 ppm	–	–	–	–
S201	3200.0	34.1	1.5	–	–	–	–	–	100
S202	3200.0	35.0	70.0	–	–	–	–	–	100
S203	3200.0	–18.0	70.0	–	–	–	–	–	100
S204	3200.0	–163.2	1.5	–	–	–	–	–	100
S205	3200.0	–92.2	1.5	–	–	–	–	–	100
LBM	592.8	–191.4	1.0	99.99	47 ppm	–	–	–	–
LCO ₂	407.0	10.9	50.5	1.79	97.97	0.24	–	–	–

compression takes place in liquid form through pumps.

The amount of required work in case 2 is approximately 27% less than that in case 1, but the need of additional heat at elevated temperature levels increases the energy use in case 2. The refrigeration cycle in case 2 consumes 64.3% of the total work followed by biogas compression, CO₂ compression and MDEA compression with 25.5%, 7.7%, and 2.5%, respectively. Moreover, a large amount of heat is required to regenerate MDEA in the stripper column in case 2 (i.e. 97.3% of the total heat demand) and 2.7% of the total heat requirement is used in the dehydration units to regenerate TEG.

Results from Table 7 demonstrate that the work requirement for the refrigeration cycle in case 2 is approximately 42% lower than that in case 1. This is mainly because of selecting the single expander refrigeration cycle. Therefore, modifications regarding the type of refrigeration cycle such as employing cascade liquefaction processes or mixed refrigerant processes, which is appropriate for delivering cooling duties at different temperature levels in the condensers of the distillation columns, can benefit the energy use of the refrigeration cycle.

The specific energy use for the two optimized cases is indicated in Fig. 3. The results for models considering necessary units of operation for LBM production illustrate a specific energy use of 2.07 kWh/kg of LBM for case 1. Nevertheless, the specific energy requirement for case 2 consists of work with 1.54 kWh/kg of LBM and heat with 1.81 kWh/kg of LBM for a mixture of raw biogas with 60 mol% methane, 59.9 mol% CO₂ and 0.1 mol% H₂S.

The specific energy use as a function of CH₄ and H₂S concentration

in the raw biogas for case 1 and case 2 is given in Figs. 4 and 5, respectively. The higher the methane content in the raw biogas, the lower the specific energy requirement. Fig. 4 illustrates that the energy use per kg of produced LBM is reduced from 3.08 to 1.93 kWh/kg of LBM when the methane content in the raw biogas is increased from 40 mol% to 70 mol%. However, an increase in the H₂S concentration from 0.01 mol% to 1.0 mol% does not influence the specific energy use. The total specific energy use for case 2 presents the same trend as in case 1, where the specific energy use is reduced from 5.97 to 2.58 kWh/kg LBM by increasing the methane content from 40 mol% to 70 mol% (see Fig. 5).

The overall efficiency for the two cases is illustrated in Fig. 6. For case 1, the overall energy efficiency is 87.2% whereas it reduces to 80.1% for case 2. Moreover, the results indicate that the methane loss in case 1 is 80% less than that in case 2 (see Fig. 6).

Results from the net equivalent methane method is given in Fig. 7. For case 1, 72.7% of the methane available in the raw biogas for case 1 can be converted into LBM after using the required amount of methane for process operations, whereas in case 2, 62.8% of the methane available in the raw biogas can be utilized as LBM. In other words, the methane utilization of the cryogenic upgrading scheme is approximately 14% greater than that in the chemical absorption upgrading scheme.

Performing a detailed energy analysis of the two studied cases implies that a synergetic approach of upgrading and liquefaction through employing cryogenic distillation columns not only improves the energy

Table 7
Energy distribution for different processes in case 1 and case 2.

Cryogenic upgrading scheme (Case 1)				Chemical absorption upgrading scheme (Case 2)			
	MW		%		MW		%
Work	19.9	Biogas compression	19.2	Heat	17.2	Biogas compression	25.5
		Refrigeration cycle	80.8			Refrigeration cycle	64.3
		CO ₂ compression	< 0.1			CO ₂ compression	7.7
						MDEA compression	2.5
						MDEA regeneration	97.3
						Dehydration units	2.7

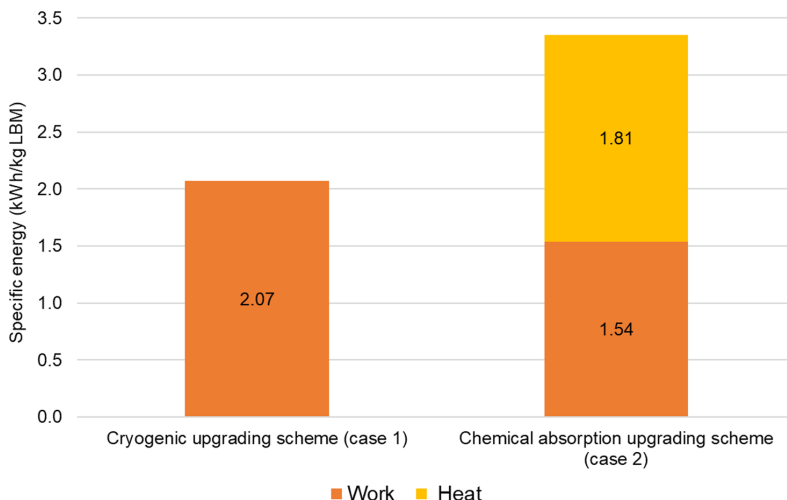


Fig. 3. Specific energy use for case 1 and case 2.

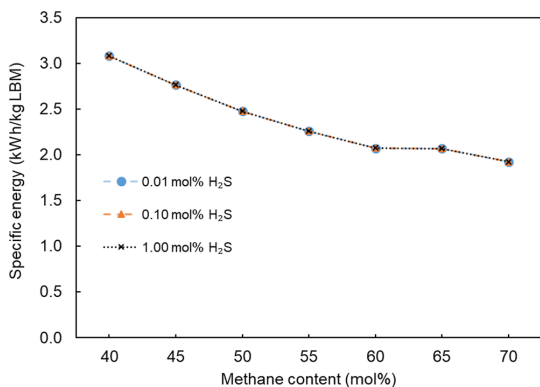


Fig. 4. The specific energy use as a function of CH₄ and H₂S concentration in raw biogas for case 1.

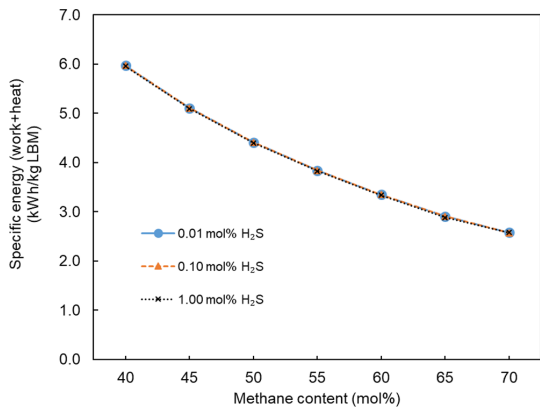


Fig. 5. The specific energy use as a function of CH₄ and H₂S concentration in raw biogas for case 2.

efficiency of the LBM production plant, but also converts a higher amount of the methane available in the raw biogas into LBM. However, in order to provide a better estimation of the performance of the two proposed cases, implementation of novel combined heat and power plants (CHP) with back pressure steam turbines should be considered since CHP plants can provide both heat and work with higher energy efficiencies. Moreover, the use of back pressure steam turbines can result in vacuum operation condition in the stripper column, which may lead to reduced heating requirements in the reboiler.

In Fig. 7, a comparison of the results in this study with results provided by Pellegrini et al. [25] (where the power consumption of the liquefaction process is estimated based on the temperature levels of the cooling requirements and a second law efficiency of 60%) illustrates that considering a complete model with refrigeration cycle and dehydration units in the two proposed configurations reduces the methane utilization by approximately 15% and 12% for case 1 and case 2, respectively. This is primarily due to the fact that the most energy intensive process in the LBM production is the liquefaction process. Consequently, simulation of the refrigeration cycles is required to provide a better understanding of the potential improvement of different LBM production configurations.

5. Conclusions

Complete models of two different configurations to produce LBM from raw biogas have been considered and optimized using Aspen HYSYS[®] V9.0. In case 1, a cryogenic biogas upgrading method by means of two distillation columns at different pressure is integrated with liquefaction, while case 2 investigates a conventional chemical absorption upgrading using MDEA followed by a refrigeration cycle.

The raw biogas comprises a mixture of 60 mol% CH₄, 59.9 mol% CO₂ and 0.1 mol% H₂S. Important design variables of models were optimized using an exhaustive search method in order to minimize the energy use of each model.

Energy analysis was performed by considering the overall energy efficiency of the LBM production plant and the equivalent methane method. For case 1, the required specific work is 2.07 kWh/kg LBM while this value for case 2 is 1.54 kWh/kg LBM. However, the additional specific heat of 1.81 kWh/kg LBM is required for case 2 in order to regenerate MDEA and TEG in the upgrading step and dehydration units, respectively.

The overall energy efficiency of case 1 and case 2 is 87.2% and

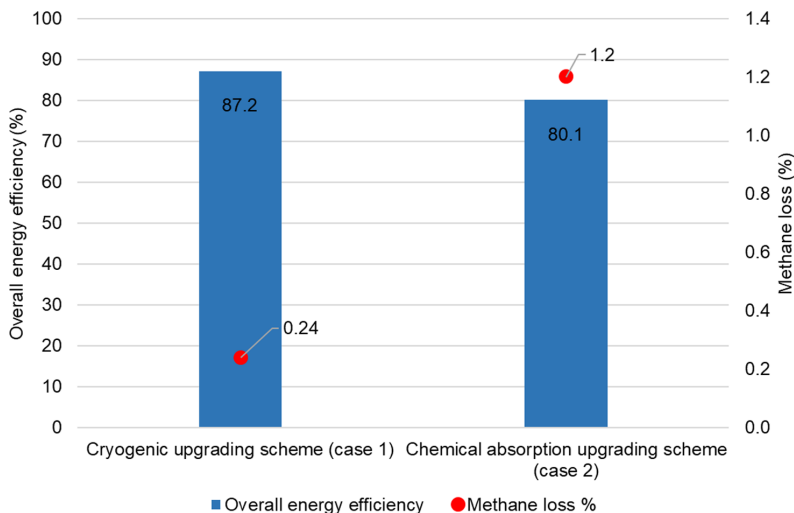


Fig. 6. The overall energy efficiency and the methane loss for case 1 and case 2.

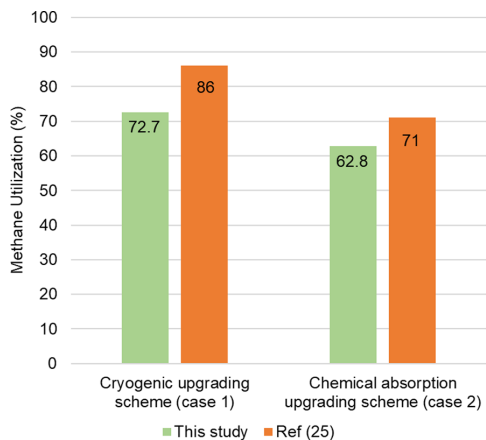


Fig. 7. Methane utilization in case 1 and case 2.

80.1%, respectively. In addition, case 1 is able to utilize 72.7% of the available methane in the raw biogas as LBM whereas this value is 62.8% in case 2. The energy analysis shows that a cryogenic upgrading scheme converts approximately 14% more of the available methane in the raw biogas into the LBM compared with a chemical absorption upgrading scheme. Results from the energy analysis demonstrates that a cryogenic upgrading scheme is favorable in terms of the overall efficiency of the LBM production plant and methane utilization.

Furthermore, results from energy distribution reveal that the main share of required work in the LBM production is used in liquefaction, approximately 81% and 64% in case 1 and case 2, respectively. Therefore, considering an appropriate type of liquefaction process with respect to the biogas upgrading method is worth being studied further. Meanwhile, heat integration potential from the LBM production plants will also be investigated in further work. For this future work, a more comprehensive optimization method will be applied.

Acknowledgements

Financial support from the Norwegian University of Science and

Technology (NTNU) through the Strategic Research Program ENERSENSE is greatly acknowledged.

References

- [1] Network-REN21 REP, "Renewables 2018 Global Status Report," REN21 Secretariat, Paris, 2018.
- [2] International Energy Agency. Technology roadmap delivering sustainable bioenergy. Paris: OECD/IEA; 2017.
- [3] Arteconi A, Polonara F. LNG as vehicle fuel and the problem of supply: the Italian case study. Energy Policy 2013;62:503–12.
- [4] Tybirk K, Solberg FE, Wennerberg P, Wiese F, Danielsen CG. Biogas Liquefaction and use of Liquid Biomethane. Status on the market and technologies available for LNG/LBG/LBM of relevance for biogas actors in 2017. BioGas 2017;2020.
- [5] Angelidaki I, et al. Biogas upgrading and utilization: current status and perspectives. Biotechnol Adv 2018;36(2):452–66.
- [6] He T, Karimi IA, Ju Y. Review on the design and optimization of natural gas liquefaction processes for onshore and offshore applications. Chem Eng Res Des 2018;132:89–114.
- [7] Lim W, Choi K, Moon I. Current status and perspectives of liquefied natural gas (LNG) plant design. Ind Eng Chem Res 2013;52(9):3065–88.
- [8] Chang HM. A thermodynamic review of cryogenic refrigeration cycles for liquefaction of natural gas. Cryogenics 2015;72(Part 2):127–47.
- [9] Austbo B, Løvseth SW, Gundersen T. Annotated bibliography—use of optimization in LNG process design and operation. Comput. Chem. Eng. 2014;71(Supplement C):391–414.
- [10] Yentekakis IV, Goula G. Biogas management: advanced utilization for production of renewable energy and added-value chemicals. Front Environ Sci 2017;5:1–18.
- [11] Bauer F, Persson T, Hulteberg C, Tamm D. Biogas upgrading – technology overview, comparison and perspectives for the future. Biofuels, Bioprod Biorefin 2013;7(5):499–511.
- [12] Rotunno P, Lanzini A, Leone P. Energy and economic analysis of a water scrubbing based biogas upgrading process for biomethane injection into the gas grid or use as transportation fuel. Renew Energy 2017;102(Part B):417–32.
- [13] Budzianowski WM, Wylock CE, Marciniak PA. Power requirements of biogas upgrading by water scrubbing and biomethane compression: comparative analysis of various plant configurations. Energy Convers Manage 2017;141:2–19.
- [14] Haider S, Lindbräthen A, Hagg MB. Techno-economical evaluation of membrane based biogas upgrading system: a comparison between polymeric membrane and carbon membrane technology. Green Energy Environ 2016;1(3):222–34.
- [15] Iovane P, Nanna F, Ding Y, Bikson B, Molino A. Experimental test with polymeric membrane for the biogas purification from CO₂ and H₂S. Fuel 2014;135:352–8.
- [16] Valenti G, Arcidiacono A, Nieto Ruiz JA. Assessment of membrane plants for biogas upgrading to biomethane at zero methane emission. Biomass Bioenergy 2016;85:35–47.
- [17] Ullah Khan I, et al. Biogas as a renewable energy fuel – a review of biogas upgrading, utilisation and storage. Energy Convers Manage 2017;150:277–94.
- [18] Ferella F, Puca A, Taglieri G, Rossi L, Gallucci K. Separation of carbon dioxide for biogas upgrading to biomethane. J Clean Prod 2017;164(Supplement C):1205–18.
- [19] Augelletti R, Conti M, Annesini MC. Pressure swing adsorption for biogas upgrading. A new process configuration for the separation of biomethane and carbon dioxide. J Clean Prod 2017;140(Part 3):1390–8.

- [20] Jiang Y, et al. Simultaneous biogas purification and CO₂ capture by vacuum swing adsorption using zeolite NaUSY. *Chem Eng J* 2018;334:2593–602.
- [21] Sun Q, Li H, Yan J, Liu L, Yu Z, Yu X. Selection of appropriate biogas upgrading technology—a review of biogas cleaning, upgrading and utilisation. *Renew Sustain Energy Rev* 2015;51(Supplement C):521–32.
- [22] Langé S, Pellegrini LA, Vergani P, Lo Savio M. Energy and economic analysis of a new low-temperature distillation process for the upgrading of high-CO₂ content natural gas streams. *Ind Eng Chem Res* 2015;54(40):9770–82.
- [23] Nejat T, Movasati A, Wood DA, Ghanbarabadi H. Simulated exergy and energy performance comparison of physical–chemical and chemical solvents in a sour gas treatment plant. *Chem Eng Res Des* 2018;133:40–54.
- [24] Vo TTO, Wall DM, Ring D, Rajendran K, Murphy JD. Techno-economic analysis of biogas upgrading via amine scrubber, carbon capture and ex-situ methanation. *Appl Energy* 2018;212:1191–202.
- [25] Pellegrini LA, De Guido G, Langé S. Biogas to liquefied biomethane via cryogenic upgrading technologies. *Renew Energy* 2017;124(C):75–83.
- [26] Kadam R, Panwar NL. Recent advancement in biogas enrichment and its applications. *Renew Sustain Energy Rev* 2017;73(Supplement C):892–903.
- [27] Berstad D, Nekså P, Anantharaman R. Low-temperature CO₂ removal from natural gas. *Energy Procedia* 2012;26:41–8.
- [28] Yousef AM, Eldrainy YA, El-Maghlany WM, Attia A. Upgrading biogas by a low-temperature CO₂ removal technique. *Alexandria Eng J* 2016;55(2):1143–50.
- [29] Yousef AM, Eldrainy YA, El-Maghlany WM, Attia A. Biogas upgrading process via low-temperature CO₂ liquefaction and separation. *J Nat Gas Sci Eng* 2017;45:812–24.
- [30] Baccanelli M, Langé S, Rocco MV, Pellegrini LA, Colombo E. Low temperature techniques for natural gas purification and LNG production: an energy and exergy analysis. *Appl Energy* 2016;180(Supplement C):546–59.
- [31] Holmes AS, Ryan JM. Cryogenic distillative separation of acid gases from methane. Google Patents 1982.
- [32] Holmes AS, Ryan JM. Distillative separation of carbon dioxide from light hydrocarbons. Google Patents, 1982.
- [33] Clodic D, Younes M. A new method for CO₂ capture: frosting CO₂ at atmospheric pressure. Presented at the sixth international conference on greenhouse gas control technologies. 2002.
- [34] Clodic D, El Hitti R, Younes M, Bill A, Casier F. CO₂ capture by anti-sublimation thermo-economic process evaluation. Presented at the 4th annual carbon sequestration conference. 2005. Alexandria, United States.
- [35] Baccioli A, Antonelli M, Frigo S, Desideri U, Pasini G. Small scale bio-LNG plant: comparison of different biogas upgrading techniques. *Appl Energy* 2018;217:328–35.
- [36] Birgen C, Garcia Jarque S. Investigation of cryogenic technique for synthetic natural gas upgrading. *Int J Hydrogen Energy* 2015;40(34):11161–7.
- [37] Gandhidasan P. Parametric analysis of natural gas dehydration by a triethylene glycol solution. *Energy Sources* 2003;25(3):189–201.
- [38] Netusil M, Ditl P. Comparison of three methods for natural gas dehydration. *J Nat Gas Chem* 2011;20(5):471–6.
- [39] Kinigoma BS, Ani GO. Comparison of gas dehydration methods based on energy consumption. *J Appl Sci Environ Manage* 2016;20(2):253–8.
- [40] Aspelund A, Berstad DO, Gundersen T. An Extended Pinch Analysis and Design procedure utilizing pressure based exergy for subambient cooling. *Appl Therm Eng* 2007;27(16):2633–49.
- [41] AspenTech, Aspen Hysys Guide. Property methods and calculations, 2017.
- [42] Kelley BT, Valencia JA, Northrop PS, Mart CJ. Controlled Freeze Zone™ for developing sour gas reserves. *Energy Procedia* 2011;4:824–9.
- [43] Stoecker WF. Design of thermal systems. third ed. New York: McGraw-Hill; 1989.

Optimization of an absorption-based biogas upgrading and liquefaction process

SAYED EBRAHIM HASHEMI¹, KRISTIAN M. LIEN¹, SONDRÉ K. SCHNELL² AND BJØRN AUSTBØ^{1,*}

1. DEPARTMENT OF ENERGY AND PROCESS ENGINEERING,
NORWEGIAN UNIVERSITY OF SCIENCE AND TECHNOLOGY,
NO-7491 TRONDHEIM, NORWAY

2. DEPARTMENT OF MATERIAL SCIENCE AND ENGINEERING,
NORWEGIAN UNIVERSITY OF SCIENCE AND TECHNOLOGY,
NO-7491 TRONDHEIM, NORWAY

* CORRESPONDING AUTHOR

THIS ARTICLE WAS PUBLISHED IN *CHEM. ENG. TRANS.* (2019) 76: 697.



Optimization of an Absorption-Based Biogas Upgrading and Liquefaction Process

Sayed Ebrahim Hashemi^a, Kristian M. Lien^a, Sondre K. Schnell^b, Bjørn Austbø^{a,*}

^aDepartment of Energy and Process Engineering, Norwegian University of Science and Technology (NTNU), NO-7491 Trondheim, Norway

^bDepartment of Materials Science and Engineering, Norwegian University of Science and Technology (NTNU), NO-7491 Trondheim, Norway
 bjorn.austbo@ntnu.no

The present work proposes a methodology for optimization of a liquefied biomethane (LBM) production plant. The LBM production plant comprises amine-based absorption upgrading followed by a single expander refrigeration cycle. The processes were modeled using Aspen HYSYS[®] and optimized through a Sequential Quadratic Programming algorithm. Any changes in the operating conditions of the upgrading process will affect the cooling demand in the liquefaction, while the opposite is not true. Based on this, a sequential optimization approach starting with the upgrading process is proposed. In order to accommodate the connection between the processes, different objective functions were formulated for the sequential optimization approach. The results from the sequential approach were compared with an overall optimization approach, where the entire LBM plant was optimized simultaneously. The results indicate that the same solution was obtained both for the sequential approach and the simultaneous approach. For the sequential approach, however, the best result was observed when the interaction between the upgrading and liquefaction processes was accounted for by considering the effect of the upgrading process on the exergy requirement in the liquefaction process.

1. Introduction

Mitigation of CO₂ from the transportation sector is challenging as fossil fuels are still dominant. Facilitating the use of alternative fuels characterized by higher energy density increases the share of sustainable energy in this sector (REN21, 2018). As an alternative fuel for heavy-duty vehicles, liquefied biomethane (LBM) produced from biogas has gained much interest because it can replace liquefied natural gas (LNG). However, production of LBM involves two energy intensive processes: biogas upgrading and liquefaction.

In biogas upgrading, the amount of CO₂ and trace compounds is reduced in order to produce high quality biomethane. Amine-based absorption is a widely used technology for gas separation in various industrial applications that can also be applied for biogas upgrading. As opposed to alternative upgrading methods such as membrane separation, pressure swing adsorption or water scrubbers, biogas upgrading through amine-based absorption can satisfy the specific purification requirements in LBM production (i.e. CO₂ content below 50 ppm (Bauer et al., 2013)) without additional polishing steps (Hashemi et al., 2019).

The energy supply to an LBM production plant with absorption upgrading consists of compression work and heat for amine regeneration. Law et al. (2017) optimized the energy and CO₂ removal efficiency of an absorption unit, observing large reductions in operating cost. Maile et al. (2017) conducted experiments regarding biogas upgrading through amine-based absorption. They showed that the CO₂ removal from the biogas mixture increased as the temperature in the absorber increased. Dara and Berrouk (2017) indicated that the trade-off between solubility of the CO₂ in the chemical solvent and the kinetic of chemical reaction determined the optimum temperature of the lean amine solution for maximum CO₂ removal. Øi et al. (2014) minimized the energy use of different chemical absorption configurations, for which the best result was observed in a vapor recompression configuration.

Once high quality biomethane is obtained from the upgrading, biomethane is liquefied through a refrigeration cycle. Refrigeration cycles are well studied in literature in terms of not only process design but also energy optimization (Austbø et al., 2014). However, studies regarding the combination of a refrigeration cycle with other processes, such as biogas upgrading, has received limited attention in literature. The present work aims to develop an optimization methodology in order to minimize the exergy supply for a LBM production plant comprising amine-based absorption upgrading and a single expander refrigeration cycle. The processes are simulated using Aspen HYSYS® and optimized using a Sequential Quadratic Programming (SQP) algorithm.

2. Process description

A detailed LBM production plant layout is presented in Figure 1. The plant consists of an amine-based absorption upgrading process followed by a single expander refrigeration cycle. These two processes are connected through high quality biomethane and CO₂ streams. A detailed process description is available in the work by Hashemi et al. (2019). Biomethane and CO₂ in liquid form are considered as final product and byproduct, respectively, from the plant.

Once raw biogas is compressed in the compression unit, it enters the bottom of the absorber column and interacts with lean amine solvent from the top of the column in order to obtain high quality biomethane. Rich amine solvent from the bottom of the absorber column is depressurized through an expansion valve. After precooling a recycled lean amine solvent stream, the low-pressure rich amine solvent enters a stripper column where amine is regenerated by adding heat in the reboiler at the bottom of the stripper. The top product of the stripper column is high purity CO₂, whereas regenerated amine from the bottom of the stripper column is recycled to the absorber column. In order to compensate water and amine losses in columns, a make-up unit is considered. Moreover, cooling water is used to reduce the temperature of the lean amine solvent before it enters the absorber. Here, methyl diethanolamine (MDEA) is used as solvent.

In order to avoid ice formation during liquefaction, water is removed from the high quality biomethane and CO₂ streams in dehydration units before being sent to the liquefaction process. Here, a single expander refrigeration cycle with nitrogen as working fluid is considered. After liquefaction, the LBM stream is expanded to atmospheric pressure. The work and heat requirements in the plant are implemented independently without considering the potential energy integration.

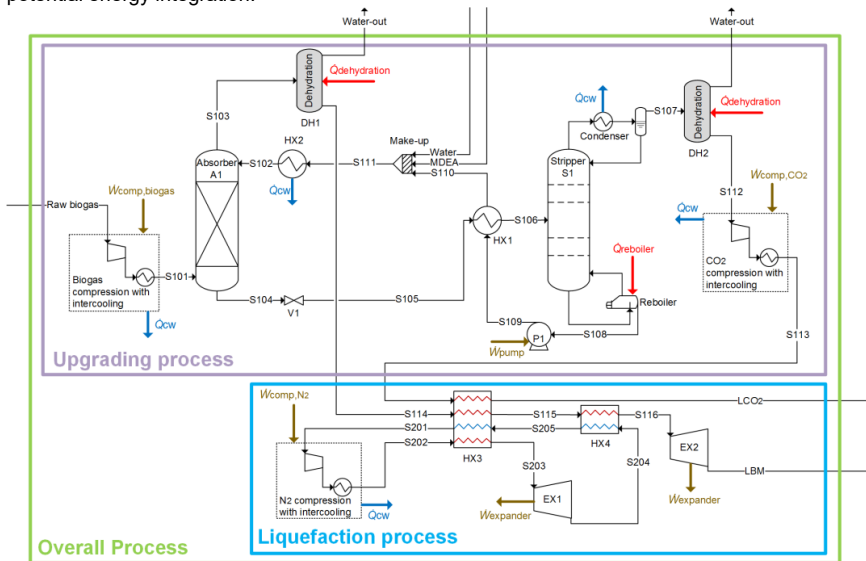


Figure 1: LBM production plant layout and different process boundaries

3. Methodology

3.1 Process modeling

The LBM production plant was simulated with Aspen HYSYS® (Aspen Technology Inc., V9.0). The Soave-Redlich-Kwong (SRK) equation of state was employed for the biogas mixture in the compression units and the

refrigeration cycle, whereas the “Acid gas – chemical solvent” package was used for the absorption process (AspenTech, 2017). The raw biogas stream contained 60 mol% CH₄, 39.9 mol% CO₂ and 0.1 mol% H₂S, with a molar flow rate of 1000 kmol/h at 35 °C and atmospheric pressure. It was assumed that the LBM was produced at atmospheric pressure with CO₂ content below 50 ppm. The LCO₂ comprised all the H₂S from the raw biogas, at 35 °C and 110 bar, which are suitable conditions for CO₂ pipeline transportation (Yousef et al., 2016).

In order to ensure satisfying the CO₂ content specification, the absorber and the stripper had 25 and 20 theoretical trays, respectively (Hashemi et al., 2019). The lean amine solvent was introduced at the 9th stage from the top of the stripper column. For the stripper, a reflux ratio of 1.25 and 95 mol% of CO₂ in the top stream were specified, which differs from what were considered in the work by Hashemi et al. (2019). MDEA with a concentration of 45 wt% was considered. In order to improve the kinetics of the chemical reaction between CO₂ and MDEA, the inlet temperature of lean amine solvent to the absorber was 10 °C higher than the temperature of the compressed raw biogas (Lange et al., 2015). The inflow streams entered the absorber column with identical pressure.

All the water present in the biomethane stream from the absorber and the CO₂ stream from the stripper was removed in the dehydration units. The dehydration units were based on tri-ethylene-glycol (TEG) absorber/regeneration columns, where the TEG regeneration temperature was assumed to be 200 °C and the outlet temperature of the dehydration units 35 °C. The heat requirement in the reboiler of the TEG regeneration column was calculated according to Hashemi et al. (2019). Furthermore, the following assumptions were taken into account in model simulations:

- Gas compression units were treated as four-stage compressors with identical pressure ratio and intercooling to 35 °C
- The cooling required in the condenser of the stripper column was provided by cooling water with inlet and outlet temperature of 20 and 25 °C, respectively
- Pressure drops in heat exchangers, columns and dehydration units were neglected, along with heat losses and gains
- Isentropic efficiency of 80 % was assumed for the compressors and the expander, while the pump had 85 % isentropic efficiency

3.2 Process evaluation

The thermodynamic performance of the LBM production plant was evaluated using exergy analysis. Exergy is supplied to the LBM production plant in the form of work (\dot{E}_x^W) and heat (\dot{E}_x^Q), which are calculated as

$$\dot{E}_x^W = \sum_i \dot{W}_i, \quad (1)$$

$$\dot{E}_x^Q = \sum_i \dot{Q}_i \cdot \left(1 - \frac{T_0}{T_i}\right). \quad (2)$$

Here, T_0 and T_i denote the ambient temperature and the temperature at which the heat (\dot{Q}_i) is transferred, respectively. Moreover, \dot{W} refers to the amount of work supplied or extracted from the plant. In this study, the exergy supply associated with heating was provided by saturated steam at 3.5 bar. The exergy of material streams was calculated by means of a Visual Basic code in Aspen HYSYS® flowsheet according to the methodology described by Kotas (2012). In this methodology, the exergy of matter is split into physical exergy and chemical exergy. Neglecting kinetic and potential energy, the physical exergy ($\bar{\epsilon}_x^{\text{phy}}$) can be expressed as

$$\bar{\epsilon}_x^{\text{phy}} = (\bar{h} - \bar{h}_0) - T_0 \cdot (\bar{s} - \bar{s}_0), \quad (3)$$

where \bar{h} and \bar{s} are the molar enthalpy and entropy of the material stream in the actual state (T, p), respectively. The subscript “0” denotes that the specific enthalpy and entropy are calculated at environment state ($T_0 = 25$ °C, $p_0 = 1$ atm = 1.01325 bar). The chemical exergy ($\bar{\epsilon}_x^{\text{chem}}$) for an ideal mixture can be expressed by

$$\bar{\epsilon}_x^{\text{chem}} = \sum_i x_i \cdot \bar{\epsilon}_{x,i}^{\text{std}} + T_0 \cdot \bar{R} \cdot \sum_i x_i \cdot \ln x_i, \quad (4)$$

where x_i and $\bar{\epsilon}_{x,i}^{\text{std}}$ are the molar fraction and standard chemical exergy of component “i” in the mixture, respectively. \bar{R} is the universal gas constant. The standard chemical exergy of each component was obtained in reference tables provided by Szargut et al. (1988). However, the standard chemical exergy of MDEA in liquid phase was estimated according to the group contribution method proposed by Szargut et al. (1988). In this method, the standard chemical exergy of MDEA (with molecular formula of C₅H₁₃NO₂) was estimated to 3.386·10⁶ kJ/kmol.

3.3 Process optimization

The objective of the optimization was to maximize the thermodynamic performance of the LBM production plant, for given inlet and outlet conditions (temperature and pressure), which is equivalent to minimizing the exergy

supply to the plant. Due to a large number of degrees of freedom and challenges associated with convergence of unit operations and recycles, optimizing the overall plant is challenging. Any changes in pressure, flow rate or composition of the streams leaving the upgrading process affect the operating conditions of the liquefaction process. However, changes in the liquefaction process will not influence the upgrading process. Hence, an alternative approach in which the upgrading and liquefaction processes are optimized sequentially, starting with the upgrading process, is proposed. In this case, however, the objective functions should be formulated such that they account for the effects of changes in the upgrading process on the liquefaction process.

Three different objective function formulations for the upgrading process are given in Table 1. In the first objective function (Obj1), the upgrading and liquefaction processes are optimized independently, considering only the exergy supply in the upgrading process. The purpose of the liquefaction process is to remove the heat required for liquefaction of the biomethane and CO₂ streams. Therefore, the sum of the exergy supply in the upgrading process and heat removal in the liquefaction process (\dot{Q}^{liq}) is minimized in the second objective function (Obj2). Likewise, in the third objective function (Obj3), the sum of the exergy supply in the upgrading process and the exergy of the heat removed in the liquefaction process ($\dot{E}_x^{Q,liq}$) is minimized. In all formulations, the liquefaction process is optimized by minimizing the net work supply.

Table 1: Objective function formulations for optimization of LBM production plant

Simultaneous optimization		
Overall	$\min(\dot{W}_{net}^{overall} + \dot{E}_x^{Q,reboiler} + \dot{E}_x^{Q,dehydration})$	
Sequential optimization		
	Upgrading	Liquefaction
Sequential Obj1	$\min(\dot{W}_{net}^{upg} + \dot{E}_x^{Q,reboiler} + \dot{E}_x^{Q,dehydration})$	$\min(\dot{W}_{net}^{liq})$
Sequential Obj2	$\min(\dot{W}_{net}^{upg} + \dot{E}_x^{Q,reboiler} + \dot{E}_x^{Q,dehydration} + \dot{Q}^{liq})$	$\min(\dot{W}_{net}^{liq})$
Sequential Obj3	$\min(\dot{W}_{net}^{upg} + \dot{E}_x^{Q,reboiler} + \dot{E}_x^{Q,dehydration} + \dot{E}_x^{Q,liq})$	$\min(\dot{W}_{net}^{liq})$

For this study, a limited number of degrees of freedom was examined. The chosen decision variables and inequality constraints for the upgrading and liquefaction processes are listed in Table 2. A minimum temperature difference of 2 °C was considered for the heat exchangers and the CO₂ content of the LBM stream was limited to 50 ppm. Equality constraints such as mass and energy balances were handled by the process simulator. It is worth mentioning that the selection of variable bounds is particularly important for the upgrading process due to nonlinearity of constraints and issues regarding column convergence in Aspen HYSYS[®]. In order to avoid convergence issues, secure variable bounds were determined through several simulation runs prior to optimization, although the optimization problem was limited to a certain domain. For the liquefaction process, the lower and upper pressure levels were set to 1 and 140 bar, respectively. Moreover, the upper pressure of the stripper was limited by the temperature of the reboiler, which should not exceed 127 °C (Lange et al., 2015). The proposed nonlinear optimization problem was solved using the Hyprotech SQP solver from Aspen HYSYS[®]. Based on experience, all convergence tolerances were set to 10⁻⁶ both for the optimizer and the unit operations. In order to reduce the likelihood of getting trapped in local optima, each objective function was examined with 30 random starting points. When optimizing the liquefaction process in the sequential optimization approach, the best result obtained for the upgrading process was used. The study was performed on a 2.67 GHz Intel[®] Xeon[®] X5650 CPU with 192 GB RAM.

4. Results and discussion

Variable values for the best solution obtained for each objective function formulation are given in Table 3, with corresponding objective function values in Table 4. In Table 5, the exergy supply to the two processes is given, along with the cooling demand in the liquefaction process and its corresponding exergy demand.

As expected, all the inequality constraints are active. The results indicate that the same solution is obtained for the simultaneous approach and the sequential approach with Obj3. Similar results are obtained also for Obj1 and Obj2, but with slightly larger exergy supply. However, the best solution obtained from the present work is different from the previous work provided by Hashemi et al. (2019). In the previous work, the optimization was performed based on an exhaustive search method considering sequential optimization of the absorber and the stripper. Therefore, the CO₂ content constraint dominated the optimization, resulting in lower absorber pressure and higher amine flow rate. In addition, the variable bounds for the reboiler temperature and the high pressure level in the liquefaction process have been changed due to practical considerations.

Table 2: Decision variables and constraints of optimization problem for upgrading and liquefaction

Decision variables	Unit	Variable range	Constraints
Upgrading process			
Absorber pressure (p_{S101})	bar	50 – 70	$x_{CO_2,LBM} \leq 50$ ppm
Stripper pressure (p_{S106})	bar	1 – 2	$\Delta T_{min,HX1} \geq 2$ °C
Stripper inlet temperature (T_{S106})	°C	75 – 90	
Lean amine flow rate (\dot{n}_{S102})	kmol/h	5000 – 8000	
Liquefaction process			
Refrigerant flow rate (\dot{n}_{S201})	kmol/h	1600 – 4000	$\Delta T_{min,HX3} \geq 2$ °C
Low pressure (p_{S201})	bar	1 – 7	$\Delta T_{min,HX4} \geq 2$ °C
High pressure (p_{S202})	bar	80 – 140	
Intermediate temperature (T_{S203})	°C	-50 – 30	

Table 3: Variable values for the best solution obtained for each objective function

	p_{S101} (bar)	p_{S106} (bar)	T_{S106} (°C)	\dot{n}_{S102} (kmol/h)	\dot{n}_{S201} (kmol/h)	p_{S201} (bar)	p_{S202} (bar)	T_{S203} (°C)
Simultaneous	66.6	1.7	90	5000	1789	2.1	140	5.3
Sequential Obj1	61.7	1.7	90	5361	1848	2.3	140	1.8
Sequential Obj2	66.0	1.7	90	5038	1796	2.2	140	4.8
Sequential Obj3	66.6	1.7	90	5000	1789	2.1	140	5.3

Table 4: Assessment of different objective functions

	Objective function values				Avg. running time (min)	Avg. model evaluations (-)
	Overall (kW)	Obj1 (kW)	Obj2 (kW)	Obj3 (kW)		
Simultaneous	14664	8821	11112	10102	88	64
Sequential Obj1	14701	8807	11113	10112	45	36
Sequential Obj2	14667	8817	11110	10104	61	45
Sequential Obj3	14664	8821	11112	10102	56	43

The cooling requirement of the high quality biomethane decreases with increasing pressure level in the absorber (and thereby in the liquefaction process). Since the absorber pressure is lower in the solution obtained for Obj1 than for the other formulations, the net work in the upgrading process is lowest. Nevertheless, the exergy of heat supply in the upgrading process is higher due to larger amine flow rate. Still, the smallest exergy supply to the upgrading process is observed for Obj1 because of higher savings in work. However, as the cooling requirement of the liquefaction process is larger, the exergy supply to the liquefaction process and the overall exergy supply are larger than for the other objective formulations. This interaction is accounted for in Obj2 and Obj3, but with different weighting of the cooling demand.

As can be observed in Table 3, some of variables are on the bounds, which indicates that better solutions are likely to be found if the bounds are extended. In this case, the difference between different objective formulations is also expected to be larger. The simulation model must, however, be able to handle/avoid convergence issues related to the columns in the upgrading process.

In the plant studied here, the interaction between the upgrading and liquefaction processes is limited to the pressure level of the high quality biomethane stream after upgrading, as the temperature and composition are fixed. For the high quality CO₂ stream after upgrading, both the temperature and the pressure are fixed, and the variations in composition are negligible. This partly explains the similarity in results for the different formulations. As can be observed in Table 4, the average number of model evaluations, and thereby the running time of the optimizer, is reduced when the optimization problem is solved sequentially. It is also worth mentioning that the same solution was obtained for liquefaction process regardless of the starting point, whereas the solution obtained for the upgrading process was highly dependent upon the starting point.

The results suggest that the sequential approach performs well for the optimization of the LBM production plant with amine-based absorption and a single expander refrigeration cycle for liquefaction.

Table 5: Exergy and energy supply for the LBM production for different objective functions

	Upgrading process			Liquefaction process		
	$\sum \dot{E}_x^Q$ (kW)	\dot{W}_{net}^{upg} (kW)	$\sum \dot{E}_x^{upg}$ (kW)	\dot{Q}^{liq} (kW)	$\dot{E}_x^{Q,liq}$ (kW)	\dot{W}_{net}^{liq} (kW)
Simultaneous	2,847	5,974	8,821	2,291	1,281	5,843
Sequential obj1	2,906	5,901	8,807	2,306	1,305	5,894
Sequential obj2	2,854	5,963	8,817	2,293	1,287	5,850
Sequential obj3	2,847	5,974	8,821	2,291	1,281	5,843

5. Conclusions

An LBM production plant using amine-based absorption upgrading followed by a single expander refrigeration cycle was modeled in Aspen HYSYS® and optimized using an SQP algorithm. The objective was to minimize the exergy supply to the plant in terms of work and heat. Different problem formulations in which the upgrading and liquefaction processes were optimized sequentially have been proposed and compared with a conventional approach where the whole plant is optimized simultaneously.

The results indicate that the same solution was obtained for the sequential optimization approach and the simultaneous approach. However, the objectives should be formulated such that the interaction between the two processes is accounted for, i.e. the influence of the upgrading process on the exergy demand of the liquefaction process. In this study, only a limited number of degrees of freedom was used, with relatively tight variable bounds in order to avoid convergence issues in simulation. The results suggest that further studies on the sequential optimization approach should be conducted, especially as the complexity of the two processes is increased with more design variables and larger variable ranges. In this case, the choice of objective function formulations is expected to have larger impact. For future studies, more complex refrigeration processes (e.g. mixed-refrigerant cycles) and convergence challenges will be investigated.

Acknowledgments

Financial support from the Norwegian University of Science and Technology (NTNU) through the strategic research program ENERSENSE is greatly acknowledged.

References

- Aspen Technology, Inc., 2013, Aspen Physical Property System: Physical property methods and Models. Burlington, USA.
- Austbø B., Løvseth S.W., Gundersen T., 2014, Annotated bibliography – Use of optimization in LNG process design and operation, *Computers & Chemical Engineering*, 71, 391-414.
- Bauer F., Persson T., Hulteberg C., Tamm D., 2013, Biogas upgrading – Review of commercial technologies, *Svenskt Gastekniskt Center Rapport*: 270, 1-83.
- Dara S., Berrouk A.S., 2017, Computer-based optimization of acid gas removal unit using modified CO₂ absorption kinetic models, *International Journal of Greenhouse Gas Control*, 59, 172-183.
- Hashemi S.E., Sarker S., Lien K.M., Schnell S.K., Austbø B., 2019, Cryogenic vs. absorption biogas upgrading in liquefied biomethane production – An energy efficiency analysis, *Fuel*, 245, 294-304.
- Kotas T.J., 2012, *The Exergy Method of Thermal Plant Analysis*, Exergon Publishing Company, London, UK.
- Langè S., Pellegrini L.A., Vergani P., Lo Savio M., 2015, Energy and Economic Analysis of a New Low-Temperature Distillation Process for the Upgrading of High-CO₂ Content Natural Gas Streams, *Industrial & Engineering Chemistry Research*, 54, 9770-9782.
- Law L.C., Azudin N.Y., Shukor S.R.A., 2017, Optimization of operational parameter and economic analysis of amine based acid gas capture unit, *Chemical Engineering Transactions*, 56, 73-78.
- Maile O.I., Tesfagiorgis H., Muzenda E., 2017, The potency of monoethanolamine in biogas purification and upgrading, *South African Journal of Chemical Engineering*, 24, 122-127.
- REN21, 2018, *Renewables 2018 Global Status Report*, Renewables Energy Policy Network for 21st Century <<http://www.ren21.net/gsr-2018/pages/foreword/foreword/>> accessed 14.03.2019.
- Szargut J., Morris, D.R., Steward, F.R., 1988, *Exergy Analysis of Thermal, Chemical and Metallurgical Processes*. Hemisphere Publishing Corp, New York, US.
- Yousef A.M., Eldrainy Y.A., El-Maghlany W.M., Attia A., 2016, Upgrading biogas by a low-temperature CO₂ removal technique, *Alexandria Engineering Journal*, 55, 1143-1150.
- Øi L.E., Bråthen T., Berg C., Brekne S.K., Flatin M., Johnsen R., Moen I.G., Thomassen E., 2014, Optimization of configurations for amine based CO₂ absorption using Aspen HYSYS, *Energy Procedia*, 51, 224-233.

Objective function evaluation for optimization of an amine-based biogas upgrading and liquefaction process

SAYED EBRAHIM HASHEMI¹, DONGHOI KIM² AND BJØRN AUSTBØ^{1,*}

1. DEPARTMENT OF ENERGY AND PROCESS ENGINEERING,
NORWEGIAN UNIVERSITY OF SCIENCE AND TECHNOLOGY,
NO-7491 TRONDHEIM, NORWAY

2. GAS TECHNOLOGY DEPARTMENT,
SINTEF ENERGY RESEARCH,
NO-7034 TRONDHEIM, NORWAY

* CORRESPONDING AUTHOR

THIS ARTICLE HAS BEEN SUBMITTED TO *IND. ENG. CHEM. RES.*

This paper is submitted for publication and is therefore not included.

Thermodynamic analysis of different methanation reactors for biogas upgrading

SAYED EBRAHIM HASHEMI¹, KRISTIAN M. LIEN¹, SONDRÉ K. SCHNELL² AND BJØRN AUSTBØ^{1,*}

1. DEPARTMENT OF ENERGY AND PROCESS ENGINEERING,
NORWEGIAN UNIVERSITY OF SCIENCE AND TECHNOLOGY,
NO-7491 TRONDHEIM, NORWAY

2. DEPARTMENT OF MATERIAL SCIENCE AND ENGINEERING,
NORWEGIAN UNIVERSITY OF SCIENCE AND TECHNOLOGY,
NO-7491 TRONDHEIM, NORWAY

* CORRESPONDING AUTHOR

THIS ARTICLE WAS PUBLISHED IN *COMPUT. AIDED CHEM. ENG.* (2020) 48:
367.

Thermodynamic Analysis of Different Methanation Reactors for Biogas Upgrading

Sayed Ebrahim Hashemi^a, Kristian M. Lien^a, Sondre K. Schnell^b, Bjørn Austbø^{a,*}

^a*Department of Energy and Process Engineering, Norwegian University of Science and Technology (NTNU), NO-7491, Trondheim, Norway.*

^b*Department of Materials Science and Engineering, Norwegian University of Science and Technology (NTNU), NO-7491, Trondheim, Norway.*

bjorn.austbo@ntnu.no

Abstract

Biomethane production from biogas can be increased by methanation of carbon dioxide with hydrogen through the Sabatier reaction. In this work, the performance of the methanation process is investigated under isothermal and adiabatic conditions for different temperature and pressure levels. The processes were modelled assuming equilibrium conditions, minimizing the Gibbs free energy. The results indicate that the exergy of heat removed from the process, and thereby the integration potential, increases with increasing temperature. The internal irreversibility is smaller and the heat integration potential larger for adiabatic reactors than for isothermal reactors.

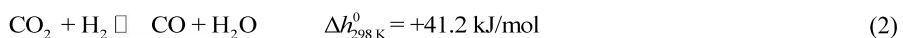
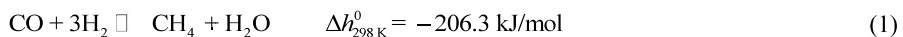
Keywords: Biogas upgrading, Sabatier reaction, Exergy analysis, Process integration

1. Introduction

The global share of renewable energy in the transportation sector is limited to 3.3 % (REN21, 2019). High quality biomethane in liquid form, with characteristics similar to liquefied natural gas (LNG), is considered to be one alternative to fossil fuels. However, production of LBM requires upgrading biogas whereby undesired contaminants (mainly CO₂) are removed, increasing the CH₄ content of the final product. In conventional approaches, biogas is upgraded through gas separation technologies such as absorption, adsorption, and membrane separation (Kadam and Panwar, 2017). One drawback of conventional biogas upgrading technologies is that the removed CO₂, typically 25–55 mol% of the biogas (Kadam and Panwar, 2017), is emitted to the atmosphere.

Recently, application of the Sabatier reaction for biogas upgrading has gained attention (Witte et al., 2018). Here, CO₂ in the raw biogas reacts with H₂ in order to increase the CH₄ content in the final product. Depending on the CO₂ content in the raw biogas, the biomethane production can increase up to 80 % compared to common biogas upgrading technologies (Witte et al., 2018). As a Power-to-Gas concept, biomethane can be used as an energy carrier for intermittent energy sources, with hydrogen produced from excess electricity (Wang et al., 2018).

The Sabatier reaction is a catalytic reaction that is a linear combination of the CO methanation reaction (Eq. (1)) and the reverse water gas shift reaction (Eq. (2)) (Witte et al., 2018):



The Sabatier reaction is typically carried out under either isothermal or adiabatic conditions. Gao et al. (2012) conducted a detailed thermodynamic equilibrium analysis for carbon oxides methanation under isothermal conditions through minimization of Gibbs free energy, reporting results in good accordance with experimental data. Jürgensen et al. (2015) considered biogas methanation through the Sabatier reaction under equilibrium and isothermal conditions. They observed that the starting temperature for carbon formation increased with increasing pressure. Moreover, they demonstrated that the CO_2 conversion was highly influenced by the CH_4 content of biogas at pressure levels below 8 bar.

The design of isothermal reactors for the Sabatier reaction is complex and costly. Hence, a series of adiabatic reactors with intercooling is often used in practice (Walspurger et al., 2014). Since heat will be available at different temperature levels for isothermal and adiabatic conditions, the heat integration potential will also be different.

This study aims to evaluate the performance of methanation reactors for biogas upgrading running under isothermal and adiabatic conditions. In addition, potential use of available heat from the reactors is examined through exergy analysis.

2. Methodology

2.1. Model description

Process configurations for isothermal and adiabatic reactors are illustrated in Figure 1. Under isothermal conditions (Figure 1 (a)), the biogas methanation takes place in a single stage reactor at constant temperature, assuming that heat is removed at the reactor temperature. Under adiabatic conditions (Figure 1 (b)), a series of reactors with intercooling is used, and heat will be removed at higher temperature than for the isothermal case. The number of reactors was chosen such that the composition of the final product stream was the same for both designs.

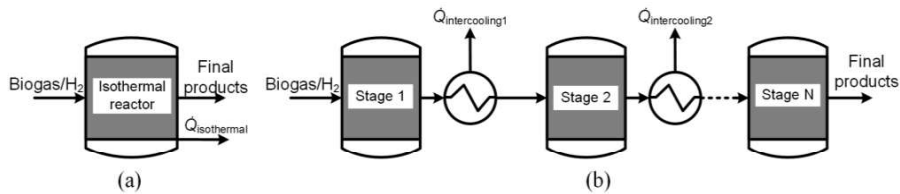


Figure 1. Methanation process configuration for (a) Single stage isothermal reactor (b) Series of adiabatic reactors with intercooling

In this study, it was assumed that equilibrium was reached in all the reactors. The two models were simulated for different temperatures and pressures with Aspen HYSYS[®] V9.0, using Gibbs reactors and Soave-Redlich-Kwong (SRK) equation of state. The advantage of using Gibbs reactors is that the final equilibrium composition is determined in accordance with the minimum Gibbs energy of the system without considering the equilibrium constants of the involving reactions. However, the Gibbs reactors do not provide information regarding kinetics or size of the reactors. The pressure drops within reactors and intercoolers were assumed negligible.

In order to make a reasonable comparison between isothermal and adiabatic conditions, it was assumed that the temperature after each intercooler was equal to the temperature of the feed stream, except for the last reactor, where the inlet temperature was manipulated in order to obtain the same final product as for the isothermal reactor.

The temperature of the isothermal reactor was assumed to be 10 °C above the feed stream temperature (Wang et al., 2018). The feed stream contained biogas (a mixture of

60 mol% CH₄ and 40 mol% CO₂) with a molar flow rate of 1 kmol/h, and H₂ with a flow rate four times as large the flow rate of CO₂ (stoichiometric ratio).

First, the performance of the Sabatier reaction was examined in terms of CO₂ conversion (Eq. (3)) and CH₄ yield (Eq. (4)), comparing the single stage isothermal reactor with the first stage of the adiabatic reactors:

$$X_{\text{CO}_2} = \frac{\dot{n}_{\text{CO}_2,\text{in}} - \dot{n}_{\text{CO}_2,\text{out}}}{\dot{n}_{\text{CO}_2,\text{in}}}, \quad (3)$$

$$Y_{\text{CH}_4} = \frac{\dot{n}_{\text{CH}_4,\text{out}} - \dot{n}_{\text{CH}_4,\text{in}}}{\dot{n}_{\text{CO}_2,\text{in}}}. \quad (4)$$

Here, \dot{n} denotes the molar flow rate.

Second, potential use of available heat from the methanation reactors was assessed through exergy analysis, comparing the single stage isothermal reactor and the complete series of adiabatic reactors with intercooling. The exergy of material streams was calculated in accordance with the methodology described by Kotas (2012), implemented as in the work by Hashemi et al. (2019). At steady state operation, the irreversibility rate within the system can be expressed as

$$\dot{I} = \dot{E}_{x,\text{in}} - \dot{E}_{x,\text{out}} + \dot{E}_x^Q, \quad (5)$$

where $\dot{E}_{x,\text{in}}$ and $\dot{E}_{x,\text{out}}$ denotes the exergy of inlet and outlet material streams, respectively. The exergy of heat is given as

$$\dot{E}_x^Q = \dot{Q} \cdot \left(1 - \frac{T_0}{T}\right), \quad (6)$$

where \dot{Q} is the amount of heat supplied (negative if removed), T_0 the ambient temperature (assumed to be 25 °C) and T the temperature at which the heat is transferred. For the intercoolers, the exergy of the heat removed is equal to the difference in exergy for the inlet and outlet material streams.

Unlike the internal irreversibilities within the methanation reactors, the exergy of the heat produced in the reactors can potentially be utilized. However, if the generated heat is not utilized, the total exergy loss in the system can be expressed as

$$\dot{E}_x^{\text{loss}} = \dot{I} - \dot{E}_x^Q \quad (7)$$

In the present study, the use of available heat was investigated only for temperatures at which the methanation reaction occurs.

3. Results and discussion

3.1. Isothermal vs. adiabatic (conversion performance)

Figure 2 illustrates the effects of temperature and pressure on CO₂ conversion and CH₄ yield for the isothermal reactor and the first stage of the adiabatic reactors. The CO₂ conversion is higher for the isothermal reactor than for the first stage of the adiabatic reactors. The CO₂ conversion decreases with increasing temperature, and is higher at higher pressure.

As can be seen from Figure 2, an increase in temperature reduces the CH₄ yield, while the CH₄ yield increases at higher pressure under both isothermal and adiabatic conditions. The changes in CO₂ conversion and CH₄ yield with temperature and pressure are smaller for the first stage of the adiabatic reactors than for the isothermal reactor.

The results demonstrate that optimal CO₂ conversion and CH₄ yield are obtained at lower temperature and higher pressure, which is in accordance with Le Chatelier's principle.

While the Sabatier reaction is limited by the chemical equilibrium at high temperature, it is limited by reaction kinetics at low temperature (depending on the type and quantity of the catalyst) (Wang et al., 2018). Hence, an operating temperature below 200 °C is not favorable. Moreover, the optimal operating pressure for the Sabatier reaction depends on the application of the produced CH₄ and a trade-off between extra compression work and improvements in the CO₂ conversion.

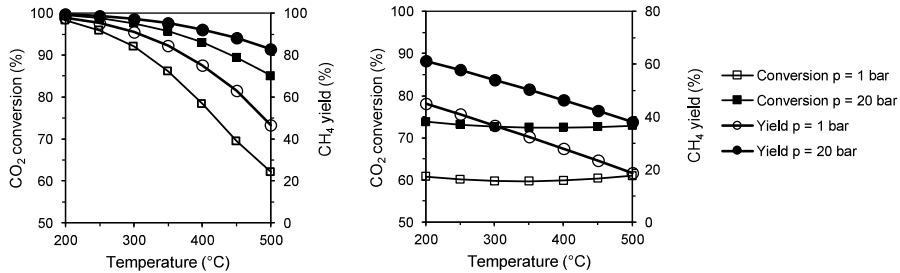


Figure 2. CO₂ conversion and CH₄ yield as functions of temperature and pressure within isothermal reactor (left) and the first stage of adiabatic reactors (right)

3.2. Isothermal vs. adiabatic (potential use of available heat)

Figure 3 demonstrates the effects of temperature and pressure on the amount of heat supplied to the isothermal reactor. The negative values illustrate exothermic reactions, where heat is removed from the reactor. The amount of heat supplied to the single stage isothermal reactor and the series of adiabatic reactors is equal since the feed and product streams are identical. The higher the pressure, the larger the heat removal from the reactor. As can be seen from Figure 3, increasing the inlet temperature reduces the heat generated within the reactor until the point at which the reaction becomes endothermic. This means that the reverse water gas shift reaction (Eq. (2)) dominates the overall reaction, producing more CO and less CH₄.

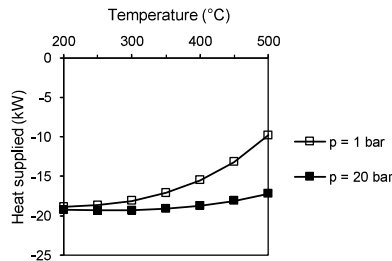


Figure 3. Heat supplied for isothermal reactor

The number of stages required under adiabatic conditions (see Figure 1 (b)) is indicated in Figure 4. The number of required stages increases with increasing feed stream temperature, while it reduces with increasing pressure.

Results from the exergy analysis for the two reactor models are given in Table 1. Since the inlet and outlet streams are the same, the total exergy loss is the same for both reactor models if the heat from the processes is not utilized. However, under adiabatic conditions, the internal irreversibility rate is smaller and the exergy content of the heat is higher (due to higher temperature). Moreover, operating the methanation reactors at lower pressure and higher temperature results in lower exergy loss within the reactors. The maximum exergy

of heat at fixed pressure is achieved at lower temperature for the methanation reactors running under adiabatic conditions

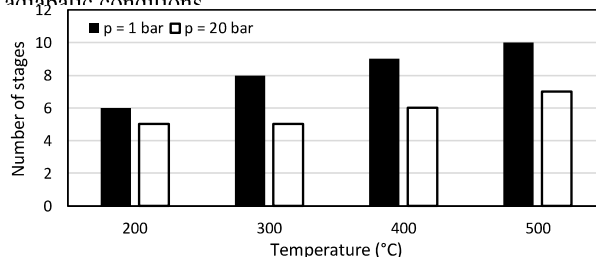


Figure 4. Required stages for adiabatic conditions as a function of temperature and pressure

As can be noticed, favourable pressure and temperature for higher CH₄ yield contradicts the reduction in the irreversibilities within the reactors. Hence, for system level process integration, the CH₄ yield must be weighed against the irreversibilities when determining the operating temperature and pressure.

Table 1 demonstrates that running the Sabatier reaction within the series of adiabatic reactors leads to the larger amounts of exergy of heat and lower irreversibilities within reactors at given temperature and pressure. This suggests that a series of adiabatic reactors could provide improved process integration potential compared to an isothermal reactor.

Table 1. Results from the exergy analysis for isothermal and adiabatic reactors

<i>Isothermal</i>								
<i>Temp.</i> (°C)	<i>p</i> = 1 bar				<i>p</i> = 20 bar			
	$\dot{n}_{CH_4,out}$ (kg/h)	\dot{I}	\dot{E}_x^Q	\dot{E}_x^{loss}	$\dot{n}_{CH_4,out}$ (kg/h)	\dot{I}	\dot{E}_x^Q	\dot{E}_x^{loss}
(kWh/kg CH ₄)								
200	15.9	0.28	-0.45	0.73	16.0	0.38	-0.46	0.84
300	15.5	0.16	-0.56	0.72	15.9	0.26	-0.59	0.84
400	14.5	0.09	-0.58	0.66	15.5	0.17	-0.67	0.84
500	12.6	0.05	-0.43	0.47	14.9	0.11	-0.69	0.80
<i>Adiabatic</i>								
200	15.9	0.16	-0.57	0.73	16.0	0.21	-0.63	0.84
300	15.5	0.10	-0.62	0.72	15.9	0.15	-0.69	0.84
400	14.5	0.06	-0.60	0.66	15.5	0.11	-0.73	0.84
500	12.6	0.04	-0.43	0.47	14.9	0.08	-0.72	0.80

In order to complete the present analysis with respect to the potential use of available heat, consideration of reaction kinetics is essential, as the performance of the reactor is highly dependent on the catalyst and operating temperature.

From a practical point of view, the application of the Sabatier reaction for biogas upgrading depends on the availability of hydrogen, because the production of hydrogen is a major cost driving factor. Besides, the temperature and pressure within the reactors influence the amount of unreacted hydrogen. In this sense, operating with less hydrogen than the stoichiometric amount and operating the series of adiabatic reactors, which improves the usable exergy of heat, might benefit the economy of the overall process. However, further studies must be conducted to determine the appropriate ratio between H₂ and CO₂.

4. Conclusions

Biogas upgrading through the Sabatier reaction was examined for a single stage isothermal reactor and a series of adiabatic reactors with intercooling, with respect to conversion of CO₂ to CH₄ and the potential use of available heat from the reactors. The reactor models were simulated in Aspen HYSYS[®] V9.0 using Gibbs reactors. The use of available heat was evaluated by exergy analysis.

The results indicate that the performance of the single stage isothermal reactor is better than the first stage of adiabatic reactors in terms of CH₄ yield. In order to achieve the isothermal performance, a series of adiabatic reactor with intercooling is required.

On the one hand, operating the methanation reactors at higher pressure and lower temperature leads to greater CO₂ conversion and CH₄ yield. On the other hand, the total exergy loss decreases with decreasing pressure and increasing temperature. The number of adiabatic reactors required to reach the same product conditions as for the isothermal reactor increases with increasing temperature and decreasing pressure. Ideally, the internal irreversibilities would be minimized and the heat integration potential maximized if the Sabatier reaction was carried out in stages at gradually reducing temperature, keeping the process close to equilibrium all the way. The heat integration potential must, however, be balanced against reaction kinetics and equipment size.

Acknowledgments

Financial support from the Norwegian University of Science and Technology (NTNU) through the strategic research program ENERSENSE is greatly acknowledged.

References

- J. Gao, Y. Wang, Y. Ping, D. Hu, G. Xu, F. Gu, F. Su, 2012, A thermodynamic analysis of methanation reactions of carbon oxides for the production of synthetic natural gas, *RSC Advances*, 2, 6, 2358-2368.
- S.E. Hashemi, K.M. Lien, S.K. Schnell, B. Austbø, 2019, Optimization of an Absorption-Based Biogas Upgrading and Liquefaction Process, *Chemical Engineering Transactions*, 76, 697-702.
- R. Kadam, N.L. Panwar, 2017, Recent advancement in biogas enrichment and its applications, *Renewable and Sustainable Energy Reviews*, 73, 892-903.
- T.J. Kotas, 2012, *The Exergy Method of Thermal Plant Analysis*, Exergon Publishing Company, London, UK.
- L. Jørgensen, E.A. Ehimen, J. Born, J.B. Holm-Nielsen, 2015, Dynamic biogas upgrading based on the Sabatier process: Thermodynamic and dynamic process simulation, *Bioresource Technology*, 178, 323-329.
- REN21, 2019, *Renewables 2019 Global Status Report*, Renewables Energy Policy Network for 21st Century, accessed 14.11.2019.
- S. Walspurger, G.D. Elzinga, J.W. Dijkstra, M. Sarić, W.G. Haije, 2014, Sorption enhanced methanation for substitute natural gas production: Experimental results and thermodynamic considerations, *Chemical Engineering Journal*, 242, 379-386.
- L. Wang, M. Pérez-Fortes, H. Madi, S. Diethelm, J.V. Herle, F. Maréchal, 2018, Optimal design of solid-oxide electrolyzer based power-to-methane systems: A comprehensive comparison between steam electrolysis and co-electrolysis, *Applied Energy*, 211, 1060-1079.
- J. Witte, J. Settino, S.M.A. Biollaz, T.J. Schildhauer, 2018, Direct catalytic methanation of biogas – Part I: New insights into biomethane production using rate-based modelling and detailed process analysis, *Energy Conversion and Management*, 171, 750-768.

Thermodynamic insight in design of methanation reactor with water removal considering nexus between CO₂ conversion and irreversibilities

SAYED EBRAHIM HASHEMI¹, KRISTIAN M. LIEN¹, MAGNE HILLESTAD³, SONDRÉ K. SCHNELL² AND BJØRN AUSTBØ^{1,*}

1. DEPARTMENT OF ENERGY AND PROCESS ENGINEERING,
NORWEGIAN UNIVERSITY OF SCIENCE AND TECHNOLOGY,
NO-7491 TRONDHEIM, NORWAY

2. DEPARTMENT OF MATERIAL SCIENCE AND ENGINEERING,
NORWEGIAN UNIVERSITY OF SCIENCE AND TECHNOLOGY,
NO-7491 TRONDHEIM, NORWAY


3. DEPARTMENT OF CHEMICAL ENGINEERING,
NORWEGIAN UNIVERSITY OF SCIENCE AND TECHNOLOGY,
NO-7491 TRONDHEIM, NORWAY

* CORRESPONDING AUTHOR

THIS ARTICLE WAS PUBLISHED IN *ENERGIES* (2021) 14(23): 7861.

Article

Thermodynamic Insight in Design of Methanation Reactor with Water Removal Considering Nexus between CO₂ Conversion and Irreversibilities

Sayed Ebrahim Hashemi ^{1,*}, Kristian M. Lien ¹, Magne Hillestad ², Sondre K. Schnell ³  and Bjorn Austbø ¹

¹ Department of Energy and Process Technology, Norwegian University of Science and Technology (NTNU), NO-7491 Trondheim, Norway; kristian.m.lien@ntnu.no (K.M.L.); bjorn.austbo@ntnu.no (B.A.)

² Department of Chemical Engineering, Norwegian University of Science and Technology (NTNU), NO-7491 Trondheim, Norway; magne.hillestad@ntnu.no

³ Department of Material Science and Engineering, Norwegian University of Science and Technology (NTNU), NO-7491 Trondheim, Norway; sondre.k.schnell@ntnu.no

* Correspondence: ebrahim.hashemi@ntnu.no

Abstract: The inevitable nexus between energy use and CO₂ emission necessitates the development of sustainable energy systems. The conversion of CO₂ to CH₄ using green H₂ in power-to-gas applications in such energy systems has attracted much interest. In this context, the present study provides a thermodynamic insight into the effect of water removal on CO₂ conversion and irreversibility within a CO₂ methanation reactor. A fixed-bed reactor with one intermediate water removal point, representing two reactors in series, was modeled by a one-dimensional pseudo-homogeneous model. Pure CO₂ or a mixture of CO₂ and methane, representing a typical biogas mixture, were used as feed. For short reactors, both the maximum conversion and the largest irreversibilities were observed when the water removal point was located in the middle of the reactor. However, as the length of the reactor increased, the water removal point with the highest conversion was shifted towards the end of the reactor, accompanied by a smaller thermodynamic penalty. The largest irreversibilities in long reactors were obtained when water removal took place closer to the inlet of the reactor. The study discusses the potential benefit of partial water removal and reactant feeding for energy-efficient reactor design.

Keywords: methanation; water removal; reactor design; CO₂ conversion; irreversibility



Citation: Hashemi, S.E.; Lien, K.M.; Hillestad, M.; Schnell, S.K.; Austbø, B. Thermodynamic Insight in Design of Methanation Reactor with Water Removal Considering Nexus between CO₂ Conversion and Irreversibilities. *Energies* **2021**, *14*, 7861. <https://doi.org/10.3390/en14237861>

Academic Editor: Pouya Ifaei

Received: 31 October 2021

Accepted: 18 November 2021

Published: 24 November 2021

Publisher's Note: MDPI stays neutral with regard to jurisdictional claims in published maps and institutional affiliations.



Copyright: © 2021 by the authors. Licensee MDPI, Basel, Switzerland. This article is an open access article distributed under the terms and conditions of the Creative Commons Attribution (CC BY) license (<https://creativecommons.org/licenses/by/4.0/>).

1. Introduction

Economic growth, energy use, and CO₂ emissions are associated with one another. He et al. [1] stated that rapid growth in the economy and energy use has caused an increase in CO₂ emissions. Pao and Tsai [2] investigated the economy-energy-sustainability nexus. They illustrated that the reduction of CO₂ emission without negative effect on the economic growth could obtain by increasing energy efficiency. Balsalobre et al. [3] pointed out that the implementation of energy strategies that emphasizes shifting towards renewable energy sources could effectively reduce the dependency on fossil fuels, and thereby also reduce CO₂ emissions.

In modern energy systems, an increased share of renewable energy sources like solar and wind has been seen as a solution for mitigating CO₂ emissions [4]. However, the intermittent nature of renewable energy sources entails a need to consider energy storage when renewable power generation does not match the demand [5]. Among possible energy storage technologies [5,6], Power-to-Gas (PtG) concepts provide the possibility of converting surplus renewable electricity to chemical energy through the production of energy carrier components such as hydrogen (H₂), methane (CH₄), and methanol (CH₃OH) [7].

Essentially, the production of H₂ from water electrolysis run by surplus renewable electricity is considered the first step in these PtG applications. The production of H₂ from renewable energy has multiple advantages such as low harmful emissions fewer steps of energy conversion to produce alternative fuel from renewable electricity, and direct utilization in fuel cell vehicles. Nonetheless, lacking storage capacity and distribution infrastructure limit the use of H₂ [8]. An alternative is the further chemical conversion of the H₂ into other energy carriers, e.g., CH₄ or CH₃OH. Although the overall process efficiency is reduced by additional chemical conversion steps, higher energy density and mature infrastructure motivate the use of alternatives [9]. Moreover, CH₄ is used for power generation, transportation, and as a precursor for other chemicals [9,10]. In PtG applications, the methane is produced through catalytic or biological methanation using CO₂ from renewable carbon sources such as biogas, or captured CO₂ from industrial processes, and H₂ from water electrolysis.

In catalytic methanation, CO₂ reacts with H₂, in the presence of a catalyst, through a reversible and highly exothermic reaction, known as the Sabatier reaction, producing CH₄ and water (H₂O) [11].



Although methanation has been in use for many years in different industries like ammonia production plants and synthetic natural gas (SNG) production, the development of the methanation reactor design is still an attractive topic in research to improve the performance of the methanation process in terms of CO₂ conversion, cost efficiency, and stability of the reactor with respect to the load fluctuation from renewable sources [12]. The traditional methanation reactors are fixed-bed reactors (FBR) [13–18] and fluidized bed reactors [19–21]. Recently, three-phase slurry reactors [22–24] and microchannel reactors [25,26] have also been developed for the methanation process. Inclusive reviews of the mentioned reactor concepts can be found in the literature [7,12]. The majority of commercial CO₂ methanation processes are based on catalytic FBR, operating under adiabatic conditions in a series of reactors with intermediate cooling or operating under isothermal conditions [12]. Hashemi et al. [27] indicated that the operation of the methanation process in a series of adiabatic reactors would reduce the irreversibility rate within the reactors, in comparison with isothermal reactors, improving the process integration potentials.

One important aspect of the methanation reactor design is the highly exothermic nature of the CO₂ methanation reaction, and many reactor concepts have been developed to overcome challenges regarding heat management and temperature control along the reactor [12]. Optimal heat management within the reactor can lead to higher CO₂ conversion. Sun et al. [28] performed a simulation-based study considering a kinetic model for the CO₂ methanation in an FBR to observe the effect of heat removal on the methane yield. They proposed a new design configuration with a molten salt-cooled heat exchanger to improve the cooling rate within the reactor, leading to increased methane yield. In another work by Sun et al. [29], it was observed that the molten salt flow rate, which indicated the cooling rate, was a crucial parameter for the reactor performance. They observed that the methane yield improved with reduced temperature (increased cooling rate), but also that overcooling would hinder the reaction. Moreover, they demonstrated that although the methane yield improved by increasing the space velocity, there was a threshold above which further increase in the space velocity led to reduced conversion. Kiewidt and Thöming [30] proposed a method to optimize the temperature profile within an FBR by balancing the heat production rate and the cooling rate. They illustrated that the methane yield improved by optimizing the temperature profile. Their results demonstrated that the optimal temperature profile was located between the temperature profiles obtained from isothermal and adiabatic operations, when balancing the kinetics and thermodynamic limitations along the reactor.

In PtG applications, it is essential to convert as much H₂ as possible since it is a major driving factor for the cost [29]. Improving the hydrogen conversion is equivalent

to improving the CO₂ conversion for a given amount of hydrogen. Besides the reactor design aspects concerning heat management within the reactor, many studies regarding reactor design focus on CO₂ conversion improvement by manipulating thermodynamic equilibrium within the reactor.

Water removal in the methanation process can shift the thermodynamic equilibrium of the Sabatier reaction towards the product side, enhancing the CO₂ conversion. Recently, this has triggered reactor concepts such as sorption enhanced methanation (SEM) and water-selective membrane reactors (MR) [9,31]. Within SEM and MR concepts, the produced H₂O in the methanation process is locally removed from the gas phase stream within the reactor by means of sorption materials such as zeolite and silica. A complete overview regarding SEM and MR with respect to sorption materials and reactor configuration design can be found in the work by van Kampen et al. [32] and Diban et al. [33], respectively.

Walspurger et al. [34] investigated the effect of water removal in an SEM reactor experimentally. They indicated that a CO₂ conversion near to 100% was possible in an SEM reactor with a commercial nickel-based catalyst and zeolite 4A as H₂O adsorbent when the operating temperature was between 250 and 350 °C. Based on Gibbs' free energy minimization, Faria et al. [35] studied in-situ water removal in an equilibrium model methanation reactor. In addition to the species present in the Sabatier reaction, they also included carbon monoxide and coke in their simulations. They illustrated that the CO₂ conversion increased with increasing water removal fraction, independently of the operating temperature and pressure. However, the methane yield was maximized at an optimal water removal fraction, depending on the temperature and pressure, above which coke formation was observed [35]. Najari et al. [36] investigated the effect of in-situ water removal from a methanation reactor using kinetic models. They illustrated that removing water locally improved the reactor performance in terms of conversion, but this also increased the risk of hot spots within the reactor, which could have a negative impact on the functionality of the catalysts [36]. Their study suggested that further examination of the effects of kinetics and temperature on the reactor performance was required [36].

Although in-situ water removal provides apparent advantages for the methanation process from a thermodynamic point of view, practical aspects, such as heat management and membrane characterization, must also be considered [32]. For reactors operated in series, as previously mentioned, water may be removed in between the stages, as an alternative to in-situ water removal. This suggests investigating the effect of water removal in stages can be considered an alternative to continuous water removal through SEM or MR. Hillestad [37] proposed a systematic staging method for the design of chemical reactors. He demonstrated that staging provided additional degrees of freedom to obtain better performance in the reactor.

Even though water removal between the methanation reactor stages has been considered as a method to increase the CO₂ conversion, investigation regarding how the design of staging with intermediate water removal should consider the reactor length (i.e., representing reactor volume) is missing in the literature. In this regard, the optimal water removal location point is expected to be dependent on the length of the reactor. Further, the energy efficiency of methanation reactors with intermediate water removal has received limited attention in the literature; most research studies in the field of reactor design emphasize performance improvement in terms of CO₂ conversion and heat management. The present study aims to fill these research gaps by conducting a fundamental thermodynamic study to examine the concept of water removal for different reactor lengths. The optimal water removal point within a reactor is determined for different operating conditions. The performance of the reactor is assessed in terms of improvement in the CO₂ conversion. Moreover, alternative objectives related to the total irreversibility within the reactor and the minimum required work for water removal are also discussed.

In Section 2, the reactor model development, reaction kinetics, and numerical solution strategy for the model are given. The methods employed to investigate the effect of water removal at different locations along the reactor are explained in Section 3. Further, a de-

scription regarding the calculation of irreversibility rate and minimum work requirements for water removal is presented. Results for the optimal location for water removal in the reactor with respect to conversion and irreversibility are presented in Section 4. Remarks and suggestions for further studies are provided in Section 5. Finally, conclusions are presented in Section 6.

2. Model Development

According to the conclusions drawn by Fischer et al. [38], a simplified one-dimensional pseudo-homogenous model, known as a plug flow reactor (PFR) model, provides sufficient accuracy to predict the CO₂ conversion within an FBR. In the present study, the pseudo-homogeneous model was combined with an effectiveness factor to accommodate the intra-particle mass and heat transport limitations between solid (catalyst pellets) and fluid (gas mixtures) phases [30]. Here, it was assumed that a concept similar to the isothermal reactor concept developed by Linde can provide isothermal operating conditions for the methanation [39]. However, it should be noted that operating under isothermal conditions is a challenging task in practice, and might not be economically feasible, as the highly active catalyst causes large heat production and potential hot spots in the reactor. The irreversibility associated with heat transfer may contribute significantly to overall process irreversibility. Test simulations within this study showed that the pressure drop along the reactor length (obtained from the Ergun equation) was on a scale of 0.1 kPa for the studied dimension and flow rates. Therefore, the pressure drop in the reactor was neglected in the PFR model, to focus on the variation of driving forces caused by reaction along the reactor. Further, the ideal gas law was applied as an equation of state. The mathematical model for the FBR is presented in the following subsections.

2.1. Reactor Modeling

The FBR in the present study was modeled by considering a plug flow reactor [40] assuming steady-state conditions. In the plug flow assumption, gradients of temperature and concentration are only considered in the axial direction, not the radial direction or the angular direction. Material balances for all the chemical substances involved along the length of the reactor (CO₂, H₂, CH₄, and H₂O) can be expressed as

$$\frac{dF_i}{dx} = \rho_c \cdot (1 - \varepsilon) \cdot A_c \cdot \eta \cdot \nu_i \cdot r. \quad (2)$$

Here, F_i is the molar flow rate of component i in the direction x along the reactor, while ρ_c , ε , and A_c denote the catalyst density, the void fraction, and the cross-sectional area of the reactor, respectively. Further, ν_i is the stoichiometric coefficient of component i in reaction (1). Explicit expressions for the reaction rate (r) and the effectiveness factor (η) are given in the following subsections.

2.2. Reaction Kinetics

The kinetic model of Koschany et al. [41], where the CO₂ methanation reaction over a Ni-based catalyst is considered, was used in this work. The reaction kinetics, and thereby the CO₂ conversion, is influenced by the operating temperature, pressure, and inlet gas mixture composition. The reaction rate model of Koschany et al. [41] can be applied in temperature and pressure ranges of 180–340 °C and 1–15 bar, respectively. Under these conditions, the CO methanation through reverse-water-gas-shift (RWGS) is limited; hence considering only the CO₂ methanation reaction is reasonable [42]. The reaction rate is based on a Langmuir-Hinshelwood-Hougen-Watson approach as follows:

$$r = \frac{k \cdot p_{\text{H}_2}^{0.5} \cdot p_{\text{CO}_2}^{0.5} \cdot \left(1 - \frac{p_{\text{CH}_4} \cdot p_{\text{H}_2\text{O}}^2}{p_{\text{CO}_2} \cdot p_{\text{H}_2}^4 \cdot K_{\text{eq}}}\right)}{\left(1 + K_{\text{OH}} \cdot \frac{p_{\text{H}_2\text{O}}}{p_{\text{H}_2}^{0.5}} + K_{\text{H}_2} \cdot p_{\text{H}_2}^{0.5} + K_{\text{mix}} \cdot p_{\text{CO}_2}^{0.5}\right)^2}. \quad (3)$$

Here, p_i is the partial pressure of component i . The rate constant (k) and adsorption constants (K_j) are calculated in accordance with Arrhenius and van 't Hoff-type equations, respectively, as follows:

$$k = k_{\text{ref}} \cdot \exp\left(\frac{E_a}{R} \cdot \left(\frac{1}{T_{\text{ref}}} - \frac{1}{T}\right)\right), \quad (4)$$

$$K_j = K_{j,\text{ref}} \cdot \exp\left(\frac{\Delta H_j}{R} \cdot \left(\frac{1}{T_{\text{ref}}} - \frac{1}{T}\right)\right). \quad (5)$$

Here, E_a and ΔH are activation energy and enthalpy of adsorption, respectively. T and R are the temperature and the universal gas constant, respectively. The equilibrium constant (K_{eq}) is approximated as [43]

$$K_{\text{eq}} = 137 \cdot T^{-3.998} \cdot \exp\left(\frac{158.7 \frac{\text{kJ}}{\text{mol}}}{RT}\right). \quad (6)$$

The values of the kinetic model parameters are given in Table 1.

Table 1. Values of kinetics model parameters [41].

Variable	T_{ref}	k_{ref}	E_a	$K_{\text{OH},\text{ref}}$	ΔH_{OH}	$K_{\text{H}_2,\text{ref}}$	ΔH_{H_2}	$K_{\text{mix},\text{ref}}$	ΔH_{mix}
Unit	K	mol/bar·s·kg _{cat}	kJ/mol	bar ^{-0.5}	kJ/mol	bar ^{-0.5}	kJ/mol	bar ^{-0.5}	kJ/mol
Value	555	3.46·10 ⁻¹	77.5	0.5	22.4	0.44	-6.2	0.88	-10

2.3. Effectiveness Factor

In comparison to CO₂, H₂ diffuses much faster into the catalyst pellets. Thereby, an adopted Thiele modulus can be used to calculate the effectiveness factor, assuming CO₂ to be the limiting species for intra-particle mass transport [30]. The effectiveness factor for spherical catalyst pellets is given as

$$\eta = \frac{3}{\phi} \left(\frac{1}{\tanh\phi} - \frac{1}{\phi} \right), \quad (7)$$

where the Thiele modulus (ϕ) can be calculated considering CO₂ as the key species in the determination of the mass transfer limitations:

$$\phi = \frac{D_p}{2} \sqrt{\frac{r \cdot \rho_c \cdot (1 - \varepsilon) \cdot R \cdot T}{D_{\text{CO}_2}^{\text{eff}} \cdot y_{\text{CO}_2} \cdot p \cdot 10^5}}. \quad (8)$$

Here, D_p and y_{CO_2} denote the catalyst pellets diameter and the mole fraction of CO₂ in the gas mixture, respectively. The effective CO₂ diffusivity ($D_{\text{CO}_2}^{\text{eff}}$) is calculated according to the Bosanquet equation taking into account molecular diffusion ($D_{\text{CO}_2}^m$) for gas-gas collisions and Knudsen diffusion ($D_{\text{CO}_2}^{\text{kn}}$) for gas-wall collisions [30]:

$$\frac{1}{D_{\text{CO}_2}^{\text{eff}}} = \frac{\tau_p}{\varepsilon_p} \left(\frac{1}{D_{\text{CO}_2}^m} + \frac{1}{D_{\text{CO}_2}^{\text{kn}}} \right). \quad (9)$$

The effective CO₂ diffusivity ($D_{\text{CO}_2}^{\text{eff}}$) takes into account the catalyst pellet configuration through particle porosity (τ_p), tortuosity (ε_p), average pore diameter (D_{pore}), and molecular

interaction between different species [17]. The molecular diffusion is based on a simplified form of the mixture-averaged diffusion coefficient by Maxwell-Stefan [44]:

$$\frac{1}{D_{\text{CO}_2}^m} = \sum_i \frac{y_i}{D_{ij}} + \frac{y_j}{1 - w_j} \sum_i \frac{w_i}{D_{ij}}. \quad (10)$$

Here, $i = \text{H}_2, \text{CH}_4$ and H_2O and $j = \text{CO}_2$. Further, y and w are the mole fraction and the mass fraction, respectively. The binary diffusion coefficients (D_{ij}) are calculated by the equations from Fuller et al. [45]:

$$D_{ij} = \frac{0.00143 \cdot T^{1.75} \cdot \left(\frac{1}{M_i} + \frac{1}{M_j}\right)^{\frac{1}{2}}}{p \cdot \left((v_i)^{\frac{1}{3}} + (v_j)^{\frac{1}{3}}\right)^2}. \quad (11)$$

Here, M_i is the molar mass of component i , and v_i is the specific diffusion volume of component i (26.9, 7.07, 24.42, and 12.7 for $\text{CO}_2, \text{H}_2, \text{CH}_4$, and H_2O , respectively) [45]. The Knudsen diffusion is computed as follows, considering only CO_2 :

$$D_{\text{CO}_2}^{kn} = \frac{D_{\text{pore}}}{3} \sqrt{\frac{8 \cdot R \cdot T}{\pi \cdot M_{\text{CO}_2}}}. \quad (12)$$

2.4. Numerical Solution Strategy

The balance equations and the correlations for reaction rates and effectiveness factors generate a set of ordinary differential equations (ODEs). The ODEs were solved with MATLAB[®] R2019a using the *ode15s* function. To solve the ODEs, the initial molar flow of components at the inlet of the reactor is required. A good trade-off between model precision and computational time is achieved by assuming an equidistant step size (representing the cell size along the reactor) of 0.001 m and a relative error tolerance of 10^{-8} . Here, the relative error tolerance refers to the considered significance of digits for the computation of the ODEs. The water removal is implemented numerically by adjusting the molar flow of water to zero at the step where water removal is taking place. The reactor specifications and input values for the model are given in Table 2.

Table 2. Reactor specifications in the PFR model.

Parameter	Unit	Value	Ref.
Temperature range	K	500–600	[41]
Pressure range	bar	1–15	[41]
Catalyst density	kg/m ³	2355.2	[41]
Catalyst void fraction	-	0.4	[17]
H ₂ /CO ₂ ratio	-	4	-
CH ₄ /CO ₂ ratio range	-	0–1.5	-
Inlet CO ₂ molar flow rate	mol/s	0.002	-
Tube diameter	m	0.0254	-
Catalyst diameter	m	0.002	[17]
Catalyst pore diameter	nm	10	[17]
Catalyst porosity	-	0.6	[17]
Catalyst tortuosity	-	2	[17]
Ambient temperature	K	298.15	-
Ambient pressure	bar	1.01325	-

3. Methodology

The hypothesis behind removing water at different positions along an FBR is that the CO_2 conversion (and thereby the CH_4 yield) would change by moving the water removal position. In the present study, water is only removed at one point along the reactor, and

the influence of moving the water removal point on the CO₂ conversion is investigated. For the sake of fair comparison, the water produced after the water removal point is removed at the end of the reactor. Before studying the effect of water removal, the reactor length required to reach equilibrium without water removal is identified. At equilibrium, the reaction rate approaches zero, which would require an infinitely long reactor. Here, the equilibrium length ($L_{EQ,1}$) is defined as the point at which 99.9% of the equilibrium conversion is obtained. It is worth mentioning that the equilibrium length of the reactor is correlated to the tube diameter. The smaller the tube diameter, the longer is the reactor required to reach the equilibrium composition.

Figure 1a illustrates a tubular FBR, with diameter D and the equilibrium length ($L_{EQ,1}$), in which the entire water removal takes place at the end of the reactor. The case with intermediate water removal along the reactor length is demonstrated in Figure 1b. Conventional directions of material and energy streams are specified in Figure 1. When studying the effect of water removal, reactors lengths (L) shorter than the equilibrium length are examined, varying the water removal point along the reactor. Water is removed at a point z along the reactor. In practice, this assumption can be interpreted as dividing the original reactor with length L into two reactors with lengths of z and $L-z$, with water removal between the two reactors. In this work, it is assumed that 100% of produced water present at this location is removed. A case with no internal water removal (WR) (i.e., all water removed at the end of the reactor) is given by $z = 0$ or $z = L$. Even though 100% continuous water removal along the reactor is practically impossible, a continuous WR case is considered to account for the theoretical cases of SME and MR. In this case, the water produced in each cell of the reactor model is assumed to be removed in the same cell.

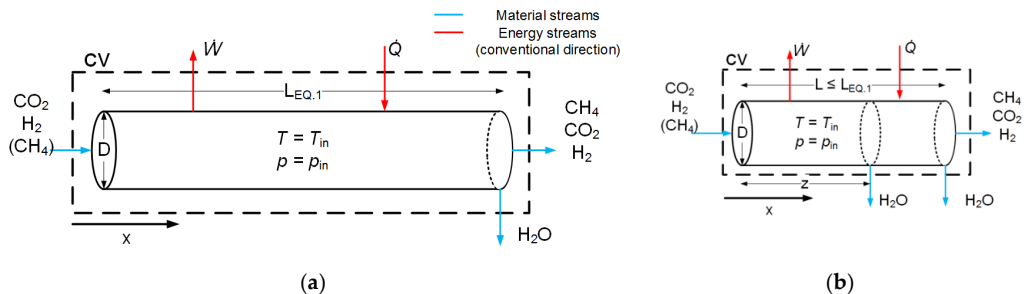


Figure 1. A schematic of a tubular FBR operating under isothermal conditions; (a) equilibrium length case, (b) intermediate water removal case.

Here, the ratio between H₂ and CO₂ is equal to the stoichiometric ratio of the Sabatier reaction (i.e., 4). Moreover, the ratio between CH₄ and CO₂ (here defined as A) is zero or 1.5, representing pure CO₂ methanation and methanation of a biogas mixture with 60 mol% CH₄ and 40 mol% CO₂, respectively. In the present study, the initial CO₂ molar flow rate is kept constant; accordingly, the initial molar flow rate of H₂ and CH₄ is calculated using the stoichiometric ratio between H₂ and CO₂ and the studied ratio between CH₄ and CO₂, respectively.

The performance of the reactor is evaluated with respect to the CO₂ conversion and the irreversibilities within the reactor. The CO₂ conversion is defined as the change between inlet and outlet CO₂ molar flow in the reactor:

$$X_{CO_2} = \frac{F_{CO_2}^{in} - F_{CO_2}^{out}}{F_{CO_2}^{in}} \quad (13)$$

Since only the Sabatier reaction is considered, the CO₂ conversion will also represent the methane yield from the reactor. In order to compare the effect of water removal for different reactor lengths, the relative conversion improvement (RX_{CO_2}) is defined as the

CO₂ conversion improvement for the optimum water removal location compared to the case with no water removal:

$$RX_{\text{CO}_2} = \frac{X_{\text{CO}_2, \text{opt}} - X_{\text{CO}_2, \text{no WR}}}{X_{\text{CO}_2, \text{no WR}}}. \quad (14)$$

As the amount of water removed from the reactor and the CO₂ conversion change with the water removal location, the work requirement for water removal and the irreversibility rate within the reactor also change. These changes are investigated using exergy analysis. The total irreversibility rate (\dot{I}) within the reactor at steady-state operation, illustrated in Figure 1 is calculated based on changes in exergy of material streams ($\Delta\dot{E}_{x, \text{streams}}$), the exergy of heat rejected from the reactor ($\dot{E}_x(\dot{Q})$) and the work required for water removal within the reactor (\dot{W}) according to the methodology described by Kotas [46]:

$$\dot{I} = \Delta\dot{E}_{x, \text{streams}} + \dot{E}_x(\dot{Q}) - \dot{W}, \quad (15)$$

$$\Delta\dot{E}_{x, \text{streams}} = \sum \dot{n}_i \cdot \bar{e}_{x,i} - \sum \dot{n}_e \cdot \bar{e}_{x,e}, \quad (16)$$

$$\dot{E}_x(\dot{Q}) = \int \left(1 - \frac{T_0}{T}\right) \cdot \delta\dot{Q}. \quad (17)$$

Here, \dot{n}_i is the molar flow rate and \bar{e}_x is the molar exergy, calculated for inlet streams i and outlet streams e . Further, \dot{Q} is the heat flow transferred to the reactor at reactor temperature T and \dot{W} is the power delivered from the reactor. The subscript "0" denotes environment state (here $T_0 = 298.15$ K, $p_0 = 1$ atm = 1.01325 bar). In this study, it is assumed that water removal takes place in a reversible process; hence, \dot{W} represents the minimum work required for water removal.

The molar exergy of material streams can be decomposed into physical exergy (\bar{e}_x^{phy}) and chemical exergy (\bar{e}_x^{chem}):

$$\bar{e}_x = \bar{e}_x^{\text{phy}} + \bar{e}_x^{\text{chem}}. \quad (18)$$

By neglecting kinetic and potential energy effects, \bar{e}_x^{phy} can be expressed as

$$\bar{e}_x^{\text{phy}} = (\bar{h} - \bar{h}_0) - T_0 \cdot (\bar{s} - \bar{s}_0). \quad (19)$$

Based on ideal gas and ideal mixture assumptions, the molar enthalpy and entropy of the mixtures can be calculated as

$$(\bar{h} - \bar{h}_0) = \sum y_i \cdot (\bar{h}_i(T) - \bar{h}_i(T_0)), \quad (20)$$

$$(\bar{s} - \bar{s}_0) = \sum y_i \cdot (\bar{s}_i(T, p_i) - \bar{s}_i(T_0, p_{0,i})). \quad (21)$$

Here, y_i is the molar fraction of component i in the mixture, while \bar{h} and \bar{s} refer to the molar enthalpy and entropy of the material stream, respectively. The chemical exergy of an ideal mixture can be calculated as

$$\bar{e}_x^{\text{chem}} = \sum y_i \cdot \bar{e}_{x,i}^{\text{std}} + T_0 \cdot \bar{R} \cdot \sum y_i \cdot \ln y_i. \quad (22)$$

The standard chemical exergy of component i in the mixture (\bar{e}_x^{chem}) is obtained from the reference tables provided by Kotas [46]. Further, \bar{R} is the universal gas constant.

4. Results

4.1. Conversion

According to thermodynamic principles, operating the reactor at a lower temperature and higher pressure is favorable for improving the CO₂ conversion due to the highly

exothermic nature of the Sabatier reaction and the volume reduction after conversion. Figure 2 illustrates the CO_2 conversion within the FBR operating under different conditions when reaction (1) reaches equilibrium. As is expected, higher CO_2 conversion is obtained by increasing the operating pressure and lowering the reactor temperature. Moreover, additional CH_4 in the inlet gas mixture (i.e., cases with $A = 1.5$) results in a reduction of the CO_2 conversion. Since CH_4 is one of the products in the reaction, the presence of CH_4 in the feed shifts the equilibrium composition towards the reactant side, leading to reduced CO_2 conversion.

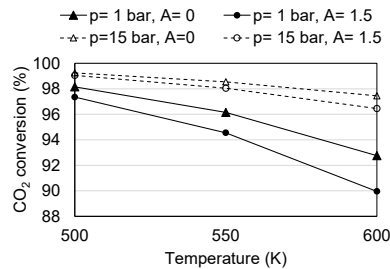


Figure 2. CO_2 conversion at equilibrium composition as a function of operating temperature, pressure, and inlet gas composition (CH_4/CO_2 ratio (A)).

Figure 3 demonstrates the influence of water removal on the CO_2 conversion and reaction rate along a reactor that is operating at 600 K and 1 bar. In Figure 3, the solid red line (EQ.1) illustrates the point at which the reaction is assumed to have reached equilibrium (99.9% of the CO_2 conversion at equilibrium). The dotted red line (EQ.2) illustrates the point at which the reaction reaches a new equilibrium if all produced water is removed at EQ.1. The solid black line (“No WR”) illustrates a case with no water removal along the reactor, while the black dotted lines represent cases with water removal at different points in the reactor. Further, the solid blue line demonstrates a case where water is removed continuously along the reactor. In all cases, the reactor is long enough to reach equilibrium after water removal. It is worth mentioning that the cases with no water removal and continuous water removal define the limiting cases with minimum and maximum CO_2 conversion, respectively.

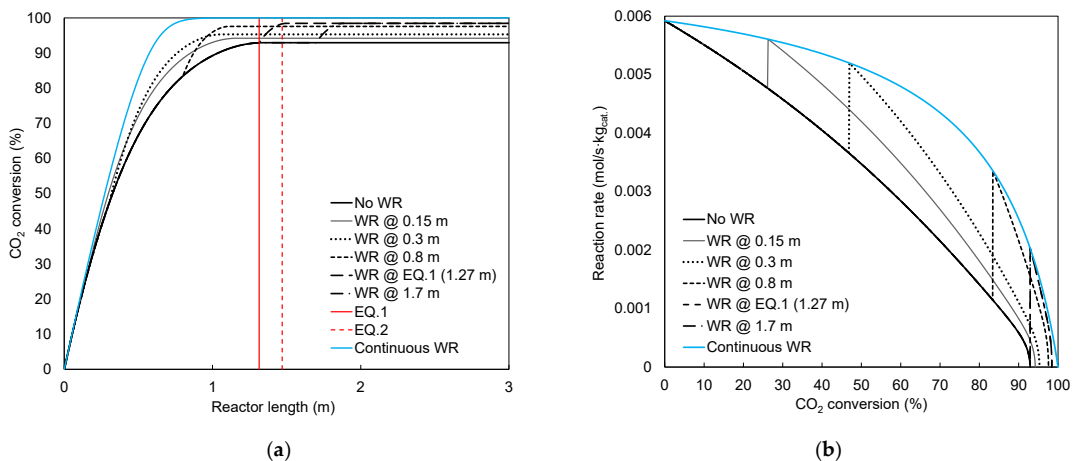


Figure 3. Effect of water removal along a reactor length operating at $T = 600 \text{ K}$, $p = 1 \text{ bar}$ and $A = 0$ on (a) CO_2 conversion and (b) reaction rate. Here, EQ.1 and EQ.2 denote the first and second equilibrium lengths. Notice that the lines for water removal at EQ.1 and 1.7 m are the same in (b).

As can be seen in Figure 3a, removing water from the reactor increases the CO₂ conversion compared to the case with no water removal. As expected, maximum CO₂ conversion is obtained when the water is removed after reaching the first equilibrium. It should be noticed that most of the conversion takes place before reaching the first equilibrium and that the length extension required to reach the second equilibrium point is smaller than the length required to reach the first equilibrium. This can be also seen in Figure 3b, where the reaction rate along the reactor is illustrated. It can be observed that water removal causes an abrupt increase in the reaction rate, increasing the average reaction rate compared to the case with no water removal. When the reaction reaches the first equilibrium, no further conversion takes place due to zero reaction rate. No matter where water is removed after reaching the first equilibrium length, the reaction rate reaches an identical maximum value and then approaches zero where the second equilibrium is obtained (see the identical lines for water removal at the first equilibrium and 1.7 m in Figure 3b). If the water removal point is located before reaching equilibrium, the total CO₂ conversion is reduced. However, the reaction rate is higher, and the conversion can be improved if the reactor is not long enough to reach equilibrium.

Figure 4 illustrates the CO₂ conversion improvement and relative length extension required to obtain maximum CO₂ conversion under different operating conditions. The length required to reach the first equilibrium point depends on the kinetics of the reaction. Operating the CO₂ methanation reactor at a higher pressure and temperature increases the reaction rate, thereby reducing the length required to reach equilibrium. Moreover, the presence of CH₄ in the inlet gas mixture reduces the reaction rate, hence increasing the length required to reach equilibrium. These trends also apply to the relative length extension required to reach the second equilibrium after removing water.

As can be observed in Figure 4, the relative conversion improvement is higher under conditions where CO₂ conversion is limited due to the thermodynamic equilibrium (i.e., low pressure, high temperature, and CH₄ in the feed). This suggests that the water removal is of more significance when the final CO₂ conversion at the first equilibrium length is lower. For instance, the highest CO₂ conversion improvement of approximately 8% is achieved for the case with the lowest conversion at the first equilibrium point (corresponding to the situation in Figure 2, i.e., at $p = 1$ bar, $T = 600$ K and $A = 1.5$).

As mentioned earlier in this section, both the CO₂ conversion and the conversion rate changes when moving the point of the water removal. This becomes important when the reactor is not long enough to reach equilibrium. The effect of the water removal location on the CO₂ conversion for a reactor with a length equal to 50% of the first equilibrium length ($L_{EQ,1}$) is illustrated in Figure 5. It should be noted that the results for water removal at either the inlet or the outlet of the reactor are the same since no water removal takes place along the reactor in both cases. As can be seen in Figure 5, there is an optimal location for the water removal at which the CO₂ conversion is maximized. Corresponding to Figure 3b, the optimal point for water removal should be where the average reaction rate is highest. The reaction rate is reduced as the number of products increases. After removing water, the driving force for the reaction, and thereby the reaction rate, increases. The later the water removal, the higher the conversion will be at equilibrium. However, if the water is removed too late, there will not be enough length left to take advantage of the increased reaction rate.

Figure 6 illustrates the effect of operating conditions on the optimum water removal location for different lengths of the reactor. The optimal location is here defined as the water removal point that gives the maximum CO₂ conversion for a given reactor length. However, the optimal point is only refined to a resolution of 0.1 in z/L . As can be observed in Figure 6, for a given operating pressure, the optimum water removal location is independent of the reactor temperature. The shorter the length of the reactor, the earlier the water removal must take place to maximize the conversion. At higher pressure, the results indicate that the optimal point of water removal is at a higher relative length of z/L .

As can be observed in Figure 3b, the reaction rate drops faster after removing the water. To overcome this limitation, the optimal value for the relative point for water removal will not be smaller than 0.5 even in short reactors. For the cases where CH_4 is present in the inlet gas mixture, the optimal value for the relative length of z/L is generally smaller. With $A = 1.5$ and low pressure, the optimal point is the same for all relative reactor lengths below 0.75. Corresponding to Figure 4, the presence of CH_4 in the feed gas reduces the reaction rate, thereby increasing the length required to reach equilibrium.

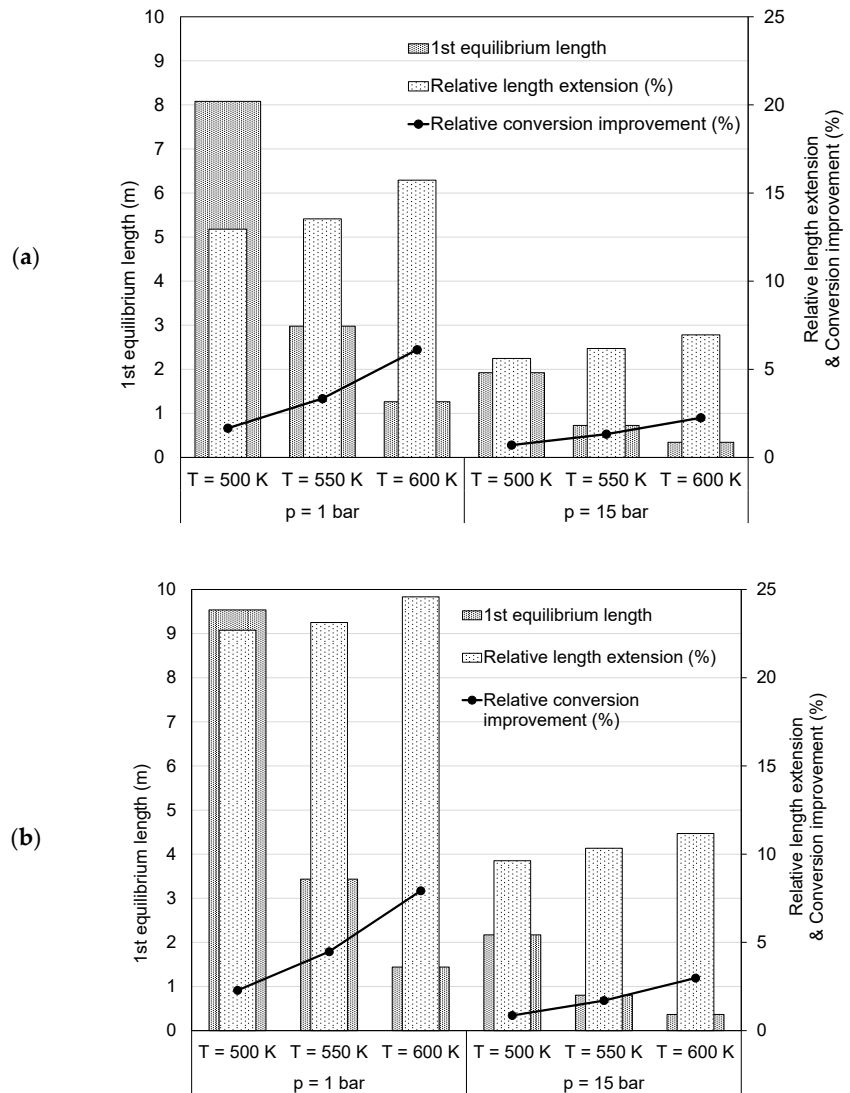


Figure 4. CO_2 conversion improvement and relative length extension required to the 2nd equilibrium under different operating conditions for (a) $A = 0$ and (b) $A = 1.5$.

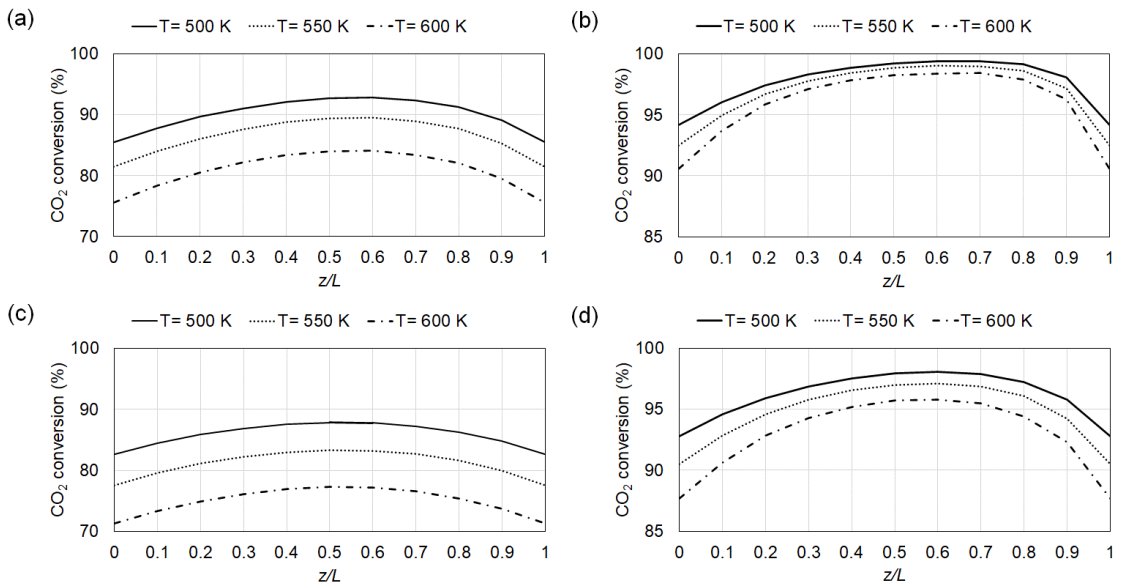


Figure 5. Effect of the water removal location on the CO_2 conversion for a reactor with $L/L_{\text{EQ},1} = 0.5$ operating under different temperature, pressure, and CH_4/CO_2 ratios (A). (a) $p = 1$ bar and $A = 0$, (b) $p = 15$ bar and $A = 0$, (c) $p = 1$ bar and $A = 1.5$, (d) $p = 15$ bar and $A = 1.5$.

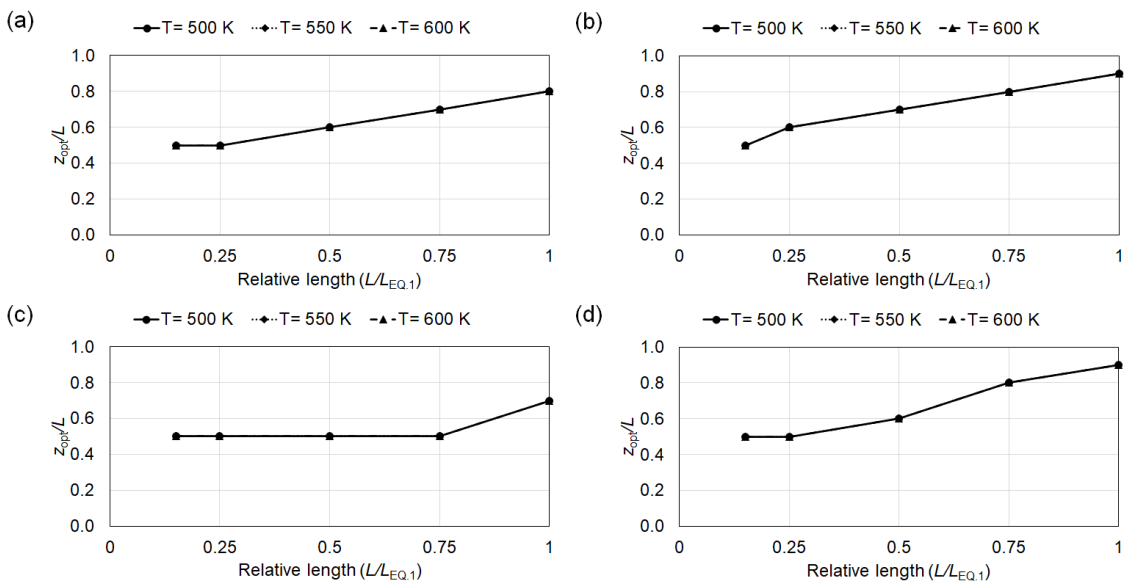


Figure 6. Effect of operating conditions on the optimum water removal point for different lengths of the reactor. (a) $p = 1$ bar and $A = 0$, (b) $p = 15$ bar and $A = 0$, (c) $p = 1$ bar and $A = 1.5$, (d) $p = 15$ bar and $A = 1.5$.

The relative conversion improvement for different reactor lengths under different operating conditions is demonstrated in Figure 7. The water removal leads to larger CO_2 conversion improvement when the length of the reactor is shorter than the first equilibrium length. At low operating pressure, the strongest effect on the relative conversion

improvement due to water removal is seen at the relative length ($L/L_{EQ,1}$) of 0.5, whereas the strongest effect is observed at the relative length ($L/L_{EQ,1}$) of 0.25 at higher operating pressure. For short reactors, the reaction will not reach equilibrium. Nonetheless, an effort to increase the average reaction rate is favorable as this gives a higher conversion. The largest relative conversion improvement due to water removal is achieved in the case without CH_4 in the inlet gas mixture, operating at high pressure and high temperature. Referring to Figure 3b, it was observed that water boosted the average reaction rate, and the new equilibrium condition would be obtained earlier. Moreover, increasing the operating temperature and pressure improves the reaction rate and this will be amplified by removing water in a short reactor.

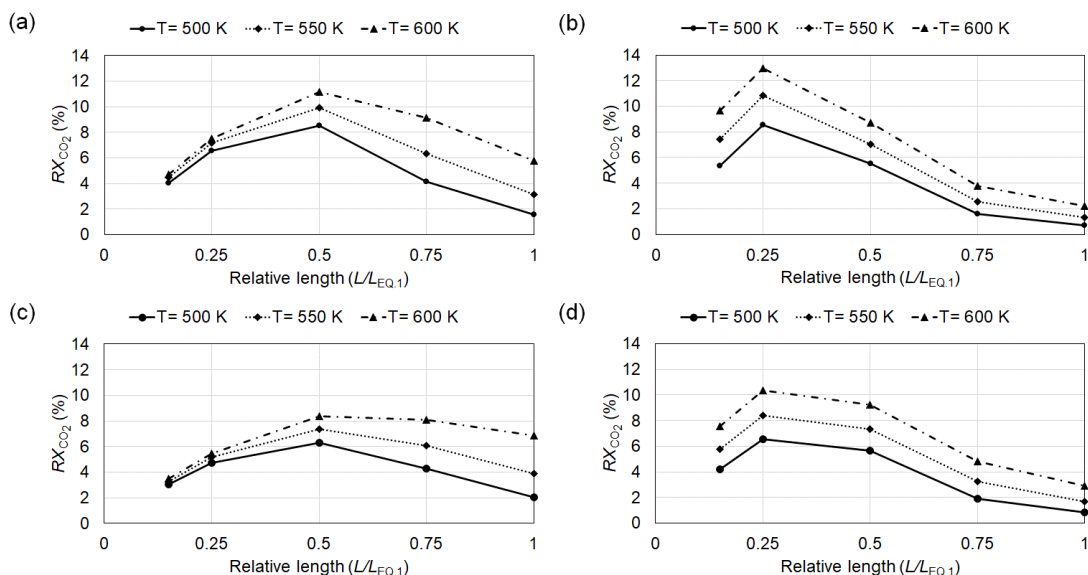


Figure 7. Relative conversion improvement for different lengths of the reactor under different operating conditions. (a) $p = 1$ bar and $A = 0$, (b) $p = 15$ bar and $A = 0$, (c) $p = 1$ bar and $A = 1.5$, (d) $p = 15$ bar and $A = 1.5$.

4.2. Irreversibility

The present section focuses on assessing the performance of the methanation reactor in terms of energy efficiency. This is realized by analyzing the irreversibility rate of a reactor with or without intermediate water removal. In cases without intermediate water removal, the analysis is presented for the final composition at the end of a reactor sufficiently long to reach equilibrium.

Figure 8 illustrates the specific irreversibility (i.e., the ratio between the total irreversibility rate and the amount of CH_4 produced) within a reactor operating under different conditions for cases without intermediate water removal. As can be observed in Figure 8, operating at lower pressure and higher temperature decreases the specific irreversibility within the reactor. Also, the existence of CH_4 in the inlet gas mixture reduces the specific irreversibility within the reactor. Contrarily, results in Figure 2 illustrated that the CO_2 conversion decreased if the reactor operated at low pressure, high temperature, and in the presence of CH_4 in the inlet gas mixture. These two perspectives suggest that the reactor design should reflect a compromise between CO_2 conversion and irreversibility. From a reversibility point of view, to reduce the thermodynamic losses within the reactor the reaction should follow a path where the magnitude of the reaction driving forces along the reactor approaches zero (i.e., theoretically preceding the chemical reaction infinitesimally close to equilibrium). Here, in cases with no intermediate water removal, the final CO_2

conversion and the specific irreversibility are only influenced by the fixed operating conditions. Therefore, the degrees of freedom to manipulate the driving forces, and thereby the extent of reaction, are limited.

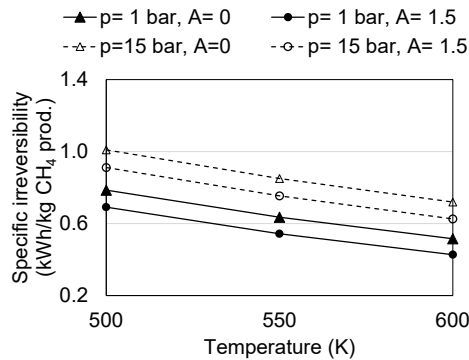


Figure 8. Specific irreversibility within a reactor operating under different conditions with no intermediate water removal.

Figure 9 illustrates the specific work required for water removal, the specific exergy of heat rejected from the reactor, and the change in specific exergy of material streams for a reactor operating under different conditions. As can be seen in Figure 9a, the work required to remove water from the reactor increases with increasing temperature. The presence of CH_4 in the inlet gas mixture also leads to an increase in the work requirement for water removal, as part of the work would be used to separate water from the additional CH_4 in the gas mixture. However, an increase in operating pressure decreases the work required to remove water. Figure 9b illustrates that the exergy of heat extracted from the reactor is independent of the operating pressure and the inlet gas composition. Running the reactor at higher temperature results in increased available exergy of heat, which can be utilized in the overall process design when potential process integration options are considered, contributing to reduced total irreversibility rate at higher temperatures. As can be observed in Figure 9c, operating the reactor at higher temperature and pressure enables extracting more exergy from the material streams, which is also observed in the CO_2 conversion in Figure 2. For a given temperature and pressure, additional CH_4 in the inlet gas mixture leads to a reduction in the exergy extraction from the material streams. The results in Figure 9c are reflected in the specific irreversibility presented in Figure 8.

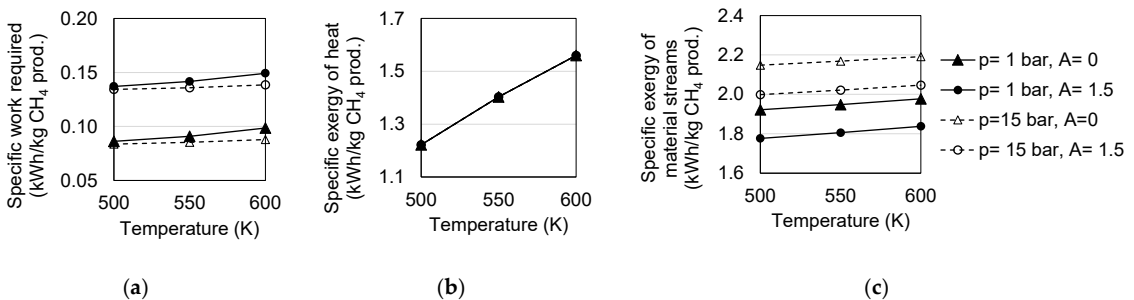


Figure 9. Contribution of the exergy terms for a reactor at the equilibrium operating under different conditions (a) specific work ($\dot{W}/\dot{m}_{\text{CH}_4 \text{ prod.}}$) (b) specific exergy of heat ($\dot{E}_x(\dot{Q})/\dot{m}_{\text{CH}_4 \text{ prod.}}$) and (c) specific exergy change for material streams ($\Delta\dot{E}_{x,\text{streams}}/\dot{m}_{\text{CH}_4 \text{ prod.}}$).

Here, the effect of the intermediate water removal location on the irreversibility rate within the reactor is studied. In cases with intermediate water removal, the water produced after the removal point is removed at the end of the reactor, to provide a fair comparison between the different cases. Figure 10 demonstrates the effect of the water removal location on the accumulated irreversibility rate and specific irreversibility along a reactor operating at $T = 600$ K, $p = 1$ bar, and $A = 0$. It is worth mentioning that the results in Figure 10 are considered for the same cases as in Figure 3. Here, the specific irreversibility refers to the ratio between the irreversibility rate and the amount of produced CH_4 in each cell of the reactor. As can be observed in Figure 10a, compared to the case with no intermediate water removal, removing water at the intermediate point increases the total irreversibility rate within the reactor. It can be observed that the increase in the irreversibility rate reaches a maximum value when the water is removed at a certain intermediate point. Continuous water removal yields the highest irreversibility rate within the reactor (solid blue line).

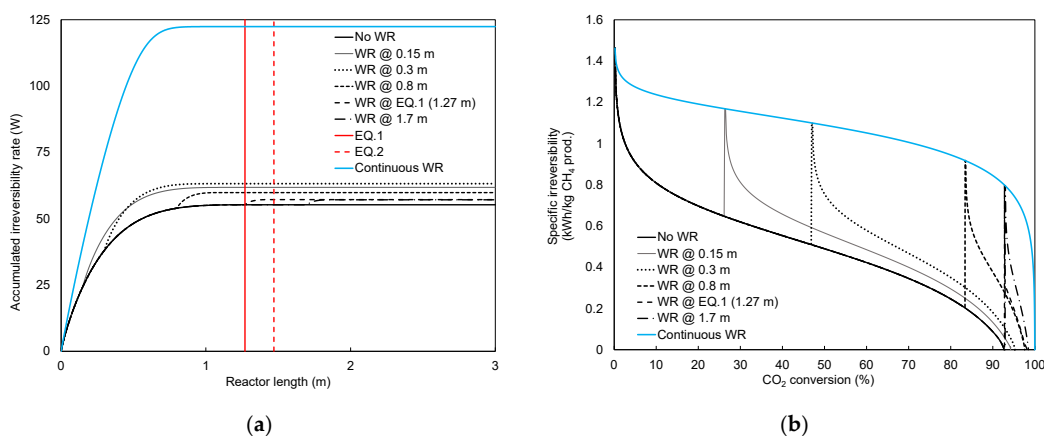


Figure 10. Effect of water removal location on (a) accumulated irreversibility rate and (b) specific irreversibility for a reactor operating at $T = 600$ K, $p = 1$ bar, and $A = 0$. Notice that the lines of water removal at EQ.1 and 1.7 m are the same in (b).

In Figure 10b, the intermediate water removal point is observed as a sudden jump in the curves, which leads to higher average specific irreversibility within the reactor. The areas below the curves in Figure 10b indicate the total irreversibility rate within the reactor. As can be observed in Figure 10b, the CO_2 conversion improvement is accompanied by a smaller increase in the irreversibility rate when the intermediate water removal point moves towards the end of the reactor. A smaller increase in the average specific irreversibility can be seen when the water is removed after the first equilibrium length (i.e., where the specific irreversibility becomes zero since no reaction occurs in the reactor). In this particular case study, with no length limitation and fixed operating conditions, the results of the irreversibility analysis suggest that water should be removed when the reaction reaches equilibrium.

Results for the specific irreversibility within a reactor operating at $T = 600$ K, $p = 1$ bar, and $A = 0$ are tabulated in Table 3 when the water is removed at different intermediate locations. An increase in the CO_2 conversion due to moving the water removal point towards the end of the reactor length is accompanied by a decrease in the change of specific exergy of material streams. Since the temperature and heat of the reaction are constant, the specific exergy of heat remains constant when moving the water removal point. When the water is removed after reaching the first equilibrium, a smaller total specific irreversibility is obtained compared to the case with no intermediate water removal. This is because the average specific irreversibility before the removal point would be higher than the obtained peak value for the specific irreversibility due to the water removal. Therefore, the amount of total specific irreversibility would reduce.

Table 3. Summarized results for the effect of water removal location (z) along a reactor operating at $T = 600$ K, $p = 1$ bar, and $A = 0$, considering an FBR with a length of 3 m.

x (m)	X_{CO_2} (%)	$\Delta \dot{E}_x, \text{ streams} / \dot{m}_{CH_4 \text{ prod.}}$ (kWh/kg CH_4 Prod.)	$\dot{E}_x(\dot{Q}) / \dot{m}_{CH_4 \text{ prod.}}$ (kWh/kg CH_4 Prod.)	$\dot{W} / \dot{m}_{CH_4 \text{ prod.}}$ (kWh/kg CH_4 Prod.)	$\dot{I} / \dot{m}_{CH_4 \text{ prod.}}$ (kWh/kg CH_4 Prod.)
No WR	92.9	1.976	1.560	0.098	0.514
0.15	94.2	1.972	1.560	0.155	0.567
0.3	95.3	1.968	1.560	0.166	0.574
0.8	97.6	1.958	1.560	0.132	0.530
1.27 *	98.4	1.954	1.560	0.109	0.502
1.7	98.4	1.954	1.560	0.109	0.502
Continuous WR	100.0	1.942	1.560	0.678	1.060

* The intermediate water removal occurs at the first equilibrium length (EQ.1).

As it is assumed that the water separation is achieved through a reversible process, no additional irreversibility caused by the water removal process is expected. As can be seen in Table 3, in comparison with no water removal case, the increase in the total specific irreversibility due to water removal is accompanied by additional reversible specific work. This suggests that considering the specific work required for water removal from a reactor operating at fixed conditions can be an alternative approach to investigate how the water removal location would influence the irreversibility rate.

The minimum work comprises the work required for water removal at the intermediate location and the end of the reactor. The effect of the water removal location on the amount of removed water and the specific work is demonstrated in Figure 11a,b, respectively, for a reactor operating at $T = 600$ K, $p = 1$ bar, and $A = 0$. By moving the water removal point from the inlet of the reactor towards the outlet of the reactor, the amount of removed water at the intermediate location increases, reaching a maximum amount when the intermediate water removal occurs at the first equilibrium length. As illustrated in Figure 11, the amount of water removed at the intermediate point would not necessarily reflect the required specific work at the intermediate point. The specific work at the intermediate point decreases as the intermediate point moves towards the end of the reactor, reaching a constant value when equilibrium is obtained. Moreover, the larger the amount of water removed at the intermediate point, the higher the specific work required at the end of the reactor to separate the additional produced water after the water removal point. The work required for water removal depends on the composition of the gas mixture, and the specific work requirement for water removal increases as the water fraction reduces.

As discussed earlier, removing water from the reactor increases the average reaction rate. Hence the same conversion can be obtained in a shorter reactor. However, the increase in the average reaction rate would cause an unavoidable increase in irreversibility when the operating conditions for the reaction are fixed. Here, the aim is to investigate how the water removal location can influence the irreversibility rate within reactors shorter than the required equilibrium length (similar to the case studies in Section 4.1.). The effect of the water removal point on the specific irreversibility for different relative reactor lengths operating at $T = 600$ K, $p = 1$ bar, and $A = 0$ is illustrated in Figure 12. Further, Figure 13 demonstrates the specific work required for water removal, the specific exergy of heat rejected from the reactor, and the changes in specific exergy of material streams for the cases presented in Figure 12.

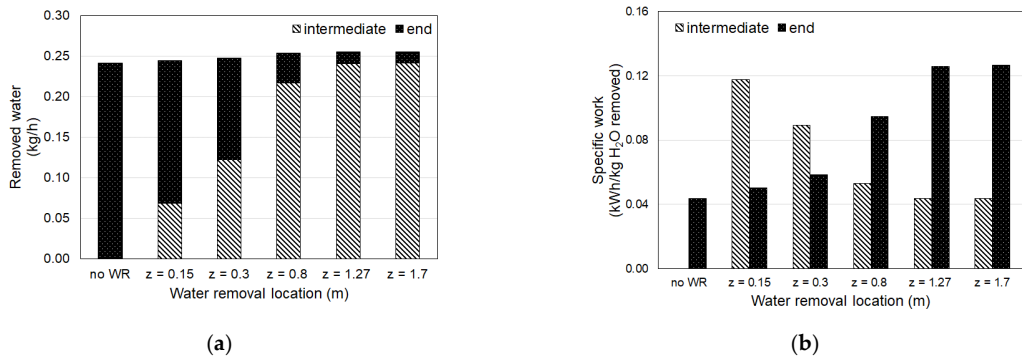


Figure 11. The effect of water removal location on (a) the amount of removed and (b) the specific water removal work at the intermediate point and the end of a reactor operating at $T = 600$ K, $p = 1$ bar, and $A = 0$ with a length of 3 m.

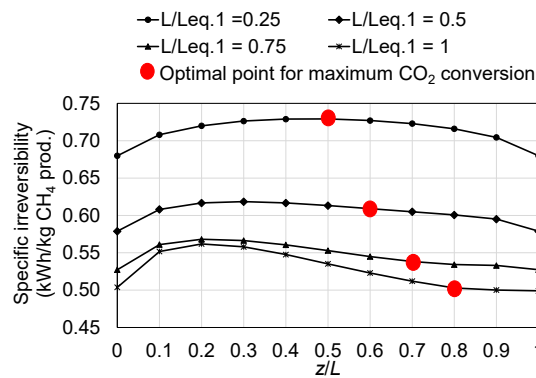


Figure 12. Effect of water removal point on the specific irreversibility for different reactor lengths operating at $T = 600$ K, $p = 1$ bar, and $A = 0$.

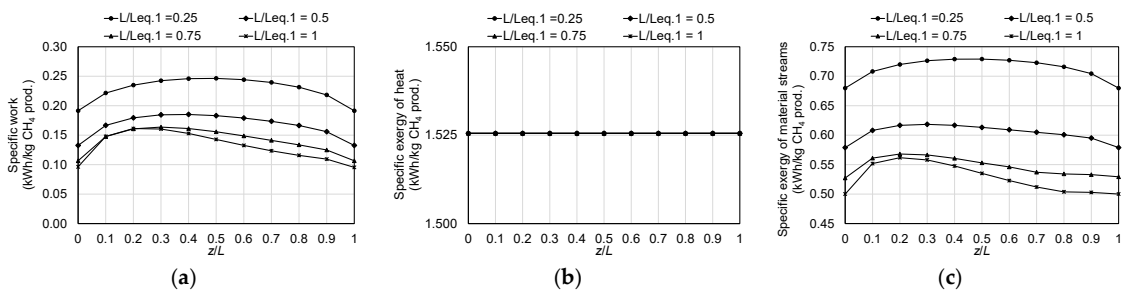


Figure 13. Effect of water removal point on (a) the specific work, (b) the specific exergy of heat, and (c) the specific exergy of material streams for different reactor lengths operating at $T = 600$ K, $p = 1$ bar, and $A = 0$.

As can be observed in Figure 12, for a short reactor (e.g., $L/Leq,1 = 0.25$), the highest specific irreversibility is obtained when the water removal occurs in the middle of the reactor. This coincides with where the maximum CO₂ conversion is obtained (at $z/L = 0.5$). As the reactor length is increased, the optimal water removal point is shifted towards the outlet of the reactor, while the largest irreversibilities are observed for water removal points closer to the inlet of the reactor. Moreover, for the optimal water removal point (in terms of conversion), the increase in specific irreversibility compared to the case with no water

removal is reduced. When the reactor length is equal to the equilibrium length EQ.1, there is only a small penalty compared to the irreversibilities in the case with no water removal. This can be explained by the direct effect of the water removal location on the average specific irreversibility and average reaction rate. As discussed earlier, the benefits from reduced specific irreversibility for longer reactors at the optimal water removal point are reflected in the required specific work and the change in specific exergy of the streams (see Figure 13).

5. Remarks

The present study illustrates that considering intermediate water removal increases the average reaction rate within the reactor and, as a result, increases the CO₂ conversion and the irreversibility rate within a reactor operating at fixed conditions. As mentioned earlier, obtaining a fixed isothermal condition for a highly activated catalytic reaction is a challenging task in practice. Besides, the fixed operating conditions limit the degrees of freedom to manipulate the driving forces within the reactor to obtain an energy-efficient reactor design. Therefore, an extended study should consider adding more complexity to the reactor model, e.g., non-isothermal operating modes.

In the present study, the examination of removing water at an intermediate point demonstrated the potential possibility of manipulation of the average reaction rate through changing driving forces leading to different irreversibility rates. To avoid a significant increase in the reaction rate at the water removal point, and thereby a significant jump in the specific irreversibility, partial water removal (instead of complete water removal at the intermediate point) or water removal at several points can be considered as alternatives. It is worth mentioning that partial water removal results in longer reactors while the effect of multiple removal points will be reduced reactor length. Nonetheless, the length of the reactor might not be an important factor if an energy-efficient reactor with a high CO₂ conversion is guaranteed.

The intermediate water removal concept can also be accompanied by a partial feeding strategy of reactants along the reactor. On the one hand, water removal increases the average reaction rate, while on the other hand, a limited concentration of the reactants would reduce the average reaction rate. This can aid in controlling the reaction rate within the reactor. Considering a combination of water removal and partial feeding of the reactants can lead to efficient heat management within the reactor, at which high CO₂ conversion can be obtained even though the irreversibility rate is low. It is observed that the work required for removing water at an intermediate location could be used as an alternative approach to investigate the irreversibility rate within the reactor. However, it should be noted that the actual work for water removal will be higher than what is presented here, as, in the present study, the produced water was removed in reversible processes.

6. Conclusions

A comprehensive thermodynamic study was performed in order to investigate the effect of water removal on the CO₂ conversion and the irreversibility in an isothermal fixed bed methanation reactor. A one-dimensional pseudo-homogenous model was applied for the reactor, considering the kinetics of the Sabatier reaction. An effectiveness factor was used to consider the intra-particle mass and heat transport limitations between the two phases. At one intermediate point in the reactor, all the water produced up until that point was removed, assuming a reversible process.

With respect to the CO₂ conversion, for short reactors, the optimal water removal point was located in the middle of the reactor. As the length of the reactor approached the length required to reach equilibrium, the water removal point resulting in the highest CO₂ conversion moved closer to the end. The location of the optimal removal point was found to be independent of the operating temperature, while the presence of CH₄ in the feed gas resulted in moving the optimal water removal point upstream.

With respect to the irreversibility within the reactor, for a short reactor, it was observed that the water removal point that gave the highest CO₂ conversion in the middle of the reactor also provided the largest irreversibility rate. For a longer reactor (i.e., reactor lengths close to the required equilibrium length), the improvement in the CO₂ conversion was accompanied by a smaller penalty in the irreversibilities compared to the case with no water removal.

The results illustrate that the length of the reactor is essential to the optimal water removal point. Further, it is demonstrated that the reactor length should not necessarily be close to the equilibrium length when the water removal takes place to obtain the best performance; the additional gains in terms of both the CO₂ conversion and the irreversibilities are not significant.

Possible conceptual ideas such as partial water removal and partial reactant feeding are suggested for future studies to develop an energy-efficient reactor. These ideas are based on manipulating the reaction rate within the reactor to control the driving forces along the reactor. The proposed model should be examined using process simulators, and for cases operating under non-isothermal conditions in future work. In this context, additional concerns such as runaway temperature limitations should be considered.

Author Contributions: Conceptualization, S.E.H. and K.M.L.; methodology, S.E.H.; software, S.E.H.; validation, S.E.H., M.H. and B.A.; formal analysis, S.E.H.; investigation, S.E.H.; resources, S.E.H. and K.M.L.; data curation, S.E.H.; writing—original draft preparation, S.E.H.; writing—review and editing, K.M.L., S.K.S., M.H. and B.A.; supervision, B.A.; project administration, B.A. All authors have read and agreed to the published version of the manuscript.

Funding: This research received no external funding.

Institutional Review Board Statement: Not applicable.

Informed Consent Statement: Not applicable.

Data Availability Statement: Data sharing not applicable.

Acknowledgments: The authors acknowledge the financial support from the Norwegian University of Science and Technology (NTNU) through the Strategic Research Program ENERSENSE.

Conflicts of Interest: The authors declare no conflict of interest.

References

1. He, W.; Abbas, Q.; Alharthi, M.; Mohsin, M.; Hanif, I.; Vo, X.V.; Taghizadeh-Hesary, F. Integration of renewable hydrogen in light-duty vehicle: Nexus between energy security and low carbon emission resources. *Int. J. Hydrogen Energy* **2020**, *45*, 27958–27968. [[CrossRef](#)]
2. Pao, H.T.; Tsai, C.M. CO₂ emissions, energy consumption and economic growth in BRIC countries. *Energy Policy* **2010**, *38*, 7850–7860. [[CrossRef](#)]
3. Balsalobre-Lorente, D.; Shahbaz, M.; Roubaud, D.; Farhani, S. How economic growth, renewable electricity and natural resources contribute to CO₂ emissions? *Energy Policy* **2018**, *113*, 356–367. [[CrossRef](#)]
4. Sinsel, S.R.; Riemke, R.L.; Hoffmann, V.H. Challenges and solution technologies for the integration of variable renewable energy sources—A review. *Renew. Energy* **2020**, *145*, 2271–2285. [[CrossRef](#)]
5. Gallo, A.B.; Simões-Moreira, J.R.; Costa, H.K.M.; Santos, M.M.; Moutinho dos Santos, E. Energy storage in the energy transition context: A technology review. *Renew. Sustain. Energy Rev.* **2016**, *65*, 800–822. [[CrossRef](#)]
6. Parra, D.; Valverde, L.; Pino, F.J.; Patel, M.K. A review on the role, cost and value of hydrogen energy systems for deep decarbonization. *Renew. Sustain. Energy Rev.* **2019**, *101*, 279–294. [[CrossRef](#)]
7. Ghaib, K.; Ben-Fares, F.Z. Power-to-Methane: A state-of-the-art review. *Renewable Sustainable Energy Rev.* **2018**, *81*, 433–446. [[CrossRef](#)]
8. Uebbing, J.; Rikho-Struckmann, L.K.; Sunmacher, K. Exergetic assessment of CO₂ methanation processes for the chemical storage of renewable energies. *Appl. Energy* **2019**, *233*, 271–282. [[CrossRef](#)]
9. Massa, F.; Coppola, A.; Scala, F. A thermodynamic study of sorption-enhanced CO₂ methanation at low pressure. *J. CO₂ Util.* **2020**, *35*, 176–184. [[CrossRef](#)]
10. Mazza, A.; Bompard, E.; Chicco, G. Applications of power to gas technologies in emerging electrical systems. *Renew. Sustain. Energy Rev.* **2018**, *92*, 794–806. [[CrossRef](#)]
11. Sabatier, P.; Senderens, J.B. New Synthesis of Methane. *C. R. Hebd. Séances Acad. Sci.* **1902**, *134*, 514–516.

12. Rönsch, S.; Schneider, J.; Matthischke, S.; Schlüter, M.; Götz, M.; Lefebvre, J.; Prabhakaran, P.; Bajhor, S. Review on methanation—From fundamentals to current projects. *Fuel* **2016**, *166*, 276–296. [[CrossRef](#)]
13. Ngo, S.I.; Lim, Y.I.; Lee, D.; Go, K.S.; Seo, M.W. Flow behaviors, reaction kinetics, and optimal design of fixed- and fluidized-beds for CO₂ methanation. *Fuel* **2020**, *275*, 117886. [[CrossRef](#)]
14. Kao, Y.L.; Lee, P.H.; Tseng, Y.T.; Chien, I.L.; Ward, J.D. Design, control and comparison of fixed-bed methanation reactor systems for the production of substitute natural gas. *J. Taiwan Inst. Chem. Eng.* **2014**, *45*, 2346–2357. [[CrossRef](#)]
15. Schlereth, D.; Hinrichsen, O. A fixed-bed reactor modeling study on the methanation of CO₂. *Chem. Eng. Res. Des.* **2014**, *92*, 702–712. [[CrossRef](#)]
16. Fache, A.; Marias, F.; Guerré, V.; Palmade, S. Optimization of fixed-bed methanation reactors: Safe and efficient operation under transient and steady-state conditions. *Chem. Eng. Sci.* **2018**, *192*, 1124–1137. [[CrossRef](#)]
17. Bremer, J.; Sundmacher, K. Operation range extension via hot-spot control for catalytic CO₂ methanation reactors. *React. Chem. Eng.* **2019**, *4*, 1019–1037. [[CrossRef](#)]
18. Zimmermann, R.T.; Bremer, J.; Sundmacher, K. Optimal catalyst particle design for flexible fixed-bed CO₂ methanation reactors. *Chem. Eng. J.* **2020**, *387*, 123704. [[CrossRef](#)]
19. Kopyscinski, J.; Schildhauer, T.J.; Biollaz, S.M.A. Methanation in a fluidized bed reactor with high initial CO partial pressure: Part II—Modeling and sensitivity study. *Chem. Eng. Sci.* **2011**, *66*, 1612–1621. [[CrossRef](#)]
20. Herce, C.; Cortés, C.; Stendardo, S. Numerical simulation of a bubbling fluidized bed reactor for sorption-enhanced steam methane reforming under industrially relevant conditions: Effect of sorbent (dolomite and CaO-Ca₁₂Al₁₄O₃₃) and operational parameters. *Fuel Process. Technol.* **2019**, *186*, 137–148. [[CrossRef](#)]
21. Li, J.; Zhou, L.; Li, P.; Zhu, Q.; Jiajian, G.; Gu, F.; Su, F. Enhanced fluidized bed methanation over a Ni/Al₂O₃ catalyst for production of synthetic natural gas. *Chem. Eng. J.* **2013**, *219*, 183–189. [[CrossRef](#)]
22. Meng, F.; Li, X.; Li, M.; Cui, X.; Zhong, L. Catalytic performance of CO methanation over La-promoted Ni/Al₂O₃ catalyst in a slurry-bed reactor. *Chem. Eng. J.* **2017**, *313*, 1548–1555. [[CrossRef](#)]
23. Lefebvre, J.; Bajhor, S.; Kolb, T. Modeling of the transient behavior of a slurry bubble column reactor for CO₂ methanation, and comparison with a tube bundle reactor. *Renew. Energy* **2020**, *151*, 118–136. [[CrossRef](#)]
24. Lefebvre, J.; Götz, M.; Bajhor, S.; Reimert, R.; Kolb, T. Improvement of three-phase methanation reactor performance for steady-state and transient operation. *Fuel Process. Technol.* **2015**, *132*, 83–90. [[CrossRef](#)]
25. Engelbrecht, N.; Chiuta, S.; Everson, R.C.; Neomagus, H.W.J.P.; Bessarabov, D.G. Experimentation and CFD modelling of a microchannel reactor for carbon dioxide methanation. *Chem. Eng. J.* **2017**, *313*, 847–857. [[CrossRef](#)]
26. Mathieu-Potvin, F.; Gosselin, L. Threshold length for maximal reaction rate in catalytic microchannels. *Chem. Eng. J.* **2012**, *188*, 86–97. [[CrossRef](#)]
27. Hashemi, S.E.; Lien, K.M.; Schnell, S.K.; Austbø, B. Thermodynamic analysis of different methanation reactors for biogas upgrading. *Comput. Aided Chem. Eng.* **2020**, *48*, 367–372. [[CrossRef](#)]
28. Sun, D.; Khan, F.M.; Simakov, D.S.A. Heat removal and catalyst deactivation in a Sabatier reactor for chemical fixation of CO₂: Simulation-based analysis. *Chem. Eng. J.* **2017**, *329*, 165–177. [[CrossRef](#)]
29. Sun, D.; Simakov, D.S.A. Thermal management of a Sabatier reactor for CO₂ conversion into CH₄: Simulation-based analysis. *J. CO₂ Util.* **2017**, *21*, 368–382. [[CrossRef](#)]
30. Kiewidt, L.; Thöming, J. Predicting optimal temperature profiles in single-stage fixed-bed reactors for CO₂-methanation. *Chem. Eng. Sci.* **2015**, *132*, 59–71. [[CrossRef](#)]
31. Faria, A.C.; Miguel, C.V.; Rodrigues, A.E.; Madeira, L.M. Modeling and Simulation of a Steam-Selective Membrane Reactor for Enhanced CO₂ Methanation. *Ind. Eng. Chem. Res.* **2020**, *59*, 16170–16184. [[CrossRef](#)]
32. Kampen, J.V.; Boon, J.; Berkel, F.V.; Vente, J.; Annaland, M.V.S. Steam separation enhanced reactions: Review and outlook. *Chem. Eng. J.* **2019**, *374*, 1286–1303. [[CrossRef](#)]
33. Diban, N.; Aguayo, A.T.; Bilbao, J.; Urriaga, A.; Ortiz, I. Membrane Reactors for in Situ Water Removal: A Review of Applications. *Ind. Eng. Chem. Res.* **2013**, *52*, 10342–10354. [[CrossRef](#)]
34. Walspurger, S.; Elzinga, G.D.; Dijkstra, J.W.; Sarić, M.; Haije, W.G. Sorption enhanced methanation for substitute natural gas production: Experimental results and thermodynamic considerations. *Chem. Eng. J.* **2014**, *242*, 379–386. [[CrossRef](#)]
35. Faria, A.C.; Miguel, C.V.; Madeira, L.M. Thermodynamic analysis of the CO₂ methanation reaction with in-situ water removal for biogas upgrading. *J. CO₂ Util.* **2018**, *26*, 271–280. [[CrossRef](#)]
36. Najari, S.; Gróf, G.; Saeidi, S. Enhancement of hydrogenation of CO₂ to hydrocarbons via In-Situ water removal. *Int. J. Hydrogen Energy* **2019**, *44*, 24759–24781. [[CrossRef](#)]
37. Hillestad, M. Systematic staging in chemical reactor design. *Chem. Eng. Sci.* **2010**, *65*, 3301–3312. [[CrossRef](#)]
38. Fischer, K.L.; Langer, M.R.; Freund, H. Dynamic carbon dioxide methanation in a wall-cooled fixed bed reactor: Comparative evaluation of reactor models. *Ind. Eng. Chem. Res.* **2019**, *58*, 19406–19420. [[CrossRef](#)]
39. Lohmuller, R.; Schneider, H.; Watson, A. Methanation Process. U.S. Patent US4294932A, 13 October 1981.
40. Fogler, H.S. *Essentials of Chemical Reaction Engineering*; Prentice Hall: Upper Saddle River, NJ, USA, 2011.
41. Koschany, F.; Schlereth, D.; Hinrichsen, O. On the kinetics of the methanation of carbon dioxide on coprecipitated NiAl(O)_x. *Appl. Catal. B Environ.* **2016**, *181*, 504–516. [[CrossRef](#)]

42. Lunde, P.J.; Kester, F.L. Carbon dioxide methanation on a Ruthenium catalyst. *Ind. Eng. Chem. Process Des. Dev.* **1974**, *13*, 27–33. [[CrossRef](#)]
43. Aparicio, L.M. Transient Isotopic Studies and Microkinetic Modeling of Methane Reforming over Nickel Catalysts. *J. Catal.* **1997**, *165*, 262–274. [[CrossRef](#)]
44. Kee, R.J.; Coltin, M.E.; Glarborg, P.; Zhu, H. *Chemically Reacting Flow: Theory, Modeling, and Simulation*, 2nd ed.; John Wiley & Sons: Hoboken, NJ, USA, 2018; Chapter 3. [[CrossRef](#)]
45. Fuller, E.N.; Schettler, P.D.; Giddings, J.C. New method for prediction of binary gas-phase diffusion coefficients. *Ind. Eng. Chem.* **1966**, *58*, 18–27. [[CrossRef](#)]
46. Kotas, T.J. *The Exergy Method of Thermal Plant Analysis*; Exergon Publishing Company: London, UK, 2012.

Direct vs. indirect biogas methanation for LBM production: A concept evaluation

SAYED EBRAHIM HASHEMI¹, MAGNE HILLESTAD² AND BJØRN AUSTBØ^{1,*}

1. DEPARTMENT OF ENERGY AND PROCESS ENGINEERING,
NORWEGIAN UNIVERSITY OF SCIENCE AND TECHNOLOGY,
NO-7491 TRONDHEIM, NORWAY

2. DEPARTMENT OF CHEMICAL ENGINEERING,
NORWEGIAN UNIVERSITY OF SCIENCE AND TECHNOLOGY,
NO-7491 TRONDHEIM, NORWAY

* CORRESPONDING AUTHOR

THIS ARTICLE WILL BE SUBMITTED TO *CHEM. ENG. RES. DES.*

This paper will be submitted for publication and is therefore not included

